Advanced Design of Sports Wheelchairs

Swansea University
Prifysgol Abertawe

Joseph O'Sullivan

Academic Supervisors:Dr Will Harrison & Dr Neil
Bezidos

Industrial Supervisor: Mr John Pitt

Industrial Sponsor:RMA Sport

Submitted to Swansea University in fulfilment of the requirements
for the Degree of
Doctor of Engineering

Swansea University

2024

Abstract

The aim of this project is to design the best possible sports wheelchair for tennis for use in competition. Initial market research was carried out on existing products from both the partner company, RMA Sport and competitor companies. The market research looked at both consumer sports wheelchairs and elite bespoke tennis wheelchairs, used by world-class athletes such as Stéphane Houdet. The comparison particularly focused on key characteristics such as weight, materials used and manufacturing methods. Optimisation techniques used in other similar engineering applications were also investigated. A product design specification (PDS) was developed based on the background research, with key design criteria for the performance, user requirements, compatibility with other components, manufacturing requirements and environmental considerations.

Practical testing was carried out on an existing product to measure loads during a range of load cases. This was done by applying strain gauges in key locations on the chair paired with camera footage to identify which movements have the largest effect on the wheelchair.

Following this, two design optimisation approaches were applied. The first looked at optimising the current design by using computational optimisation algorithms to minimize weight whilst maintaining structural integrity for all load cases. This was done initially by modifying tube dimensions in a low-fidelity finite element model, before being extended to setting both tube dimensions and chair geometry as design variables. Three different methods were used to identify the best solution: Design of Experiments (DOE), Genetic Algorithm (GA), and Particle Swarm Optimization (PSO). This resulted in a weight reduction of almost 450g when compared to the original design.

The second design optimisation approach was aimed and developing a more bespoke product for elite athletes, utilising carbon-fibre tubes with additively manufactured connectors. Topology optimisation was used to minimise the weight of these connectors whilst making joints that were strong and stiff. 48% reduction in mass of printed connectors. The final design was manufactured and assembled to prove the concept.

The PDS was used to compare the two proposed designs with the original wheelchair design to ensure they met the desired specifications.

Acknowledgements

If you have a bar on access, include the declarations below

Declarations

This work has not previously been accepted in substance for any degree and is not being concurrently submitted in candidature for any degree.
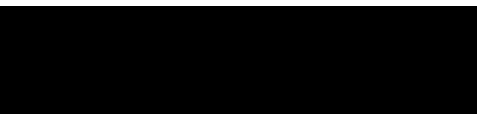
Signed.████████████████...

Date.23/01/24...

This thesis is the result of my own investigations, except where otherwise stated. Other sources are acknowledged by footnotes giving explicit references. A bibliography is appended.

Signed.████████████████..

Date...23/01/24..

I hereby give my consent for my work, if relevant and accepted, to be available for photocopying and for inter-library loans **after expiry of a bar on access approved by the University.**

Signed.████████████████..

Date.23/01/24...

The University's ethical procedures have been followed and, where appropriate, that ethical approval has been granted.

Signed.████████████████..

Date.23/01/24...

Contents

List of Figures

List of Tables

Chapter 1

Introduction

The objective of the project was to investigate different designs for high-performance tennis wheelchairs to be used by the sponsoring company RMA Sport. This was accomplished by proposing two different design approaches. The first approach involved using the current manufacturing methods while the second approach involved utilising alternative materials and manufacturing methods. Both approaches are customisable to create player-specific designs.

This was achieved by first conducting an initial review of current sport wheelchairs, ranging from entry-level wheelchairs to the more elite models sold by RMA Sport and their competitors, as well as potential restrictions on the design of the chair, such as rules or more practical transportation or manufacturing limitations.

The information from these sections was then used to establish a set of design goals in the form of a product design specification (PDS), for the two final designs to be compared against, outlining design targets and restrictions

A current RMA Sports tennis wheelchair was analysed using strain gauges to identify the main loads during the three main movements associated with wheelchair tennis. This data was paired with camera footage to identify which movements have the largest effect on the wheelchair, as well as which movements could be restricted by a new wheelchair design.

The next stage in the design process involved to analysing RMA Sports' current tennis wheelchair. This was achieved by creating a simple finite element

model of the sports wheelchair in Abaqus and verifying the model using data from the practical testing.

Once the model had been verified, the sports wheelchair was optimised. A special focus was placed on improving stiffness and reducing mass by adjusting various parameters such as geometry and tube thickness: thus, it was possible to determine whether any improvements could be made without major disruptions to RMA's manufacturing set-up. This was achieved by using different optimisation techniques for truss structures were identified, the techniques used many variables and multiple objectives to identify the best design solution. A particular focus was placed on using the design of experiments (DOE), genetic algorithms (GA) and particle swarm optimisation (PSO) techniques to filter the multiple potential design solutions.

Finally, this project focused on the design and optimisation of a modular design using additive manufacturing (AM) methods. The basis of the design is to have a chair that could start out as a dynamic jig, allowing the user to experience different geometries while playing a game and how it affects their play style. The 3D frame components printed were optimised using topology optimisation to ensure that printed parts were as light as possible without detracting from their strength.

Chapter 2

Literature Review

The aim of this chapter is to summarise the initial background to the project, providing details on the sponsoring company and wheelchair tennis as well as an overview of the current tennis wheelchairs on the market. Before going on to highlight any areas that might influence the design of the wheelchair, including user requirements, such as fit and components the wheelchair will use. The effect of the environment on the wheelchair, manufacturing, and assembly techniques. In the next section of this chapter will identifies different optimisation techniques, areas of the wheelchair to consider and methods used to solve similar problems in other industries. Before describing the current methods RMA use to test there wheelchairs.Points made through out this chapter will then be used to assemble a PDS that provides targets for future designs to meet.

2.1   Sponsoring Company

Roma Medical is one of the United Kingdom (UK)'s leading suppliers of mobility and rehabilitation aids. All the of products supplied by Roma are designed, manufactured, and assembled in-house by a large team of skilled technicians. Roma sells the products throughout the UK through mobility and rehabilitation aid distributors and supplies different types of wheelchairs to the National Health Service (NHS) [2] Roma Medical's set up is quite small, with the main offices, workshop, showroom, and stores based on an industrial estate in Bridgend, Wales. Roma Medical currently supplies 85 assorted products within the UK [3].

In 2012 Roma created a second company, initially called Roma Sport and

now called RMA Sport. This side of the company specialises in high-end sport wheelchairs. Initially focusing on wheelchair rugby or murder ball, RMA Sport designed a chair for the Great Britain Wheelchair Rugby (GBWR) and Southampton University wheelchair rugby teams. Since 2012, RMA Sport has expanded to other sport chairs such as basketball, dance, wheelchair motocross (WCMX) and tennis as well as a multi-purpose sport chair for multi-sport taster sessions [4]. RMA Sports wheelchairs are all designed using a patented Contour Body Mapping system and a pressure mapping system and then put into a computer aided design (CAD) model. This means that each chair is designed for the individual user's size and personal needs [3].

2.2 Wheelchair Sports

Wheelchair sports have grown in popularity in recent years, with an increasing number of sports becoming available to disabled athletes. Alongside this increasing interest, sports wheelchair designs have had to be adapted to become more competitive. Moreover, wheelchairs designed for different sports have varied design goals; for example, racing wheelchairs (*figure2.1 a*) must be as light as possible to improve the acceleration of the wheelchair in a straight line, whereas rugby wheelchairs (*figure2.1 b*) must be resilient to impact. Thus, wheelchairs that have been specified for a given sport give athletes a competitive edge. This project focused on the sport of wheelchair tennis.

(a) Invacare racing wheelchair [5]   (b) RMA's rugby wheelchair[6]

Figure 2.1: Racing and rugby wheelchairs

2.3 Introduction to Wheelchair Tennis

Wheelchair tennis was first showcased, although not competitively, at the 1988 Paralympics in Seoul, South Korea. The first competitive game was played at the 1992 Paralympic Games in Barcelona [7].

Wheelchair tennis is played similarly to a conventional tennis game, with no changes made to the court, net or racquet. The most noticeable change to the game is that the ball can bounce twice before it is classed as out of play, with the second bounce not being required to land within the court of play. This allows for more time to return the ball to the opponent.

A wheelchair tennis player will fit into one the following three classes: men, women or quadriplegic, with the latter being a category for those with quadriplegia, who use a racquet taped to the hand and electric wheelchairs. Like the conventional game, it can be played as a singles or doubles match.

Tennis wheelchair design characteristics can be broken down into four componants, namely driven wheels, castor wheels, a seat and the chassis/space frame. Like other court based wheelchair sports such as basket ball and badminton, the tennis wheelchair usually consists of a light weight chassis and cambered driven wheels aiding in the acceleration and stability pf the wheelchair.

2.3.1 The Rules

As previously stated, the rules of wheelchair tennis are similar to regular tennis, with the main difference being that the ball can bounce twice.[7]. There are, however, eight rules that are specific to the design of the wheelchair in the International Tennis Federation (ITF) 2020 Tennis Rules [8]:

- There are no restrictions on the material the chair can be manufactured from as long as it is not a reflective material and does not hinder the opponent.

- The wheels are only allowed to have one push rim. There can be no changes to the wheelchair that grant the player a mechanical advantage, such as levers or gears.

- Wheels can cause no permanent damage to the court surface.

- The player can only use the push rims or wheels to propel the wheelchair: no steering, braking, gearing or energy storage systems are permitted.

- The Player's buttocks shall remain in contact with the seat during the playing of a point. Strapping may be used to secure the player in the seat.

- The height of the seat must be fixed and cannot be adjusted.

- For players who are unable to move the chair on their own, an electric motor is permitted, but the chair cannot exceed 15km/h (9.3mph) and can only be controlled by the player.

- If any changes to the chair are required, then there is a 60 day period to submit the design to the ITF before the event

Hence, while there are a few rules that could restrict future design, there are no limitations on dimensions or the materials that can be used. The main focus of the rules is on any methods that would provide a substantial advantage to the player's movement. For example, the mechanical advantage rule prohibits the use of any propulsion methods other than push rims. Methods such as the lever propulsion system used by off-road wheelchairs, as can be seen in *Figure 2.3.1* would be off limits. The other rule that could potentially affect the design is the requirement for the player's buttocks to be firmly placed on the chair. This affected the tennis player Stéphane Houdet's bespoke wheelchair (*Figure 2.7*) and requiring a change from the initial saddle design to a more conventional seat.

Figure 2.2: Lever propulsion wheelchair [9]

2.4   Existing Products

This section summarises the tennis wheelchairs that are currently available on the market. Existing wheelchair designs are important to consider before beginning the design process in terms of, practical test data, the materials used, any techniques that are used to manufacture the wheelchair, and anything used to specifically suit the athlete. This section examines the tennis wheelchairs that RMA currently provides for entry-level players and the more advanced wheelchairs used by the majority of intermediate to professional tennis players. Most companies follow this example, that is they sell an entry-level and advanced-level wheelchair, all with a similar base design with the exception of Stéphane Houdet's bespoke wheelchair, which is designed around his style of play and his specific user requirements.

2.4.1   RMA Sport

RMA Sport currently offers two wheelchairs specifically designed for tennis. The first is the Grass-roots wheelchair(*figure 2.3*),which is sold in a range of prefabricated sizes, with two adult (15" and 17" seat widths) [10]and two youth (12" and 14" seat widths) wheelchairs [11]. The space frame is manufactured from steel and designed for players with a maximum weight of 95kg.

The wheelchair has several adjustable components, including the anti-tip wheel height, backrest, and footplate. These can all be changed as the player becomes more experienced.

The second wheelchair, the Elite Pro Tennis Chair is a made-to-measure wheelchair. The frame is manufactured from TIG-welded 7020 aluminium with geometry specific to the player, is set up and finalised using RMA's patented contour body mapping system. The wheelchair has a total mass of 9.6kg. As this wheelchair is more tailored to the user than the grass-roots wheelchair, fewer of the components are adjustable, with the anti-tip wheel and foot rest fixed. Still, there are some areas of adjustability included in order to fine-tune the fit, such as a canvas backrest and an ergonomic cushion on the seat [12].

(a) Adult tennis wheelchair [11]   (b) Basketball wheelchair [12]

Figure 2.3: RMA Sport wheelchairs

2.4.2 RGK

RGK is one of RMA's main competitors in the manufacture of bespoke sport wheelchairs and has 20 years of experience in wheelchair manufacturing [13]. RGK currently has three tennis wheelchairs on the market, namely the Grand Slam, Grand Slam X, and the Grand Slam CX.

The Grand Slam (*Figure 2.4 (a)*) is the company's entry level wheelchair. It has a frame manufactured from 7020 aluminium and additional components such as a knee support made from carbon fibre. This wheelchair weighs just 8.5 kg. To ensure that the chair fits the player, the Grand Slam has a wide range of adjustable options, including the backrest, side guards, anti-tip wheel and axle position. [14] The Grand Slam X and CX (*Figure 2.4 [b]*) are aimed at advanced and professional athletes. Both chairs share RGK's tri-chassis design to distribute the load more evenly throughout the frame by making the chassis wider at the bottom, therefore allowing for better triangulation in the design. Both sport wheelchairs utilise a mixture of materials while keeping 7020 aluminium for much of the frame. However, the axle is manufactured from carbon fibre in both the X and CX. The seat is replaced with a tailored carbon fibre seat in the CX. These design changes reduce the mass of the chair to 7.9kg for the Grand Slam X. and 9.2 kg for the Grand Slam CX, possibly due to the fitted carbon

fibre seat[15]. However, a better-fitting carbon fibre chair leads to improvements in comfort and responsiveness when in play on the tennis court [16].

The Grand Slam is popular with professional British Paralympians Gordon Reid, Alfie Hewett, and Jordanne Whiley, all of whom use a variant of the RGK Grand Slam [17].

(a) RGK Grand Slam [14]   (b) RGK Grand Slam CX [16]

Figure 2.4: RGK wheel chairs

2.4.3   Bromakin

Bromakin has manufactured wheelchairs for over 30 years. Currently, it sells two wheelchairs specifically designed for tennis, namely the Tennis EVO and the Tennis XL. As with the two previous companies, the entry level EVO is fully adjustable. This is achieved using telescopic tubes (*Figure 2.5*) to adjust the position of the anti-tip wheel, while the tubes that connect the seat to the lower part of the chassis are also telescopic, enabling the angle of the seat to be adjusted [18].

The Bromakin XL is also manufactured from 7020 alloy, but; some of the adjustability in the seat has been removed to improve rigidity and reduce the mass of the wheelchair. The adjustability in the anti-tip wheel and the footplate carries through to this design. The foot rest in this design allows for substantial adjustment as it is clamped to the tubes (*figure2.5 [b]*). Rather than customising the chair's geometry, Bromakin instead opts to sell the Tennis XL in a range of seat and wheel sizes, making this chair suitable to be sold to high end tennis clubs and individuals [19].

9
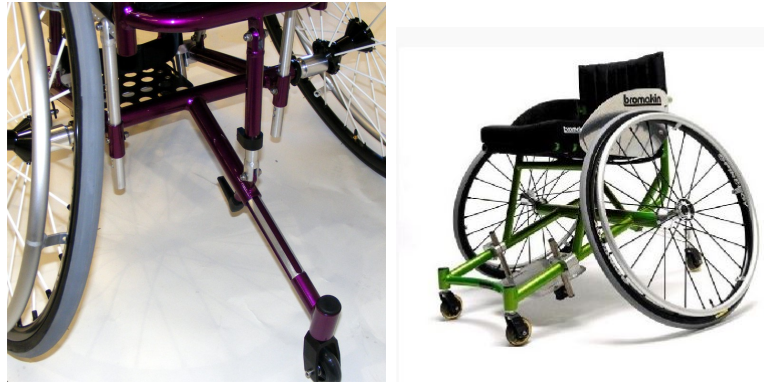
(a) Bromakin EVO adjustable anti-tip wheel[20]

(b) Bromakin tennis XL [20]

Figure 2.5: Bromakin wheelchairs

2.4.4 Invacare

Invacare has been manufacturing wheelchairs since 1885 and focuses mainly on the design and manufacture of day and home care wheelchairs, with a small area of the company dedicated to sports wheelchairs. Unlike its competitors, Invacare only produces one sports wheelchair specifically designed for tennis, the Invacare Top End T-5 7000 series.

The Top End is manufactured from heat-treated 7000 series aluminium and is aimed at professional athletes. The chair provides several opportunities to customise the fit when it is purchased. It is sold with options for different footrests, an adjustable seat, and side guards [21]
.

Invacare also produces a wheelchair that is marketed to both tennis and basketball athletes. It is named the Top End Pro, and while it is similar in design to the T-5 7000, it is available in two frame sizes. It can be easily adjusted to suit the game it is being used for, using quick release locking mechanisms for adjusting the height and angle of the chair (*figure 2.6*) [22].

(a) Top End T5 7000[21]   (b) Invacare Top End Pro[22]

Figure 2.6: Invacare wheelchairs [18]

2.4.5   Stéphane Houdet's Wheelchair

Stéphane Houdet is one of the best professional tennis players in the world, winning over 45 international tournaments and former world number 1 [23]. The bespoke wheelchair that he uses was designed by a team of engineers working with the French wheel manufacturer Cormia [24]. The wheelchair is completely individual to Houdet, taking his specific disability into consideration, as can be seen in *Figure 2.7*. The wheelchair weighs 10 kg. The main chassis of the wheelchair is a carbon fibre monocoque, that supports his amputated leg, which allows Houdet to kneel on his other leg. Due to the position of Houdet's kneeling leg, the majority of this wheelchair's chassis is lower when compared with other tennis wheelchairs, thus providing a lower centre of gravity and allowing the player to turn and reach for the ball more aggressively.

This wheelchair holds the player in an upright playing position, giving him an improved posture, better breath control, and greater reach, resulting in an advantage over other tennis players. The seat is more minimalistic than other designs, which removes any movement restrictions when Houdet leans to reach the ball.

Other features of Houdet's wheelchair are the shock absorbers on the wheelchair steering castors and the anti-tip wheel at the back of the wheelchair. The latter

11

provides a mechanical advantage in that the rear wheel is essentially spring-loaded, which increases Houdet's reach. The wheels on his current chair are manufactured by Corima and they are made from carbon fibre to save on rotational mass, therefore aiding Houdet's acceleration.

(a) Houdet's chair-front [25]   (b) Houdet's chair-rear [26]

Figure 2.7: Stéphane Houdet's wheelchair

2.4.6   Existing products summary

With the exception of Houdet's wheelchair, most tennis wheelchairs seem to follow a similar design philosophy. This includes an aluminium space frame as the chassis, which is then custom-fitted to the player with adjustable or tailored seats, a choice of wheel size, and an adjustable anti-tip wheel.

Houdet's chair is an incredibly bespoke design with its carbon fibre monocoque which is prosthetic-specific and integrates him into the wheelchair; this is a good example of how a wheelchair can provide an advantage on the tennis court.

A few companies have highlighted the importance of a player's fit with their wheelchairs, and all companies offer a level of customisation in their wheelchairs to suit the users' play style. Both RMA Sport and RGK wheelchairs both offer a

fitting service for their customers, allowing them to produce a wheelchair specific to the athlete.

2.5   User Requirements

IN 2018 a journal article was produced for the the international society of wheelchair professionals (ISWP). The article states that user requirements are one of the most critical characteristics to consider when designing a product. Areas such as size, age, postural requirements, propulsion, and changing needs must be examined [27].

As demonstrated in Section2.4(Existing Products), the majority of the sports wheelchair manufacturers offer a wheelchair for adults and younger athletes. RMA offers a youth and an adult club wheelchair as part of their standard wheelchair range. The youth wheelchair has smaller diameter wheels, more aggressive camber, and a smaller seating area compared with the adult club chair.

When optimising the design of the adult's club wheelchair, a good match between the end user and the chair is crucial. The wheelchair must fit athletes of a range of different sizes and shapes; therefore any future designs should aim to fit ranges from the 5th percentile woman to the 95th percentile man [28]. *Figure 2.8* and *Table 2.1* list areas that must be considered during the optimisation and design stages. For example, dimensions B,E,G, and H were considered when designing the seat and foot plate. As *Figure 2.1* indicates the difference between the 5th and 95th percentiles can be significant, thus, some adjustability in the design must be retained.
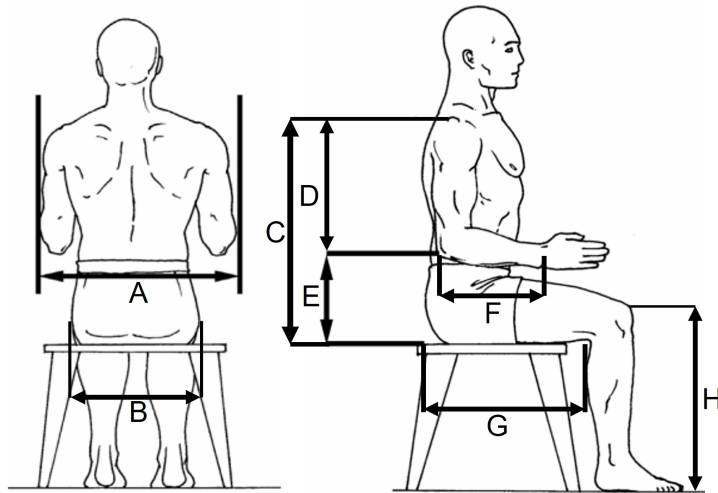
Figure 2.8: Schematic representation of the locations of anthropometric measurements (image modified from[29])

Table 2.1: Anthropometric data: Values to consider in design[29]

	Anthropometric Data Point	5th Percentile Woman (mm)	95th Percentile Man (mm)
A	Forearm-Forearm Breadth	414.7	420.6
B	Hip Breadth	307.8	376.5
C	Shoulder Height, Sitting	509.1	646.3
D	Shoulder-Elbow Length	307.6	398.8
E	Elbow Rest Height, Sitting	175.7	273.7
F	Elbow-Wrist Length	237.8	316.1
G	Buttock-Popliteal Length	440	545.5
H	Knee Height Sitting	474	615.7

The most crucial factor is the players mass. RMA's tennis wheelchair has a maximum user weight of 95 kg [12]. By using a safety factor of 1.5, recommended for use with highly reliable materials where loading and environmental conditions are not severe and weight is an important consideration[30], the player's mass for the initial simulation is 142.5 kg. As the athlete is usually strapped into the wheelchair and lower body movement is restricted, the total mass must be divided for some of the load cases. For example, the upper body is going to have

a larger effect on the Serve. In 2020, a study was conducted to interpret the body configuration of wheelchair athletes [31], where the player's mass was split into three sections; the results are displayed in *Table2.2*, where the court sports results are highlighted. Based on the results of this study, the mass configuration of the player can be broken down into percentages for each of the three componants, namely the arms (15.6%), legs (30.0%) and trunk (53.4%). This yields masses of 3.7, 23.6, and 76.2 kg for the arms, legs, and trunk, respectively. Using these values, the total mass can be split into more specific, localised loads in each load case.

Table 2.2: Fat-free mass and fat mass in various sports for three compartments[31]

Group	Number Of Participants	Fat-free mass (kg)			Fat Mass (kg)		
		Arms	Legs	Trunk	Arms	Legs	Trunk
Paracycling	11	7.8 ± 2.0	10.1 ± 4.2	22.6 ± 3.4	1.4 ± 0.8	5.0 ± 2.8	5.2 ± 3.4
Rugby	14	7.0 ± 1.6	14.1 ± 4.1	25.7 ± 5.5	1.9 ± 1.2	5.8 ± 2.9	8.0 ± 5.2
Basketball	6	9.0 ± 1.0	13.1 ± 5.5	27.6 ± 4.4	1.7 ± 0.9	4.9 ± 1.9	7.4 ± 4.7
Athletics	13	6.6 ± 2.4	6.9 ±3.8	20.5 ± 6.2	1.8 ± 0.8	5.4 ± 2.4	5.8 ± 2.4
Curling	6	7.6 ± 1.5	10.4 ± 2.8	26.0 ± 3.3	2.9 ± 0.9	8.7 ± 2.4	12.7 ± 3.8
Court Sports	8	6.3 ± 1.4	10.4 ± 3.9	22.4 ± 5.0	2.5 ± 0.9	7.1 ± 3.8	7.8 ± 4.8
Others	10	7.2 ± 2.0	10.5 ± 5.3	24.7 ± 5.3	2.2 ± 1.0	6.5 ± 2.8	7.8 ± 3.5
Total	69	7.2 ± 1.9	10.7 ± 4.8	23.9 ± 5.3	2.0 ± 1.1	6.0 ± 2.9	7.5 ± 4.4

2.5.1   Components

As already stated, a sports wheelchair can be broken down into four main components: the chassis, driven wheels, castors, and seat (*Figure 2.9*). As this project focused on optimising the chassis, into which the seat is integrated into the chassis, the wheels needed to be purchased parts, and must fit any of the chassis designs.

Figure 2.9: Tennis wheelchair components

The high-end wheelchairs at RMA are supplied with wheels by Spinergy, a company that specialises in making high quality wheels for both the bicycle and wheelchair industry[32]. Spinergy, offer four standard diameters: 24", 25", 26", and 700C [33]. Spinergy wheels are held to the wheelchair chassis using a quick-release axle (*Figure2.10*) that passes through the hub into a boss that can be welded or threaded into the wheelchair space frame. Any future designs will need to allow for the same fitting process if they are designed around the same wheel set as the current offering.

(a) Spinergy Sport Lite extreme   (b) Spinergy quick-release axel [34]
wheels [33]

Figure 2.10: Spinergy wheel and axel

As noted in Section 2.4(Existing Products), the two steering wheels and the anti-tip wheel(s) use castors. The castors used on RMAs club wheelchairs are

depicted in *Figure2.11.*They consist of a 72 mm rubber wheel held in place by anodised aluminium forks, connected to a M12 threaded shaft that is held in place with two sealed bearings housed in the frame (*figure 2.11(b)*). Any future designs must consider this.
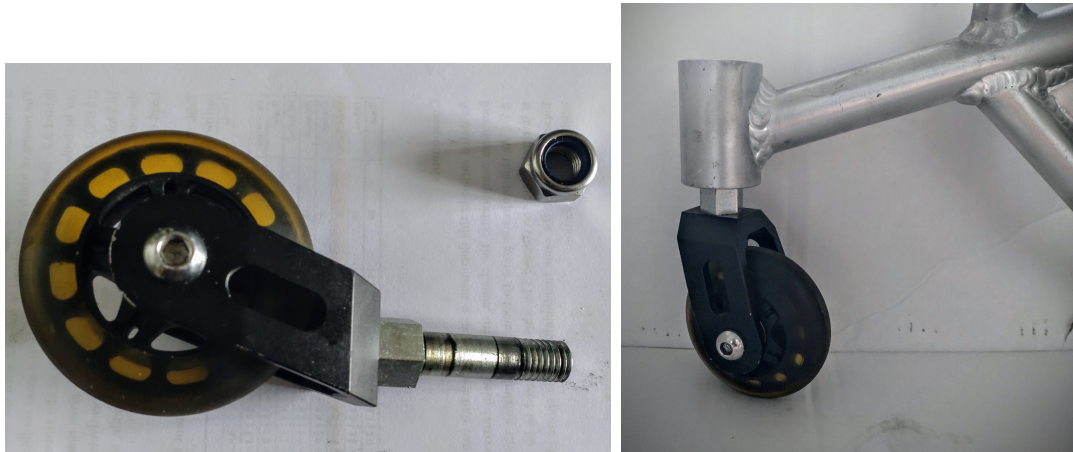
(a) Front castor   (b) Front castor assembled

Figure 2.11: Castor from an RMA Sport wheelchair

Although not currently used in wheelchair tennis, a potential option could be the Frog Legs Phase-One castor [35] (*Figure 2.12*). This frog leg castor is currently used in other wheelchair sports such as wheelchair chair motocross (WCMX) and skate wheelchairs. The rubber section of the caster helps to cushion any harsh impacts that the wheelchair and user may encounter when landing tricks. In the case of wheelchair tennis, the intention is to increase the reach of the player during the game. For example, the sprung castor gives Houdet an advantage with his playing style.

(a) Frog legs phase 1 castor[35] (b) RMA WCMX Wheelcahir using frog
legs castors [36]

Figure 2.12: Frog legs phase 1 castor and WCMX wheelchair

For this project, the chassis was chosen for two reasons: first, the chassis is the component of the wheelchair that is controlled by RMA from fabrication to assembly, whereas the other components discussed in this section are purchased parts and assembled on site. Second, optimising the frame allows the same level of customisation in components for the athletes as with the standard RMA tennis wheelchair, with the exception of the driven wheels. This might lead to the greatest improvement in the wheelchair design where mass and stiffness are the main design goals.

2.5.2 Cost

Considering the cost of sporting equipment is essential, as it can limit access to a sport at entry level. However, as the player advances in their sporting career, they may be willing to pay more for better performance, such as lighter materials, custom geometry, or more efficient components. This is evident from the difference in price between an entry-level wheelchair, like the RGK entry-level chair, costing £1548 [37], and the Grandslam, which costs £3609 [38]. The average mark-up on sporting goods is 40 per cent [39] suggesting the RGK sports wheelchairs cost £1105 for the entry wheelchair and £2577 for the Grandslam to produce.

It was an important consideration in the design process as this can provide

limitations on manufacturing methods and materials used. Two improved designs have been proposed, one that used RMA's established manufacturing methods optimising their current wheelchair. Improving the design without increasing the cost to the consumer. The second design looked to target the upper end of the market focusing on smaller batches and using different materials and manufacturing techniques that may increase the cost of the final design.

2.6 Environmental Considerations

As the wheelchair in this project was specifically designed for tennis, the main environmental areas to consider were the tennis court, any factors that would affect the wheelchair during a game of wheelchair tennis, and transportation.

As stated in the rules presented earlier in this chapter, the wheelchair can not cause any damage to the court. This rule mainly applies to the contact points (castors and driven wheels), which are purchased components; however to avoid damage in a crash as well as damage to the player during everyday use, the wheelchair also cannot have any sharp edges.

As with most court based wheelchair sports, the camber of the wheels is more aggressive than that of a standard day chair. Due to the camber, the footprint of the wheelchair can be quite large, making it difficult to transport. To solve this problem the driven wheels are easily removable using a quick-release axle that locks to a fixed point on the wheelchair frame (*figure 2.10(b)*). It is important for any future designs to consider this to avoid reducing functionality.

To optimise the wheelchair, the effect that the environment has on it must be considered. During a game of wheelchair tennis, the forces exerted on a wheelchair can be broken down into six different areas, as depicted in *Figure 2.13*. This figure outlines the interaction between the wheelchair configuration and wheeling performance in wheelchair tennis [40].
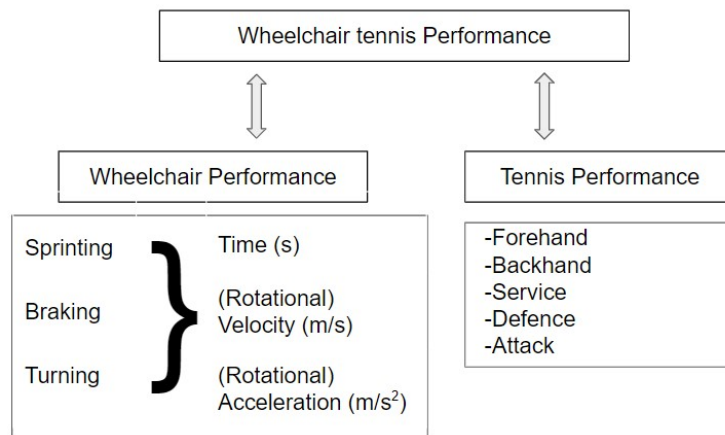
Figure 2.13: Conceptual model of wheelchair tennis performance (adapted from [40])

Forehand, backhand and service can be treated as though the wheelchair is in a fixed position and broken down into two load cases namely load-up and follow-through. Each of the load cases applies the load to a different areas of the wheelchair. Defence and attack are classified as the athlete's game plan strategy, which usually refers to the player's position on the court,(*Figure 2.14*). A more aggressive strategy positioned closer to the net. In both cases, the strategy for most wheelchair tennis athletes is to cover the width following a figure of eight. This load case can be broken down into three movements, namely acceleration, braking, and turning.
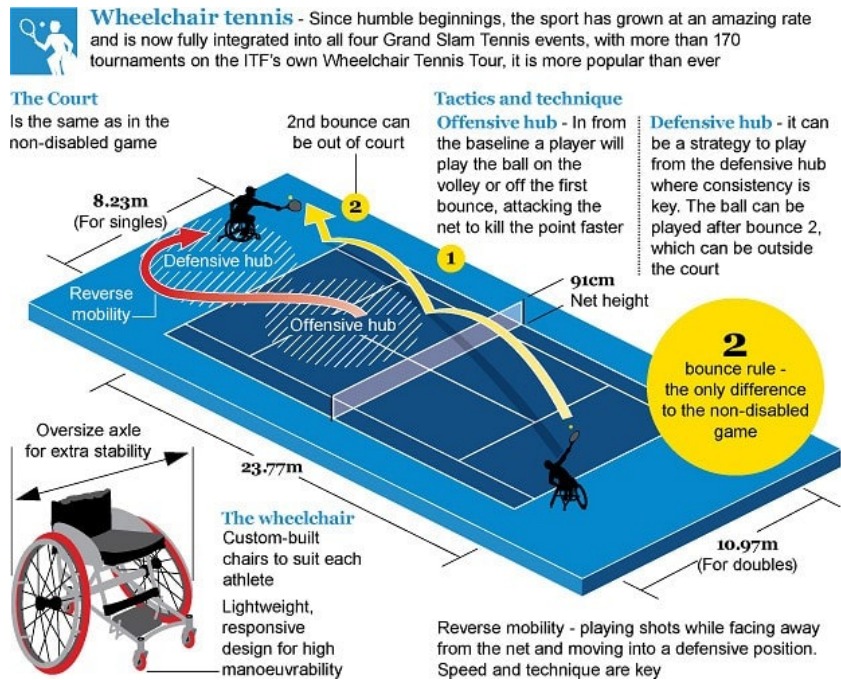
Figure 2.14: Wheelchair tennis movement [41]

The final aspect to be considered in this section is the impact that the wheelchair will have on the environment throughout its lifespan. It is essential to take into account the entire life cycle of the product and its effect on the environment. This can be achieved by utilising sustainable materials and manufacturing techniques during the design phase. Additionally, it is important to consider what will happen to the wheelchair at the end of its useful life. Can all the materials be recycled or re purposed once the user is done with it? These questions are crucial in ensuring that the wheelchair has minimal impact on the environment.

2.7 Manufacturing

There are two main options for designing and manufacturing a light weight chassis: (1) a more traditional approach with a space frame, which is used for the majority of sports wheelchairs; or (2) a monocoque chassis design, which is commonly used in motor sport and high end composite bicycles. Uniquely seen in Houdet's wheelchair. The choice of manufacturing technique is an important consideration for the PDS, in which any potential limitations for that will affect the design.

2.7.1 Welded Space Frame

It is important to consider any manufacturing limitations or capabilities that may influence the design. As discussed in Section 2.4 (Existing Products), a majority of chassis in sports chairs are aluminium space frames welded by hand, using adjustable jigs (*Figure 2.15*). This manufacturing method is quite common, and it is also used in other industries due to its many benefits such as automotive, sporting equipment, and construction. It is relatively in-expensive, simpler in design, light-weight, quick to assemble and adjustable [42]. However, there are several limitations when manufacturing the frame in this way: limited material choice (steel, aluminium, and titanium are common choices), the need for skilled labour, and potential build up of residual stress due to heat.

Figure 2.15 depicts the manufacturing method currently used by RMA. The tubes are welded by hand, with a mixture of fixturing and clamps holding the tubes in welding. To limit the impact on RMA's set-up, thus reducing the need for investment in new equipment, facilities, or specialist skills, one of the optimised designs made use of the current manufacturing set up.

Figure 2.15: RMA factory in Bridgend, UK[3]

2.7.2 Lug Space Frame

Another commonly used assembly method for space frames involves the use of traditionally machined or cast lugs where the tubes meet. Lugged space frame construction is used in a variety of industries, such as construction (scaffolding) and more traditional bike frames (see *Figure2.16*). The tube sections are permanently bonded to the lugs through the use of an adhesive or welding. In the case of scaffolding the tubes are held into the lugs using grub screws.

Manufacturing a space frame in this way has several benefits. First, the frame can be assembled quickly and easily with no need for a specialist, as with the welded and monocoque designs [43]; second, the choice of materials is not as limited as that for a welded space frame; and lastly, depending on the nature of the joint, materials can be mixed to obtain the desired properties. However, there are some disadvantages to building a space frame in this way; for example,

as there is extra material around each of the joints, the frame can be heavier than when a full composite frame is made. The lugs are commonly machined or cast, which can be a time consuming and costly manufacturing method in smaller batch sizes.

Figure 2.16: The 2003 Look KG381 road bike frame uses carbon tubes bonded to aluminium lugs

In recent years, AM has been used in high end, bespoke sports equipment. For example in the cycling industry, companies such as Bastion Cycles [44] and Atherton Bikes [45] manufacture road bicycles and downhill mountain bikes that are used in World Cup competitions. The main selling point of both the Atherton and Bastion bikes is their use of additive layer manufacturing (ALM) process to provide custom geometry for customers and athletes through printing the connecting points of the frame and connecting the lugs using carbon fibre tubes. This service is not currently offered by their competitors.

In 2014 Renishaw printed a full mountain bike frame out of titanium alloy [46] for a case study, before before using topology optimisation to improve the seat clamp. Due to the size of a bike frame and limitations on build size, the frame was split into three parts and assembled after building.

The ALM process also allows for greater design freedom with the ability to create near net shapes without the consideration of machining restrictions or casting. This process also works well when the parts are combined with topology optimisation to produce parts with a good strength-weight ratio. Once all parts have been printed and machined to the required tolerance, they should be easy

to assemble, which should reduce the manufacturing time.

(a) Bastion demon road bike [44]   (b) Renishaw Printed Mountain Bike [46]

Figure 2.17: Bikes manufactured using ALM

ALM is a form of 3D printing, that slices a 3D CAD model into layers, allows the model to be built up layer by layer until the final part has been manufactured. Many ALM methods exist, such as binder jetting, a technique that combines the metal powder with a liquid binder, to build the part layer by layer, and it requires post-processing to improve mechanical properties. Sheet lamination, which builds the part by combining each layer by brazing or using a binder, is not suitable for structural applications. Laser bed sintering constructs the part layer by layer. Once the layer of powder has been deposited, a high-power laser traces the pattern on that layer before a wiper blade pulls across and another layer of powder is deposited; then, process is repeated until the part is completed.

For this project laser bed sintering was chosen due to the machine availability and it provides parts that are quick to manufacture and that can be used almost immediately [47].
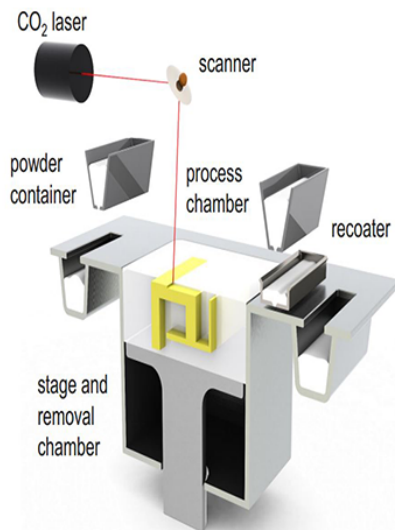
Figure 2.18: Selective laser sintering [48]

Due to the complex shapes of the modular design, the short time scale for manufacture, and the ability to customise each build, it was decided to use an additive manufacturing method to construct this wheelchair design. Using laser bed sintering provides the best mechanical properties for a printed part, giving similar material properties to those provided if the part were manufactured using more conventional methods.

The benefits of using a printing manufacturing process for the wheelchair build are the relatively short manufacturing time and low cost in the prototyping stage of design and also eliminates the need to produce moulds if the parts are cast, and reduces material waste if similar parts are machined.

2.7.3   Composite Monocoque

In section 2.4 (Existing Products), Stéphane Houdet's wheelchair (*Figure 5.7*)was the most unique tennis wheelchair, with its carbon fibre monocoque construction. Manufacturing chassis in this way is common in motor sport, boat hulls, racing drones and high end sporting equipment such as bicycle frames. How ever this method can be time consuming and initially labour intensive as the mould is one of the most important factors.

2.8 Optimisation Techniques

As stated in the previous section one of the most popular structures in similar sporting goods is a space frame. Improving the performance of a space frame can lead to a problem with a large amount of variables. This section aims to highlight different optimisation methods applied to truss structures in different industries.

Structural optimisation involves finding the best possible design (objective), by changing specified design variables based on certain constraints. This process can be applied to reducing mass, increasing stiffness, or improving the strength of the structure. Structural optimisation can be classified into three different categories namely sizing, shape, and topology. Sizing permits the dimensions and thickness to be changed while the connectivity of the design domain remains unchanged. Shape optimisation allows for the surface of a shape to be adjusted, while topology optimisation strives to optimise the substructure[49].

As demonstrated in Section 2.4, with the exception of Houdet's wheelchair, the most popular sport wheelchairs on the market use a space frame structure for the chassis. The space frame is one of the most popular structures because it can be constructed quickly at a low cost and is strong and light [50]. For these reasons, it is employed in a wide range of industries, such as construction, automotive, aerospace, and sporting goods (e.g. bicycles and wheelchairs).

Due to the popularity of space frame structures, there has been much research has been conducted on the optimisation the design process for space frames. The majority of research aimed to use genetic algorithms and particle swarm techniques to improve the design. Optimising the design in this way provides many benefits, including saving design time in the more conventional iterative design process, automating the design process and achieving a lighter structure and thus a lighter design[51].

There are many different optimisation approaches, each with their strengths and weaknesses. Methods such as the Nelder-Mead Downhill Simplex [52], gradient-based methods [53] and algorithms based on Newton's method are relatively easy to implement, but require multiple function evaluations per iteration and

are prone to converging on local minima. For challenging optimisation problems with many design variables, more complex algorithms are available which are more suited to finding global optimums. Two example of these are genetic algorithms (GA) and particle swarm optimisation (PSO).

2.8.1 Genetic Algorithms

A GA is an optimisation technique used to identify the best solution to a problem with a wide range of potential answers. The algorithm mimics biological evolution, as proposed by J.H.Holland in 1992[54].The genetic algorithm loop consists of six stages.

1.Initialisation- Random solutions are generated based on the variables provided; these points can be classified as the parent solutions in the initial stage.

2.Crossover-The parents are selected and paired at random, and certain variables are switched in the two solutions to create two new potential solutions.*Table 2.3* Depicts an example of a binary problem. The crossover technique swaps the last two variables (blue) to create two new off spring solutions

3.Mutation- To encourage the exploration of potential results, variables are selected at random and swapped with another solution, thus increasing the number of results (*Table 2.3* green).

4.Merge-The crossover and mutated solutions are then added to the range of solutions generated in the initialisation stage.

5.Evaluate-All potential solutions are evaluated against the required criteria and assigned a fitness value [54]. Any solutions with a low fitness value are removed from the space. In the problem shown in *Table 2.3*, for example, the desired goal was to obtain a solution contains only ones a value; therefore, the solutions with the most ones were assigned the largest fitness value while the bottom three solutions were removed (highlighted in red), before repeating the cycle with the new parent solutions

6.Repeat-Steps 2-5 can then be repeated through multiple generations of so-

lutions, until a suitable answer is reached.

Table 2.3: Example of crossover and mutation solution generation for a binary problem

		Variables				
Initialisation	Parent 1	1	0	1	0	0
	Parent 2	1	1	0	1	1
Crossover (Single)	Offspring 1	1	0	1	1	1
	Offspring 2	1	1	0	0	0
Mutation	Offspring 3	1	0	1	1	0
	Offspring 4	1	1	1	1	0
Merge & Evaluate	Offspring 4	1	1	1	1	0
	Parent 2	1	1	0	1	1
	Offspring 1	1	0	1	1	1
	Offspring 3	1	0	1	1	0
	Offspring 2	1	1	0	0	0
	Parent 1	1	0	1	0	0

This technique has been used to aid in the optimisation of frames, as there may be a numerous potential variables and solutions based on the design criteria.

For example, in 2013, a two-phase GA was used to identify the optimum cross-sectional area of each of the tubes in a space frame roof structure in Ottawa[55]. The structure was created using more traditional optimisation methods. By splitting the large-scale structure into different regions based on the loads that affect each region and then picking a uniform beam for each region, we saved design time and made the construction easier by introducing regularity.

The study's goal was to identify whether any mass could be saved in the structure by swapping the beams with readily available materials identified in the AISC Steel Construction Manual, which provides 1,092 potential beams for

29

the 288 members that comprise the train station structure; thus, there could be over 300,000 potential design solutions. Due to the number of variables in this design, the computational time would be significant even with the use of geometric algorithms. In this study, optimisation was performed in two stages to improve the efficiency of the process and reach the optimum solution sooner. As with the conventional design method, the structure was split into different regions. The first stage of the optimisation started with 50 design solutions, which were put through the optimiser to produce the offspring and rated against the design criteria, before being run through the GA optimiser. After each round of evolution, any overstressed members in the surviving solutions were identified, assigned to their own region, and removed from the current region so as not to affect other members, This process was repeated until the required goal was met.

The second phase started with the design generated in the first phase and aimed to optimise the previously identified overstressed members. The wall thickness of each overstressed member was incrementally increased until the design criteria were met. Optimising the design in this way led to a 13% weight reduction in the first structure and an 8% reduction in the second structure, with an optimisation time of 10 hours for the first structure and one of approximately 4 hours for the second.

This optimiser was further elaborated in 2013 [54], by adding more variables to the optimisation process, thus improving the structure as well as the beam cross-sections. The same initial process was followed by splitting the roof structure into more manageable sections and keeping the initial simulation the same. In this paper, each member was assigned a binary value, with 1 keeping the member and 0 removing the member from that solution as a topology element of the optimiser. Further variables were added to control the length of each member for shape optimisation. As in the previous paper, the initial step of the optimiser was used to produce a global solution. Subsequently, any overstressed members at each iteration were identified, and the design was fine-tuned in the second stage of the optimisation.

Optimising the structure in this way led to a 22% and 24% mass reduction in examples 1 and 2 respectively, for a significant weight saving over the conventional design and a good improvement on the initial optimisation.

2.8.2 Particle Swarm Optimisation

Partical Swarm Optimisation (PSO) is another potential optimiser suited to problems with multiple potential solutions. As with GAs, a population of solutions is generated and fills a space of potential design solutions known as particles. Using a mixture of inertia, past experience, and social influence, the particles move towards the optimum solution after each iteration [56], with each design solution compared with the current and previous results to identify each particle's best design solution (past experience) and the best particle found thus far (social influence). This data, combined with the random velocity and direction of the particle, are used to calculate the particle's next position. For the solution space to be explored effectively, the amount of influence that each of these factors has on the particle movement in each iteration must be determined. More weight is given to the initial movement (α) and personal best (β) of each particle (*Figure2.19*) in the initial stages of the optimisation to encourage exploration. In later iterations the influence of the global best (γ) is increased, which encourages the participants to converge on a single solution.
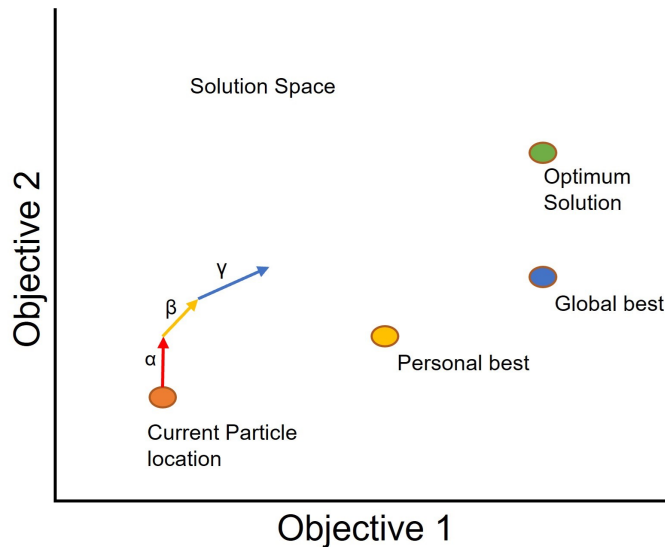
Figure 2.19: Particle movement in PSO

A hybrid version of the PSO method was used to reduce the mass of a range of truss structures in a study by Shahid Bahonar in 2021 [57]. The author sought to optimise structures built from 10,25,72, and 120 bar truss structures, with the geometry becoming increasingly complex with the addition of more members. Variants of the PSO method altered the cross sectional area of each member to

reduce the mass of the overall structure while applying a limit to the maximum displacement of the structure. For each case the mass of the structures were reduced; however, as the number of variables increased, the PSO needed to be modified to ensure greater exploration of the design space.

2.8.3 Design of Experiments

Optimising the space frame leads to a problem with multiple potential variables such as tube thickness, length and diameter. An effective strategy for organising a multiple variable problem is to use a design of experiment (DOE) method.

DoE uses the extremes of each controlled variable to create a design space that can be populated with potential outcomes. Each dimension of the space is assigned one variable of the design space to set limits (*Figure 2.20*). By gathering results from each corner of the design space (extremes),the results of these experiments can be used to improve knowledge on how each variable affects the outcome. The number of sampling points in the DoE is strongly dependent on the number of design variables, d, and the number of levels sampled for each variable, L. For a full factorial DoE, the number of sampling points, $N=L^d$. For engineering problems with a large number of design variables, it is essential to use a stratified sampling approach such as orthogonal or Latin Hypercube sampling. The Latin Hypercube method splits each design variable into a number of levels equal to the total number of sampling points. Each design point occupies a unique level for each design variable. The Latin Hypercube method can produce an uneven spread of sampling but this is minimised by using an Optimum Latin Hypercube, where the sampling points are moved to produce a more even spread across all dimensions. Producing an Optimum Latin Hypercube DoE is an optimisation process in itself and research has been done to make this process as efficient as possible [58]

Once the design space has been fully defined. The space can be populated by altering each variable at specified intervals, and then the experiment can be run. Generating results at specified intervals for each variable.
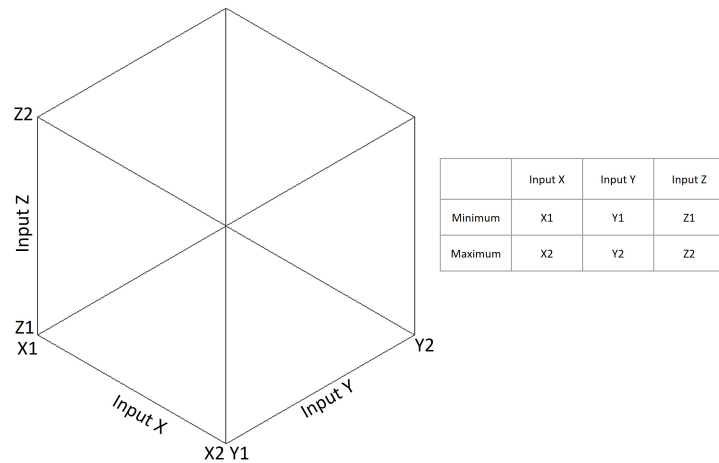
Figure 2.20: Design space generated using DOE Methodology

Once a suitable sample of design points has been identified and run, results for the DoE can be used to define a mathematical model of how the responses are influenced by each design variable. If this metamodel is sufficiently accurate, then it can be used to drive an optimisation algorithm without having to run each design point, whether it is an experiment or a simulation. This can increase the time required to optimise engineering problems with either large numbers of design variables or long-running simulations.

2.8.4 Topology optimisation

Topology optimisation is a useful tool and has design the target of minimising the mass of the designed components under set boundary conditions. There are a few key points to consider when using topology optimisation to improve parts. The process starts with the CAD model of the initial part and with the boundary conditions set. Then, using finite element analysis (FEA) is used to identify areas of stress within the component; thus, the topology optimisation process identifies the areas that do not contribute to supporting the stresses in the part. Furthermore, the material is removed to reduce the mass of the overall part (*Figure 2.8.4*).

Benefits of optimising parts in this way include the mass reduction of the part. Using the powder bed fusion process also allows for a reduction in waste material, reducing the amount of practical testing and creating a lightweight part

that enhances the performance of the final product[59].
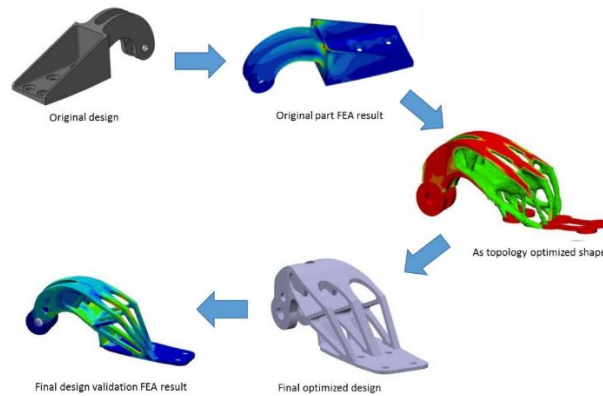
Figure 2.21: Topology optimisation process [59]

AM methods have previously been combined with topology optimisation techniques for aerospace components. Altair conducted a case study [59] to optimise a nacelle hinge bracket from an A320 (*Figure 2.8.4*) and succeeded in reducing the mass of the original part from 918g to 326g. This produced a part with more evenly distributed stresses, resulting in a more efficient use of the material in the hinge.

Topology optimisation techniques have also been used in the cycling industry, including by SRAM for developing new pedal cranks (*Figure2.22*). They created the first prototype using AM techniques as a way to save weight and stay ahead of their competitors with a mass reduction of 20%. [60].

When using topology optimisation for AM, there are several limitations and areas to consider. For example, when building the part, it is crucial for there to be no over hangs greater than 45 degrees, as any unsupported overhangs could cause the part to fail during manufacturing. This problem can be resolved to a certain degree after the optimisation process by adjusting the orientation of the part on the build plate and adding supports [61].

Figure 2.22: Topology and AM examples [60]

2.8.5 Optimisation Summary

In this section, various design optimisation techniques for different structures were analysed. The examples demonstrate that the exploratory techniques are effective in examining optimization problems with multiple variables and multiple possible design solutions. To achieve the desired design targets, variation techniques were utilised for the optimisation of the RMA's current design, which had several variables. In the case of the modular design, topology optimisation was employed to enhance the connecting points of the frame.

2.9 Testing

It is important to test the sporting equipment that will be used by any athlete to be certain that it is fit for purpose. To ensure that future designs will meet or exceed the current design specifications, it was necessary to determine how current tennis wheelchairs perform during a game, thereby setting the bar for future designs.

Wheelchair testing helps to identify the movements that occur during a game and to highlight areas of the design related to spatial awareness of the player's game. The design choices should not cause obstruction by impending the players movement or decrease efficiency. The mechanical data provided illustrated how movements can affect the wheelchair by highlighting potential load cases.

The collected data were then used to validate the finite element model of the

wheelchair at later stages in the design process, thus ensuring that the model was an accurate representation before it was used to optimise the current design.

The testing of sports equipment is essential for improving the equipments performance. For all sports equipment, there are three testing areas to consider-namely subjective, bio-mechanical, and mechanical testing[62]. As indicated in the diagram in*Figure 2.23*, the data provided by these three different testing methods ranges from qualitative data gained from human experience to full quantitative data provided by mechanical testing with the aid of technology.
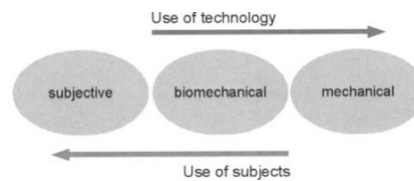
Figure 2.23: Testing methods in the development of sports equipment[62]

Subjective testing focuses on user evaluation and personal experience using the sports equipment and can vary from player to player. This testing and feedback loop is useful when the target goal is to ensure that the product is comfortable and fit for purpose according to the specifics of the athlete's needs. For example, for sports clothing [62] , there are many subjective factors to consider, such as fit, restrictiveness, and aesthetics. Ultimately the product will be a failure if the end user does not like it. Subjective feedback is useful in wheelchair testing as the wheelchair must meet the same subjective criteria as sports clothing; that is it needs to fit, not restrict movement, and be aesthetically pleasing. Subjective feedback is useful throughout the design process from idea generation to final concept, prototyping, and product testing as it ensures an iterative design process and an end product that will suit the final user.
For example, with a bespoke one off product like Houdet's wheelchair (Section 2.4: Existing products), which has been specifically designed around his play style and injury, with a fixed prosthetic used to secure him to the chair, there would have been a requirement for subjective testing throughout the design and prototyping phases. This would ensure that the end product was comfortable and fit for purpose.

Biomechanics lies in the middle of the three testing areas (*Figure2.23*), as it

considers the athlete and the sports equipment as one system; thus both quantitative and qualitative data are collected through practical testing. This is important, because a well-designed product from an engineering perspective can still fail if it integrates poorly with the end user. For example, a desirable trait for a running shoe would be a stiff sole to reduce losses when pushing from the ground; however, as excessive stiffness could injure the user's bones and muscles, the sole's stiffness would be reduced [63].

This approach can also be related to sports wheelchairs. Analysing the player's movements during a game of wheelchair tennis and noting how the player moves, can be achieved at a basic level by using camera footage to observe the movement. It could also be achieved using a motion capture system such as Vicon, where reflective markers are placed on key areas of the athlete and then paired with infrared cameras that map their movement, collecting a wide range of variables.

Finally, mechanical testing ensures that the newly designed product will be fit for purpose from an engineering point of view, ensuring the equipment can endure the loads that will be required of it not only during a match but also during the product's lifetime. For example,the RMA sports testing set-up described in *section2.9.1* uses a rolling road to ensure that the product is fit for purpose. Further engineering data can be acquired by strain gauging the equipment to understand the load cases, after which the product can be optimised. Based on these data, the design can be altered to suit a required design outcome.

2.9.1   RMA's Testing Procedure

RMA Sport currently test its new wheelchair and component designs in-house, using the set-up displayed in *Figure 2.24*. A rolling road consisting of two rollers with an uneven surface, supporting the driven wheels and castor wheels. A mass (150kg) is then strapped to the wheelchair and held down for 800,000 cycles (approximately 420 miles) [64]. This provides an accelerated lifetime test of the chair to ensure that the wheelchair and any of the chosen components can withstand the loads and are durable through the life span of the product[64].

Before this set-up was used RMA sent their wheelchairs to the TUV (Technical Inspection Association, translated from German) test facility in the Netherlands [65]. The testing facility performed a range of tests on the sports wheelchair to

ensure it met the design standards ISO 7176 and EN-12183 [66] which applied to manual wheelchairs as defined by regulations set in European Medical Device Directive 93/42/EEC (MDD) [67]. Although these standards do not apply to sports wheelchairs, they do suggest the minimum standard a wheelchair needs to meet. However, the RMA test method far exceeds the testing recommended in this standard. As the standard recommends testing the wheelchair for only 20,000 cycles.

Figure 2.24: RMA Sports rolling road[64]

2.10 Literature review summary

The aim of this chapter was to provide any information that went on to influence decisions made in this project. Initially giving an overview of wheelchair sports, with a focus on wheelchair tennis. The next step was to analyse other wheelchairs on the market, looking at materials and manufacturing techniques used by RMA's competitors. Thirdly, Areas that might influence the design of the wheelchair where highlighted including the user requirements, environmental factors and components that influenced the designs. The optimisation section of this chapter highlighted different optimisation techniques used to improve struc-

tures from different engineering sectors.

The final section then highlighted the importance of athlete feedback in the design and testing process as well as the testing methods RMA currently use for all of there sports wheelchairs before releasing to market.

The information gathered in this chapter has influenced a set of design goals that have been summarised in a PDS in the next chapter.

Chapter 3

Product Design Specification

An important part of the design process is the setting of a PDS, which provides a clear set of goals for future designs to be compared against. *Table3.1* summarises Information gathered in the areas discussed in Chapter 2 (Literature review). Information is taken from areas highlighted by a document produced by Pittsburgh University in 2018 [27]. With the aid of the International Society of Wheelchair Professionals (ISWP), said document aims to highlight key influences to consider when designing a wheelchair, including the needs of the user, environmental considerations and ergonomic considerations.

Table 3.1 presents a summary of the design considerations and targets collected in the previous chapter, as criteria for judging future designs. Each requirement is assigned a number (1=primary, 2=secondary and 3=tertiary) to indicate the importance of the goal and to the impact on the final design.

This project focused on two designs. The first can be manufactured with minimal changes to RMA's current manufacturing set-up by optimising the current wheelchair design. The second, which utilises ALM, is a modular wheelchair that allows for a greater range of adjustability and more bespoke designs.

Table 3.1: Product Design Specification

No.	Requirement	Class	Acceptance Criteria for a Pass	Source	Comments
1	Design Target				
1.1	Reduce mass	1	Wheelchair to be sub 9.6kg	2.4.1	Reducing the wheelchair mass improves acceleration performance . 9.5Kg is the mass of RMA's current wheelchair
1.2	Increase stiffness	2	Any future designs should not exceed 10% of the maximum displacement when under load, using the current wheelchair as the benchmark		Maintaining or improving stiffness will improve the efficiency of the wheelchair,
2	User requirement				
2.1	Fit a range of body shapes	2	Seat Width 307.8mm-376.5mm Seat Length 440mm-545.5 mm Knee Height 474mm-615.7mm Elbow Rest Height 175.7mm-273.7mm	2.5	Dimensions to fit 5th percentile woman to 95th percentile man. can be achieved through adjustability or custom design
3	Componants				

Table 3.1 continued from previous page

No.	Requirement	Class	Acceptance Criteria for a Pass	Source	Comments
3.1	Quick release driven wheels	2	Frame design must have attachment points for quick release hubs, either using a threaded boss or direct mount	2.5.1	Boss must be compatible with Spinergy quick-release axles and fit Spinergy wheels with 24", 25", and 26" diameters.
3.2	Castors	2	Have space to fit bearings for the M12 threaded bar on the castor	2.5.1	Must allow the wheelchair to turn on the spot, whilst supporting the wheelchair
3.3	Seat	1	Hold athletes in place securely based on dimensions stated in target 2.1	2.5.1	Also, comply with ITF rules, The seat must be fixed and cannot be adjusted and player must remain in contact with a chair ??
4	Environmental Considerations				
4.1	Cannot cause damage to court	1	No sharp edges in the design	2.3.1	Prevents damage to court and player
4.2	Distractions to other players	1	No reflective materials used	2.3.1	Any reflective materials can be considered distractions
4.3	Tight turning circle	1	A wheelchair can turn 180 degrees within a diameter of 1000mm.	2.6	Enables agile movement on the court with a turning radius of 1000mm as per EN12183 [66].

Table 3.1 continued from previous page

No.	Requirement	Class	Acceptance Criteria for a Pass	Source	Comments
4.4	Removable wheels	2	Fit quick release hubs	2.5.1	Allow for threaded boss to be fitted after frame has been assembled or manufacture into the frame
5	Load Cases				
5.1	Serve	1	Split into two load cases: load up and follow through. Wheelchair must support this yield during this movement	2.6	During the lead-up phase, the player's mass is shifted to the rear of the wheelchair, and during the follow-through, it is quickly transferred to the front of the wheelchair
5.2	Acceleration and turning	1	Wheelchair can not deform or fail under load	2.6	The load case will include accelerating in a straight line and turning on the court. Important areas to consider for this load case
5.3	Forehand and Back hand	1	Proposed designs can not deform or fail under load	2.6	Occurs when the player reaches for the ball. Applying a load to one side of the chair
5.4	Impact	3	Wheelchair can not deform or fail under load	2.6	Chair can deform after crash but more beneficial if it survives impact
6	Manufacturing				

Table 3.1 continued from previous page

No.	Requirement	Class	Acceptance Criteria for a Pass	Source	Comments
6.1	Cost	2	Wheelchair to be competitive with other wheelchairs that are on the market	2.5.2	A wheelchair can be produced for around £1600 at an entry-level and £2600 for an elite level, and both designs must justify the expense while taking prices into account.
6.2	Availability	2	Utilise available manufacturing techniques	2.7	RMA Sport should have access to all manufacturing methods, whether they are in-house or sub-contracted.
6.3	Design and manufacturing time scale	2	Wheelchair must be designed and manufactured within 4 to 6 weeks	2.7	RMA's current lead time is 4 to 6 week manufacturing lead time [68]. so the designs must use readily available manufacturing techniques that allow for changes to be made to the geometry without adding to this time.

Table 3.1 continued from previous page

No.	Requirement	Class	Acceptance Criteria for a Pass	Source	Comments
6.4	Large-scale production	2	Designs suitable to manufacture in larger batches. Using RMA's current facilities.	2.7	Machine shop set up for welded aluminium space frame chassis. Using fixed jigs for the standard sizes that can be used to speed up production using RMA's current facilities, Producing the wheelchairs in larger quantities can contribute to the cost of a single unit.
6.5	Small batch, bespoke	2	Design to allow for simple adjustments. to create one-off bespoke wheelchairs designed around specific athletes.	2.7	Potential for additive manufacture, to create unique one-off designs

Chapter 4

Practical Testing

An important part of the design process wa the practical testing of RMA's current tennis wheelchair. This provides minimum design targets that future wheelchair designs can improve upon.

The initial strategy for testing the chair was to pair the strain gauges attached to the wheelchair with the camera footage presented in the set-up in (*Figure4.4*). Using a video camera on the side of the court, the data is recorded from the strain gauges using a portable data logger.

The primary goal of the testing was to identify the movements that cause the largest loads that affect the sports chair during a game of wheelchair tennis. Player movements were simulated in a strain gauged wheelchair and these data were paired with camera footage to understand which movement causes the stress.

4.0.1 Strain Gauges

Resistance-based strain gauges have been used for over 50 years due to their simplicity, low cost, and relative accuracy [69]. A strain gauge is usually a thin length of wire arranged in a grid shape and attached to a thin backing, which is then glued to the test piece. When a load is applied to the test piece, it deforms, as does the attached strain gauge, causing a change in voltage and taking advantage of the piezoresistive effect, whereby a material changes its resistance when put under strain [69]. Using this change in resistance, it is possible to determine the strain that the tested part is under at the point where the gauge is attached using the following equation, $\Delta R/R_o = k\epsilon$ [70], where ΔR is the change in resistance

across the strain gauge; R_o initial resistance; ϵ is the applied strain, which is the goal of the experiment and k is the gauge factor (for the RS Pro Wire Lead Strain Gauge this value is 2 [71]).The normal configuration for setting up the strain gauges is in a low-power Wheatstone bridge, as can be seen in *Figure 4.1* [72]
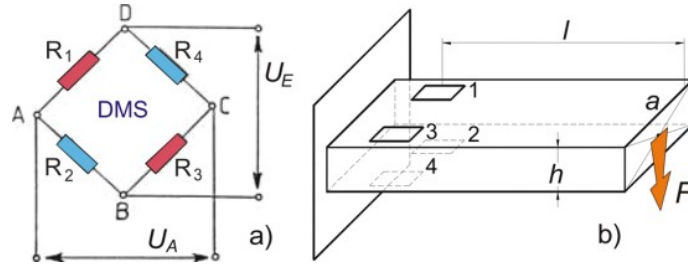
Figure 4.1: Wheatstone Bridge [72]

As the P3 data logger only has four data inputs, four locations were chosen on the wheelchair (see *Figure4.2*). These areas were chosen as most of the loads on the wheelchair will occur due to player movement. In this case, they were the four corners of the seated area of the wheelchair on the two down tubes at the rear and on the horizontal parts leading to the front of the wheelchair as can be seen in the pictures in *figure 4.2*. Placing the strain gauges in these locations will indicate how the forces are distributed around the wheelchair. As space was limited, the strain gauges where set up in a half Wheatstone bridge configuration to improve the accuracy of the test. This set-up helped to calibrate the strain gauges attached to the sports wheelchair with out taking up too much space. To complete the other half of the Wheatstone bridge, a fixed resistor was used to balance the other half of the bridge, which was done inside the P3 data logger.

Application

As previously stated, the strain gauges were set up in a half-bridge layout. When the strain gauges were applied to the wheelchair, the chosen surface was sanded back and thoroughly cleaned using an alcohol wipe to ensure that no contaminants were left between the surface of the wheelchair and also that the strain gauge, and that the strain read was as accurate as possible. Once this is complete, the strain gauges were glued to the surface of the tennis wheelchair in the previously specified positions (*Figure 4.2*).

Once the wires had been attached to the strain gauges, they could then be wired into one of the four specified channels in the data logger. Channel one was for the player's back right, channel two for the back left, channel three for the front left and channel four for the front right.

(a) Strain gauged RMA sports tennis wheelchair(strain gauge locations marked in red)
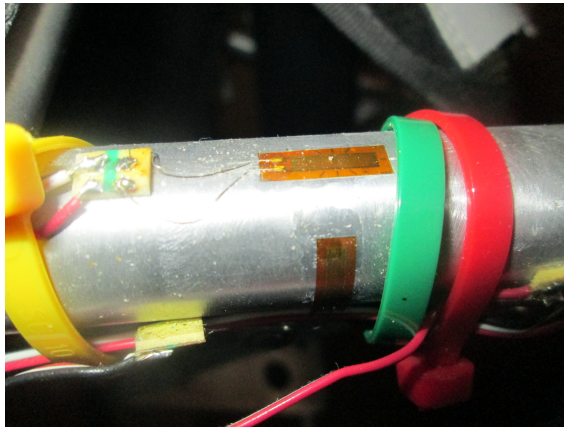
(b) Strain gauge

Figure 4.2: Strain gauged wheelchair

4.0.2 Tennis Wheelchair

The main design requirements were that the actual wheelchair must to be fast, be manoeuvrable, and not restrict the player's movement when they reach for the tennis ball. Therefore the wheels were designed to have a steep camber to improve the stability of the wheelchair when turning quickly on the court, while

the frame was designed to fit the player's body snugly around the hips, thus aiding controlled movement. The material of choice for the frame is aluminium, and the chair has two driven wheels plus two smaller castor wheels on the front of the chair, which allow for easy steering and manoeuvrability. Some of the more advanced chairs have a stability castor wheel on the back of the chair to prevent the chair from toppling over. The preferred method of attachment to the chair is for the player to be strapped in at the legs and at the waist to give the impression of being one with the chair. For this experiment, RMA's tennis wheelchair (*Figure4.2*) was used. The design consists of an aluminium space frame with two driven wheels and three castors, two on the front and one at the rear of the sports chair, to prevent tipping.

4.0.3   Data logger

A portable data logger that can be strapped to the sports wheelchair collected strain gauge data so that they can be logged while the player is playing a game or while simulating player movement. For this to work, the P3 data logger was chosen as it runs off a battery.The data logger can receive inputs from four different strain gauges, allowing for the collection of strain data from four corners of the wheelchair (*Figure4.3*).

This data logger has two data logging options. the first is manual logging, where the data are recorded when required by the user, such as in a beam experiment: data would be logged when a mass is added to the beam and the data could be added when it has settled. This method allows for a cleaner data set at the end of the experiment. The second option is automated logging, where the P3 system collects data from each of the strain gauged points at time intervals ranging from 1 second to a full minute [73].

For the present study, data was collected using an automated sampling option at a frequency of 1 Hz, which was the highest frequency that the p3 could record. A large amount of data was recorded and split into the individual load cases using video footage during the post-processing stage.

(a) P3 data logger (View 1) (b) Data logger (View 2)

Figure 4.3: P3 data logger

4.1 Experimental Procedure

The testing was conducted at an outdoor tennis court at the David Lloyd Club in Swansea. A strain gauged RMA Sports tennis wheelchair at the base line and a video camera placed at the side of the court were used to film the test, as depicted in *Figure4.4*.

The two data sets were synced by providing a visual and audio signal when the P3 data logger started recording on the video camera. Once the camera and the data logger had started to record, the player simulated a serve, acceleration, steering and ball returns (details of the movements are provided below). The data was collected by the data logger and the footage was taken using a GoPro Hero White with the frame rate set to 30 frames per second at 1080p resolution.

(a) Set up (View 1)

(b) Set up (view 2)

Figure 4.4: Practical testing set up at David Lloyd Club, Swansea

4.2 Subject Movement

The following four types of movements can be identified in a game of wheelchair tennis: the serve, ball return, acceleration, and steering. The serve can be broken down into three stages, as seen in *Figure4.5* [74]. The initial movement is the preparation phase, which includes throwing the ball in the air. In the accelera-

tion phase, the player moves forward and strikes the ball. The final phase is the follow-through where the players momentum moves to the front of the wheelchair.
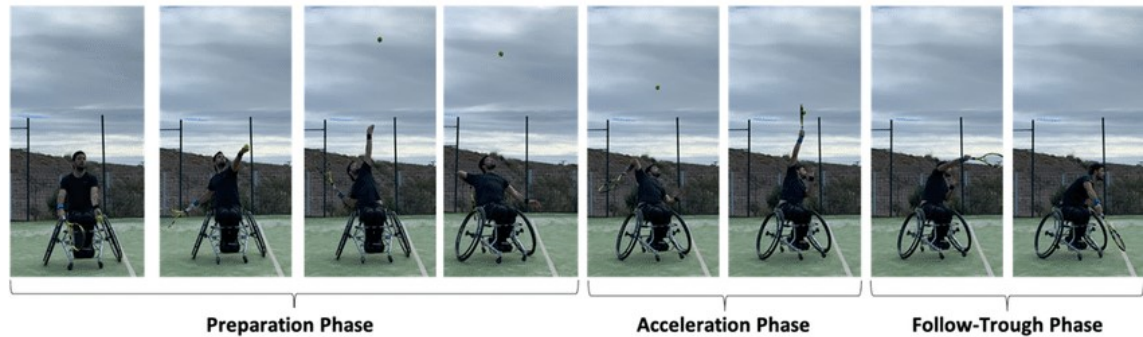
Figure 4.5: Service sequence [74]

During a volley returning the ball, there are two extreme movements, namely the backhand and the forehand. Here, the player's mass leans to reach for the ball, and most of the player's weight is over one side of the wheelchair.

Once the strain gauge data had been collected for each of the movements, the next step was to identify how the movements affected the wheelchair. The data could then be used to conform the load cases and provides an indication of how the initial finite element analysis (FEA) model would act in the first stage, before moving on to optimise the design of the sports wheelchair.

Finally, the acceleration and steering could be combined into one motion, as most players playing a defensive strategy move around the court in a figure of eight. This is a play strategy favoured by most professional tennis players, as it means that the player is always on the move and covering most of the court, who;e also including three movements of acceleration and both left-hand and a right-hand turns. It was thus both interesting and necessary to obtain strain data for the aforementioned described movements.

4.2.1 Serve movement

The serve should consist of two peaks in load. The first peak occurs during the load up phase, where the mass of the player moves to the rear of the wheelchair

as the ball is thrown up (*Figure 4.6*) before moving rapidly towards the front of the wheelchair as fast as possible to increase the acceleration of the tennis ball and win the set.

The player used their right hand to hold the racquet and serve, which suggested that there should be a load spike from the right-hand rear side of the chair, which was on channel 1 on the data logger. Moving in a diagonal motion for the serve it was safe to assume that the next load spike would be on the front left-hand side of the sports wheelchair, which was wired into channel 4. During the test, the movement was repeated five times to find a peak load and record a range of serve speeds.

(a) Serve (Start)

(b) Serve (Finish)

Figure 4.6: Serve

4.2.2   Tennis Ball Return

In wheelchair tennis, another potential load case is the return of the ball, which could occur at any point in the game. This can result in a wide range of potential loads, as the ball could be returned from any position in the wheelchair depending on the positions of the ball and the player in relation to the game in play. The movements shown in *Figure 4.7 and Figure 4.8* depict the two potential extremes in a low backhand and forehand with any movement above the head covered in the earlier serve load case.

(a) Forehand (Start)

(b) Forehand (Finish)

Figure 4.7: Forehand

As *Figure4.7* indicates, the forehand is a very simple motion that moves from the right to the left side of the wheelchair and with the racquet following a low arc to the side of the chair. With respect to the strain gauges, there should be a transfer of load from channel's 1 and 3 over to channel's 2 and 4.

Figure 4.8 illustrates the backhand motion as the opposite of the forehand motion, with the player moving from left to right rapidly. The load cases move from left to right due to the reduced reach across the player. The player can move slightly lower than in the backhand, as seen in *Figure 4.8*(a), which could result in an increased load on that side of the wheelchair.

(a) Backhand (Start)

(b) Backhand (Finish)

Figure 4.8: Backhand

4.2.3 General Movement

Moving the sports chair around the tennis court could result in loads being applied to the wheelchair. As stated, the wheelchair tends to move in a figure-of-eight pattern that can be divided into two components, namely steering and acceleration in a straight line, covering the base line of the court in a defensive manoeuvre, or moving towards the front of the court if the player has a more aggressive play style. This movement was replicated in the test by the player accelerating from side to side of the tennis court and aggressively turning at the end of the court, which ensured turns in both directions to measure the effect of braking with the racquet hand.

(a) Acceleration   (b) Turn

Figure 4.9: General movement

4.3 Practical Testing Results

After the testing was completed, the data was converted from the recorded microstrain to stress (pa) using aluminium's Young's modulus of 70 GPa to calculate the loads acting on the sports wheelchair. The data was split into the different movements that occurred during the test using footage obtained from the video camera, with the movements within those sections highlighted to help correlate the stresses with specific movements.

4.3.1 Serve Results

The graph in *Figure 4.10* plots the results from the strain gauge data after they were converted from microstrain into stress in millipascals. The green lines in the graph depict the initial part of the serve (*Figure 4.10*[a]), while the red lines represent the follow-through part of the serve (*Figure 4.8*[b]). The names of the channels (CH1, CH2, CH3, and CH4) have also been changed to relate to the location of the strain gauges on the wheelchair, namely BR, BL, FR, and FL (back right, back left, front right and front left, respectively), with data from the four locations plotted in the graph.
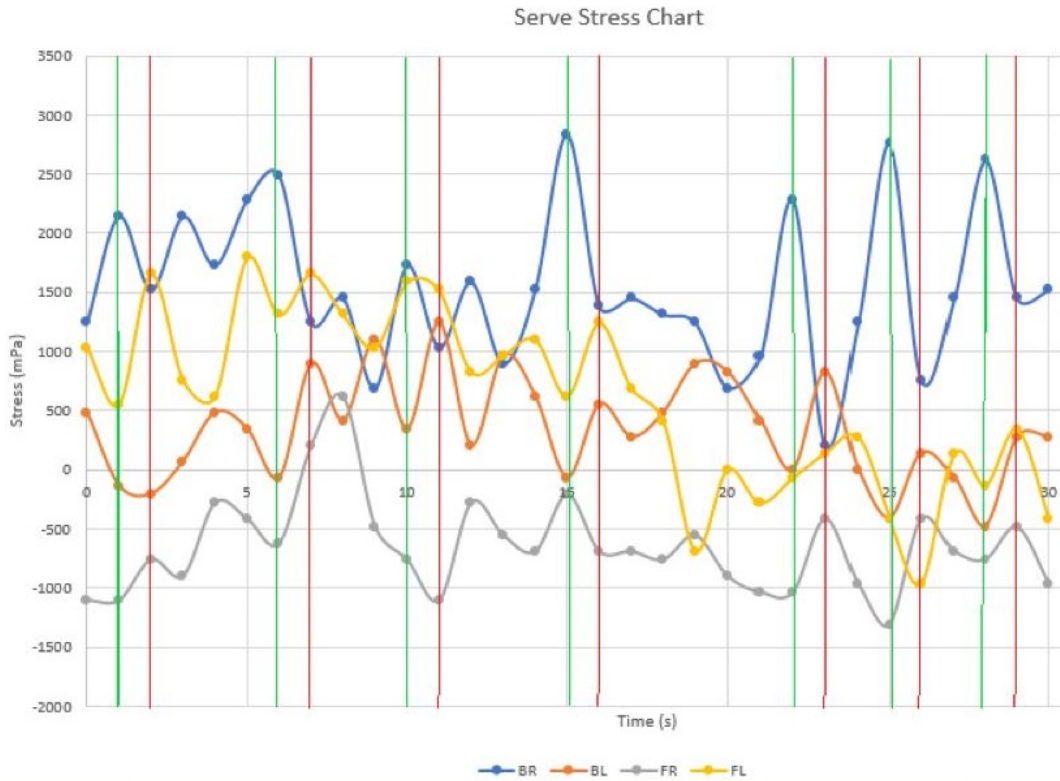
Figure 4.10: Practical stress data for serve movement

Table 4.1: Average Stress and Standard Deviation of the Serve

Serve Preparation (Green)

	Strain Gauge			
	BR	BL	FR	FL
Average (mPA)	2078.63	94.88	-853.88	603.75
Standard deviation	516.92	415.54	280.73	820.37

Follow Through (Red)

	Strain Gauge			
	BR	BL	FR	FL
Average (mPa)	1440.375	379.5	-569.25	491.625
Standard deviation	862.9435	538.2758	270.3985	983.0554

According to *Figure 4.10*, as predicted for the BR (back right [blue]) and FR (front right[yellow]) channels, the initial and final parts of the serve correlated

with the expected peaks and troughs on the graph as the player loaded up and completed the serve. A peak stress occurred at 15 seconds at 2750 mPa at the back of the wheelchair in the fourth serve. The average stress at CH1 was the largest at 2,078mPa.

It is interesting to note that the peaks on the BL (back left [Orange]) side of the wheelchair correlate with the second part of the serve. This could have been caused by to the mass transfer of the tennis player from left to right during the serve, as illustrated by the pattern revealed by the FL strain gauges.

The serve in the test did not provide a consistent load with the standard deviation for each serve being quite large. This could have been caused by to a few different factors, including different serve speeds and the range in movement of the Tennis player. If a professional more experienced athlete was used, then it would be possible to obtain a more consistent strain value for a tennis set-piece such as the serve.

It is also noteworthy that the peaks in the BL (orange) side of the wheelchair correlate with both the first and second parts of the serve. This could be have been caused by the mass transfer of the tennis player from left to right during the serve, as indicated in the pattern revealed by the FL strain gauges.

4.3.2   Ball Return Results

Figure4.11 presents the stress data for the forehand part of the test. As with the serve, the red and green lines indicates the pre movement towards the back of the wheelchair, and the red line shows the movement of striking the tennis ball. According to the graph, the movements indicated a slight correlation with the front right side of the chair as the tennis ball was struck, and the momentum of the swing carried the player's mass to the right side of the wheelchair. The fluctuations in the other sensors did not correlate with the forehand movement. These changes could be explained by small movements made by the tennis player.

The maximum stress for this movement was approximately 2.5 Pa at the back left side of the wheelchair, and stress dropped to -1.5pa on the front right strain

gauge sensor.
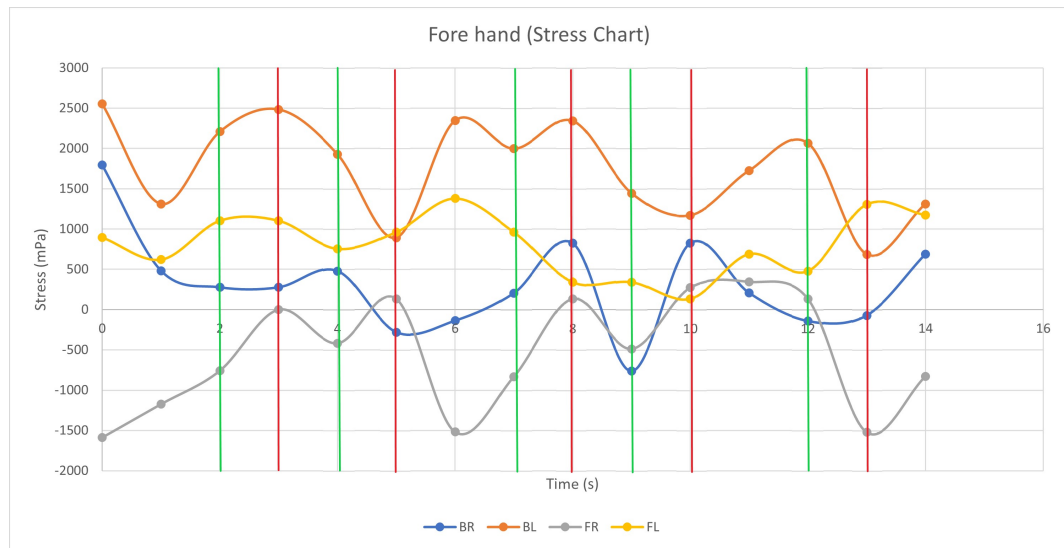
Figure 4.11: Forehand results

The graph in *Figure4.12* displays the stress data for the backhand movement during the test. As with the other graphs, the green lines depict the movement before the swing, while the red lines trace when the ball was struck. As previously mentioned, the backhand involves the player moving towards the back left side of the chair and swinging the tennis racquet towards the front of the wheelchair.

More over, the graph seems to include this pattern for most of the data, with a peak occurring at the back and front left strain gauges (represented with orange and grey lines) of the wheelchair for most of the pre-swing stages. The largest stress occurred on the first swing at a value of 3.17 Pa on the back left side of the wheelchair. For a majority of the backhands, the left sides started to peak when the swing occurred in the initial stage on back left hand side of the wheelchair (blue line) peaking on the fifth swing at -1.86 pa.

60
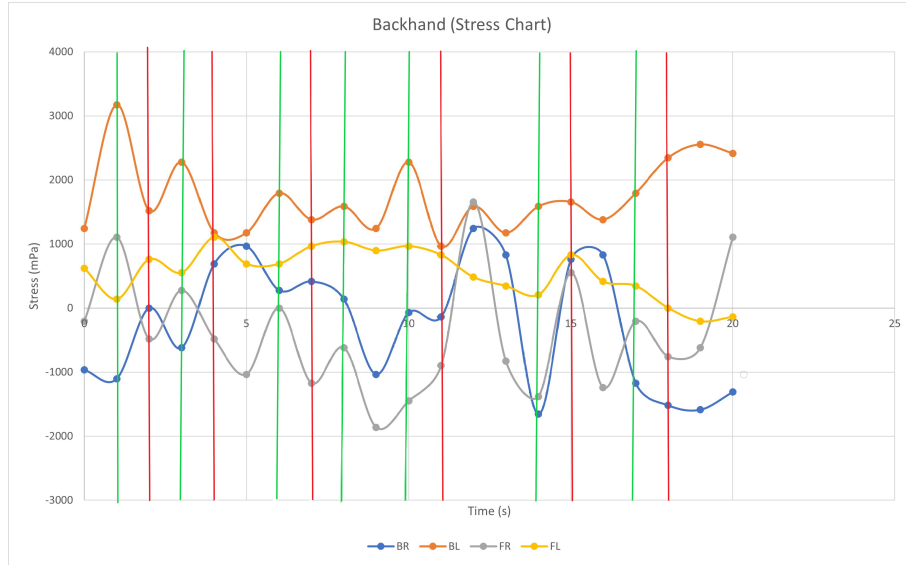
Figure 4.12: Back hand results

Table 4.2: Average Stress and Standard Deviation of the Forehand Results
Forehand Preparation (Green)

	Strain Gauge			
	BR	BL	FR	FL
Average (mPa)	51.75	1897.5	-621	793.5
Standard Deviation	479.54	893.01	328.75	456.13

Forehand follow through (Red)

	Strain Gauge			
	BR	BL	FR	FL
Average (mPa)	414	1173	-207	345
Standard Deviation	528.50	806.64	112.68	469.25

4.3.3 General Movement Results

The graph in *figure4.13* displays the results for general movement. As this was the least consistent movement, much fluctuation occurred in the data points for each of the strain gauge locations. The green lines indicate the left-hand turns,

Table 4.3: Average stress and Standard Deviation of the backhand results

Backhand Preparation (Green)

	Strain Gauge			
	BR	BL	FR	FL
Average (mPa)	-607.2	1628.4	-979.8	897
Standard Deviation	699.9497	717.5431	716.4364	446.6638

Backhand Follow through (Red)

	Strain Gauge			
	BR	BL	FR	FL
Average (mPa)	402.5	816.5	-264.5	126.5
Standard Deviation	816.9048	723.2394	1024.985	406.4563

and the red lines depict right-hand turns. During the periods of time between these turns, the wheelchair user accelerated in a straight line across the tennis court.

As seen in the graph, a left-hand turn seems to correlate with a peak in stress on the back right side of the wheelchair (blue line) because the mass of the player is thrown to the opposite side of the turn to balance the wheelchair. Turning seems to be more impactful on the sports wheelchair when turning left; this could be a result of the left hand braking more effectively because it is not holding the racquet. The peak stress occurs in the middle of two quick changes of direction in the chair between the third left turn and the second right turn. with a peak stress of 3.4 Pa at 22 seconds at the back right side of the wheelchair. The stress also peaks in the opposite direction in the same location at eight seconds during a right turn at -2.4 Pa. As that side of the sports chair un-weights.
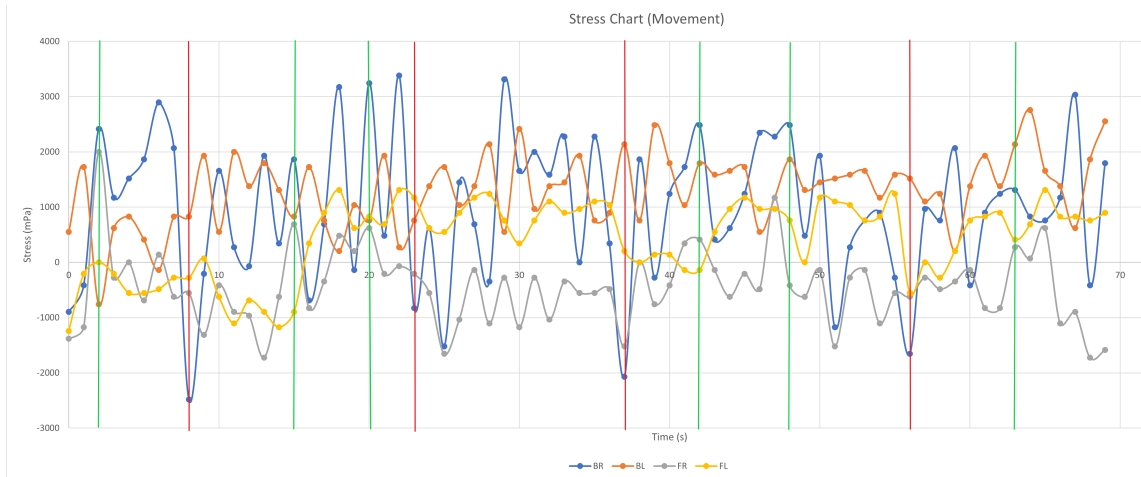
Figure 4.13: Movement Results

[H]

Table 4.4: Average stress and Standard deviation when turning results

Left turn (Green)

	Strain Gauge			
	BR	BL	FR	FL
Average (mPa)	1426	-2507	-103.5	-1127
Standard deviation	556.58	556.58	749.21	584.94

Right turn (Red)

	Strain Gauge			
	BR	BL	FR	FL
Average (mPa)	1311	-2622	-724.5	-1035
Standard Deviation	649.7246	649.7246	559.1413	757.9538

Chapter 5

Wheelchair Geometry and Load Cases

This chapter aims to describe the geometry of two designs to be considered for optimisation. First, it examines the welded aluminium space frame structure currently used by RMA, including how a model to analyse was created, before examining how the different load cases affect the wheelchair.

The second design created was a modular designed space frame. The design isolated the connecting points of the space frame to create lugs. The lugs were then analysed individually, identifying how each of the load cases would be affected during a game of tennis.

5.1   RMA Wheelchair Geometry

The initial simulation and subsequent optimisation used the same initial model as RMA's current tennis wheelchair, which was discussed in Section 2.4 (Existing Products). A model was created by exporting the coordinates from a three-dimensional sketch of the current space frame in Solidworks (*Figure 5.1*). The exported points represented features of the wheelchair, such as, where two tubes join or where there is a bend in the tube. The initial model consisted of 48 points used in the input file. The input file treated each tube as an individual part and assigned a letter, as shown in *Figure 5.2* below. Within the defined parts, the relevant coordinates, material properties, tube thickness, and radii were set to ensure greater control over the individual parts. The input geometry file could

then be imported into Abaqus as per *Figure 5.1*:
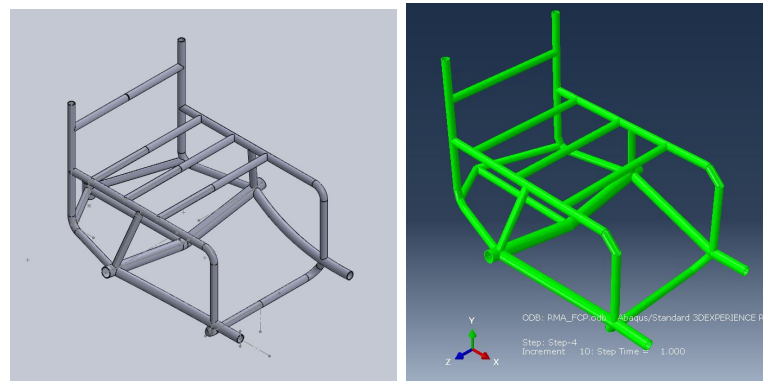
(a) Solidworks CAD model of RMA's tennis wheelchair

(b) Abaqus model of RMA's tennis wheelchair

Figure 5.1: RMA's initial tennis wheelchair model

5.1.1 Parametrisation

To optimise the wheelchair in later stages, changes were made to the initial Abaqus input deck before analysis and optimisation. First, the file was parametrised by replacing the values in the input deck with a variable parameter; for example, the tube thickness for PART-A (*Figure 5.2*) was 2.0 in the original file and was replaced with A-t. To simplify any future changes, separate input files were made for the variables that were parametrised and were called by the main input deck in the same way as the load cases were in the initial model. *Figure 5.2* and *Table 5.1* display the naming conventions for each part and its associated coordinates. In later stages of the optimisation process the longer tubes where split into more parts to allow more variables to be added. as can be seen in the second column of *Table 5.1*.
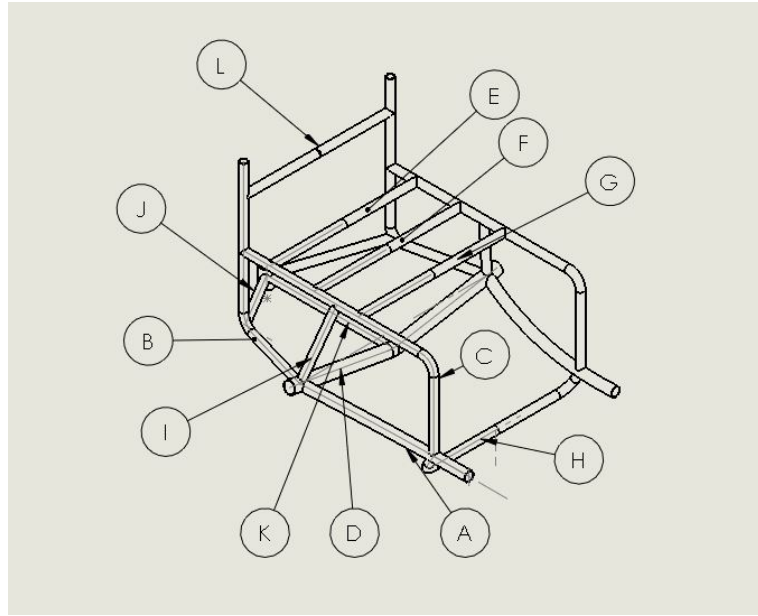
Figure 5.2: Part names for the RMA wheelchair

Table 5.1: Parameters Associated with Parts

Part Name	Split Part (Op3)	Coordinates Linked to Part
Part-A	AA,AB,AC,AD,	X1,Y1,Z1,X2,Z2,X3,Z3,
Part-B	BA,BB,BC,BD,BE,BF	X3,Y3,Z3,X4,Y4,Z4,X5,Y5,Z5 ,X6,Y6,Z2,Y7,Y30,Y8
Part-C	CA,CB,CC,CD,CE,CF,CG,CH,CI	X2,Y1,Z2,Y9,X10,Y7,X12,X11, ,X13,X14,X6,
Part-D	DA,DB,DC,	X15,Y15,Z15,Y3,Z3,Y16,Z23
Part-E	E	X14,Y7,Z2,Z19,Z24
Part-F	F	X13,Y7,Z2,Z19,Z24
Part-G	G	X12,Y7,Z2,Z21,Z24
Part-H	H	X2,Y1,Z2,X22,Y22,X23,Y23, ,Z24,Z25,Z18,Z25,Z31
Part-I	IA,IB	X3,Y3,Z3,X11,Y7,Z2
Part-J	JA,JB	X5,Y5,Z5,X18,Y18,Z23
Part-K	KA,KB	X15,Y16,Z23,X18,Y18,Z23
Part-L	L	X6,Y30,Z2,Z19,Z24

5.2 Load Cases

As elaborated in previous chapters, in a game of wheelchair tennis, there are three main movements to consider, which can be broken down into four different sets of boundary conditions. The serve is split into two different load cases, namely leaning back at the start of the movement (the preparation phase) and follow through once the player moves the mass forward to strike the ball. The third load case occurs when the player reaches for the ball during the game, with the players mass being concentrated to one side of the wheelchair. This load case can also be used to simulate wheelchair turning by concentrating the load on one side of the wheelchair. The final load case intends to simulate an impact, which is less likely in tennis than in other wheelchair sports such as rugby or basketball. Nonetheless, impact can occur when tennis players play doubles and run into other players or the border of the court.

For each load case, a separate Abaqus input file was created, and the locations of the boundary conditions were identified using the geometry points used in the main input file. This makes it easier to add or adjust the load cases in the future and could potentially be used for different wheelchair sports with different load cases and chair geometries.

5.2.1 The Serve (Step 1 and Step 2)

In the preparation phase of the serve (Step 1), as the player leaned back, most of their mass was over the rear of the wheelchair. For this reason, the total weight of the trunk (76.2kg) and legs (23.6kg) (values from *Table 2.2*) was distributed towards the rear of the seat, placing a point load of 128.44N on three points of the wheelchair in the direction of gravity, as seen in *figure5.3C (Red)*.

The effect of the arm was calculated using data from video footage of the practical testing. The footage indicated that the preparation phase occurred over 1 s, moved over 35^0 and used a trunk length of 0.7 m (95th percentile). Using these values, the tangential acceleration at the shoulder was calculated as 0.85ms^{-2}. This acceleration as well as the mass of the arm (3.7kg) and trunk (76.2kg) should provide a good approximation of the force on the backrest. Thus, there was a force of 28.6 N in the -X direction and this load was placed on the mid and left

points of the back rest (*Figure5.3C [blue]*). The driven wheels, front castors, and anti-tip wheel were pinned as depicted in *figure5.3C [Orange]*
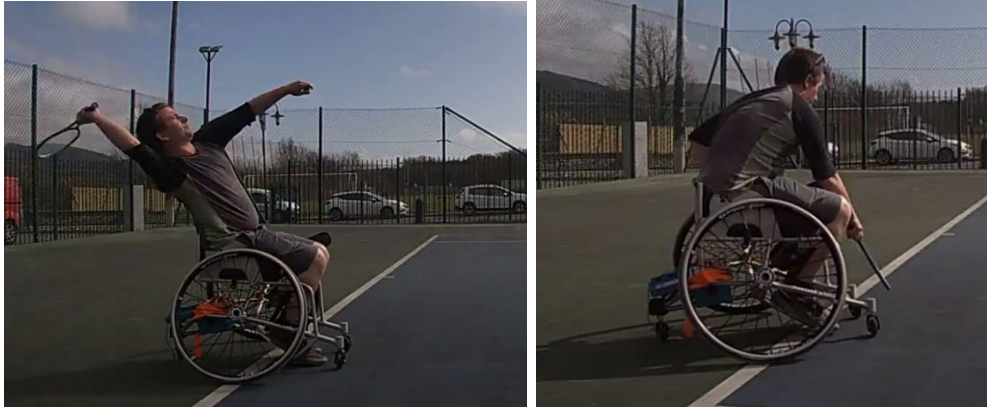
(a) Preparation phase of the serve (Step 1)

(b) Follow through phase of the serve (Step 2)
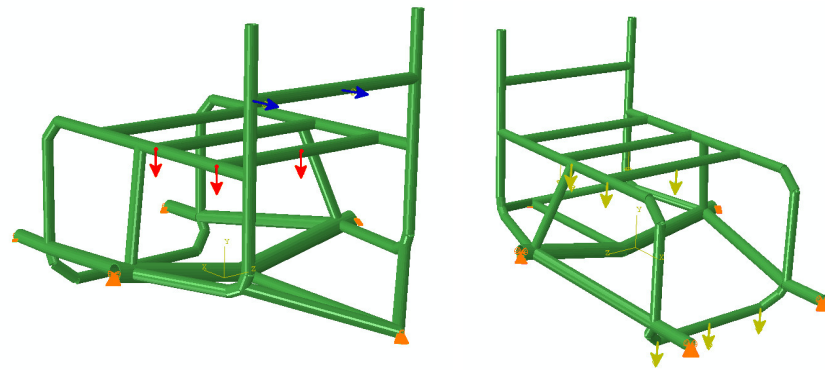
(c) Free body diagram for preparation phase of the serve (Step 1)

(d) Free body diagram for the follow through phase of the serve (Step 2)

Figure 5.3: Von Mises diagram of both stages of a serve and real world depiction

During the follow through of the serve (Step 2), the player's mass is transferred from the rear left side to the front of the wheelchair. This was simulated by distributing the player's full mass (1425N) over four points on the front right side of the seat and three points on the foot plate in the -Y direction. Again, the nodes of the space frame were pinned such that the driven wheels and both castor wheels are connected to at the front of the wheelchair, as depicted in *figure5.3D*.

5.2.2 Reach (Step 3)

During a game of tennis, the player's upper body can move quite freely while in the wheelchair. Extreme load changes occur when the player reaches for and returns the ball (*Figure 7.3*). The reach load case represents the player reaching for the ball and by focusing on the effect of loading the driven wheel to one side.
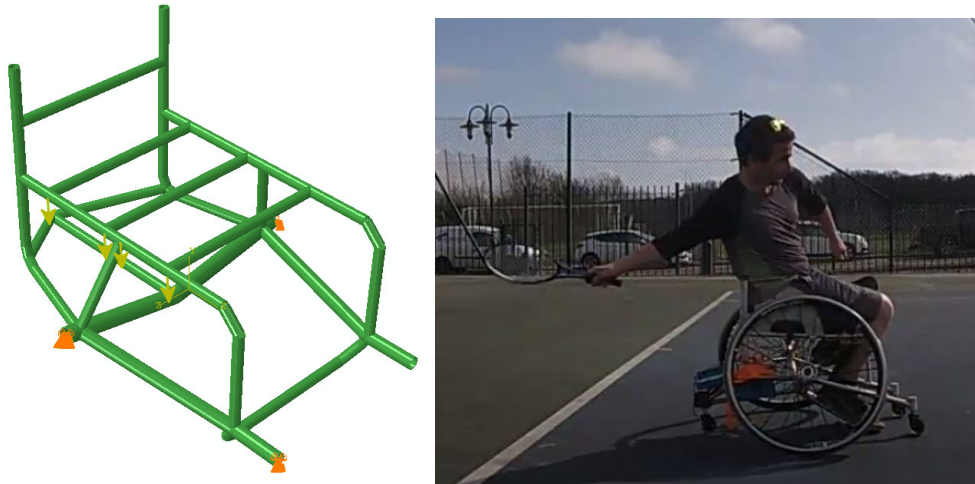
(a) Reach free body diagram (Step 3)   (b) Player reaching for the Ball (step 3)

Figure 5.4: Real world depiction and free body diagram of the reach load case

To simulate this, the mass of the wheelchair user was placed on one side of the chair, and distributed along the three points in the model that comprised the right side of the chair. A point load of 356.25N was applied to the nodes that construct the right side of the seat in the direction of gravity, while the ground contact points of the wheelchair were pinned on that side (left-hand side driven wheel and front left hand castor wheel. [Node 4011 and 1011])

5.2.3 Front Impact (Step 4)

Although impacts in wheelchair tennis do not occur very often, they are a possibility because the player could crash into the border of the court (e.g. Olsen/Gerard vs Hewitt/Reid Wimbledon final 2018) or potentially another player if playing doubles.

To simulate this, the wheelchair frame was given a velocity based on a study conducted at Loughborough University, UK, which to gauged the acceleration

profile of elite wheelchair tennis players [75] by producing the acceleration profile of the three player categories (men, women and quads) using 32 participants. The speed of the participants was measured over a 20-m sprint, with speed gates at 2.5 m, 5 m, 10 m, and 20 m. The maximum velocity recorded by the participants with a tennis racket was $4.4ms^{-1}$ at the 20m gate. In the simulation the wheelchair was given this velocity heading towards a fixed object (*Figure 5.5*).

The mass of the player (the red dot in *Figure 5.5*) was tied to the seat belt anchor points (yellow dots). The front castor nodes were then fixed in the Y direction to prevent the front of the wheelchair rotating into the floor. This dynamic load case occurred over 20 steps.
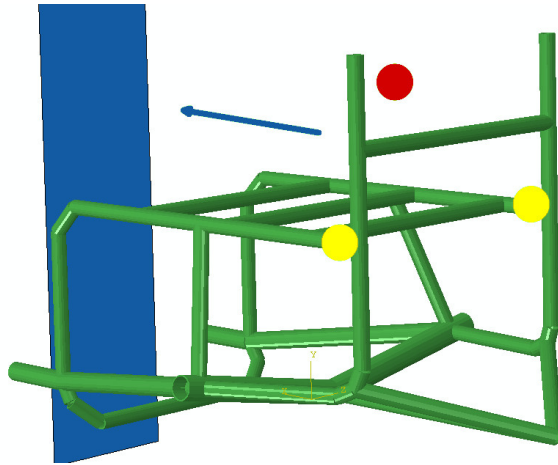
Figure 5.5: Free body diagram for front impact load case

5.3 Adjustable Wheelchair Design

This section covers the second design idea for a sports wheelchair design and focuses on a modular concept for a wheelchair. A modular design in sporting equipment has many advantages, including the ability to fit the chair to unique situations, whether that is the sport being played or the individuals play style. From a manufacturing stand point, this makes the chair easier to fit to the athlete. Having a modular design also has several secondary benefits, which include making it easier to transport the wheelchair and allowing greater adjustability throughout the product lifetime, similar to the day chairs the athletes might use.

The next iteration removed the need to use a bonding agent. Instead the connecting frame points were redesigned to incorporate a clamp to hold the carbon fibre tubes in place. This design could potentially allow the wheelchair to be used for a wider variety of sports by adjusting the geometry to suit the situation. The second application could be for younger athletes, who can adjust the geometry as they grow; thus, the chair would be made more affordable and environmentally sustainable in the long term.

Moreover, topology optimisation was used to keep the manufacturing costs and times down. The following three AM materials were investigated: steel (316L), aluminium (6061) and titanium (Ti-64). To make the most of this near net-shape manufacturing process, the parts were improved using topology optimisation to reduce the overall weight of this modular design.

5.3.1 Modular Design

The first iteration of the modular design was based around a modular base unit as seen in *figure 5.6*. The chassis and seat components are attached to the base unit by M6 t-nuts slotted into a T-profile in the base module. For the prototype wheelchair, the base unit was manufactured out of six lengths of t-section aluminium profile, joined together by welding 2 mm aluminium plates with a cross piece to increase the stiffness (*Figure 5.6*b). This manufacturing method was chosen for the prototype to keep the costs down at this stage to prove the concept. For the final part, it would be favourable for the base unit to be manufactured by extruding the unit as one piece to improve the manufacturing time and aesthetics of the final product.

(a) Initial modular design
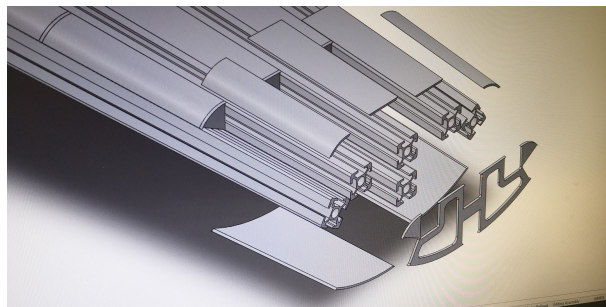
(b) Base unit

Figure 5.6: Initial modular design and base unit

This design allows for the space frame and seat components to move. Although the adjustability of this design only goes in one direction, it is an important part of the fit to get right. The position of the player can affect the power that they drive through the wheels; If it is too far forward, then there would not be enough room to push, whereas if it is too far back, then this would exclude the power of the stroke. Additionally, the player's position in relation to the wheelchair greatly affects the wheelchair's centre of gravity. If this position is wrong, then it could significantly affect the player's game. This design allows the player to fine-tune the geometry during use, which allows the effects of the small changes to elevate the player's performance.

5.3.2   Modular ALM Design

This design utilises advanced manufacturing techniques such as AM, by printing the connecting points of the space frame and then assembling the frame by gluing carbon fibre tubes together. As previously mentioned, this technique is already used to manufacture push bicycles. By using this approach, the geometry can be tailored to the athlete while keeping manufacturing costs relatively low for small production runs. The modular wheelchair utilises the design freedoms in AM by using topology optimisation to create light-weight connectors that retain their strength and stiffness.

The wheelchair design consists of 12 connectors that were optimised based on different theoretical load cases with the total player's weight acting on the parts and a safety factor of 1.5 [30].

Each connecting point of the space frame was optimised using a topology optimiser (Altair Inspire) to reduce the weight of the components, as displayed in the following figures. The components were optimised effectively, by reducing the overall mass of the connectors by 50 %.

Figure 5.7: Initial concept design of the additive layer frame

5.4   Modular Wheelchair Load cases

In order to achieve the optimised modular design, the space frame was broken down into its individual components shown in *Figure 5.8*. The loads were then

applied to each of the lugs separately. This section intends to explain how the different load cases can impact the individual components and the boundary conditions used in the optimisation process.
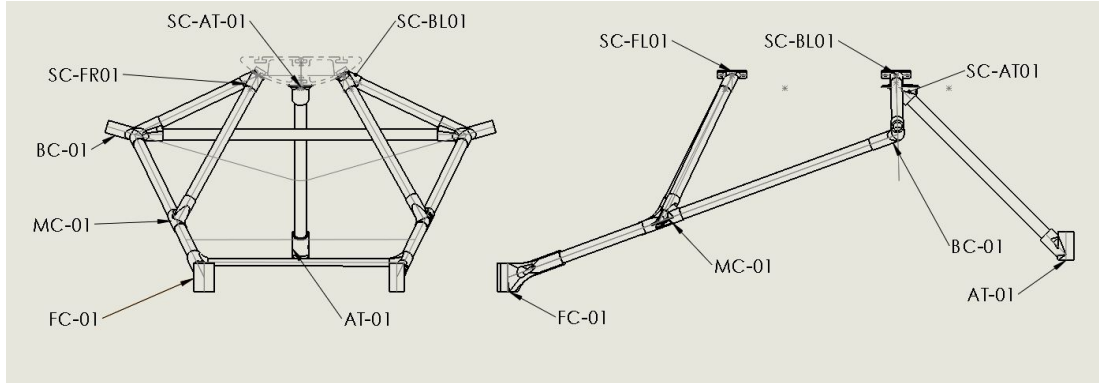
Figure 5.8: Modular Design Assembly Drawing

5.4.1   Front Connector (FC-01)

This connector supports the front castor wheels, which are currently designed around the frog legs Phase-One castor [35] (*figure 5.9*). This frog leg castor is currently used in other wheelchair sports such as in WCMX and skate wheelchairs. The rubber section of the castor helps to cushion any harsh impacts that the wheelchair and user may encounter when landing tricks. In wheelchair tennis, the idea would be to increase the reach of the Player during the game, as can be seen with the sprung castor used on Stéphane Houdet's wheelchair (*Section 2.4*) which is advantageous to his play style.

As with all of the connectors, a 3mm hole was added to the point where the carbon fibre tube is inserted. Once the part was printed this hole was threaded. A grub screw can be inserted to hold the tubes in place when dry fitting the component. This ensures that the final product is suitable for use before the final assembly.
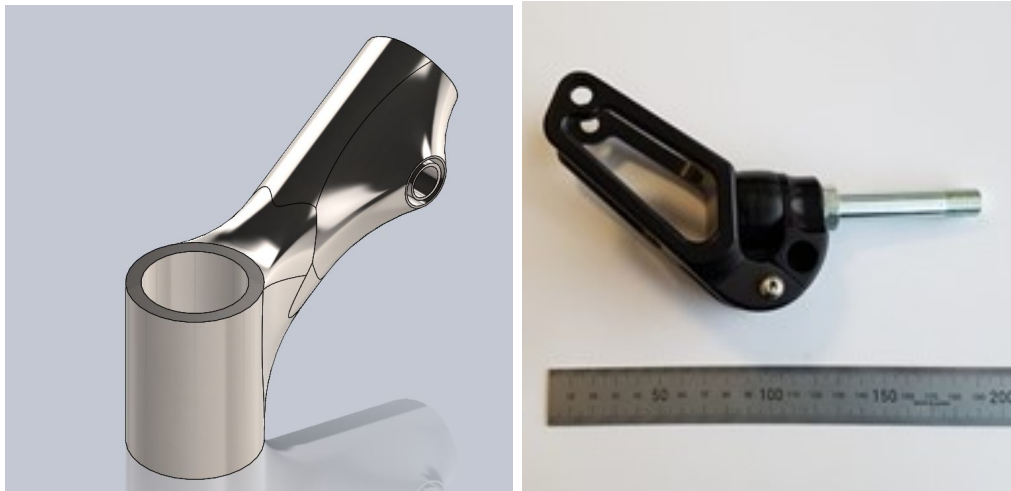
(a) Front lower node initial   (b) Frog Legs castor

Figure 5.9: Initial front connector and Frog Legs castor

FC-01 Boundary Conditions

Part of the Topology simulation requires a design space to be selected. This region is highlighted in red in (*figure 5.4.1*). The design space is the area in which the optimiser can remove material. It is important to identify areas to exclude from the design space where material should not be removed. In this case the area where the castor fits to the wheelchair was excluded from the design space keeping the area above clear to enable the nut that holds the castor in place to be tightened as well as provide ease of access when assembling the wheelchair.

The other two areas have been excluded from the design space are where the carbon tubing meets the connector as seen in (*figure 5.4.1*). This design ttook further advantage of the AM methods by adding extra gluing area to the inside of the tube: 20mm of non-design space geometry should provide enough surface area to form a strong enough bond with the glue. To find the optimum shape for this part, the CAD model was altered to increase the design space and remove any unnecessary restrictions, as seen in *Figure5.4.1*. A box was drawn around the design space. It was important to ensure that, when increasing the design space the new geometry did not impinge on the access points, such as in the area around the castors.
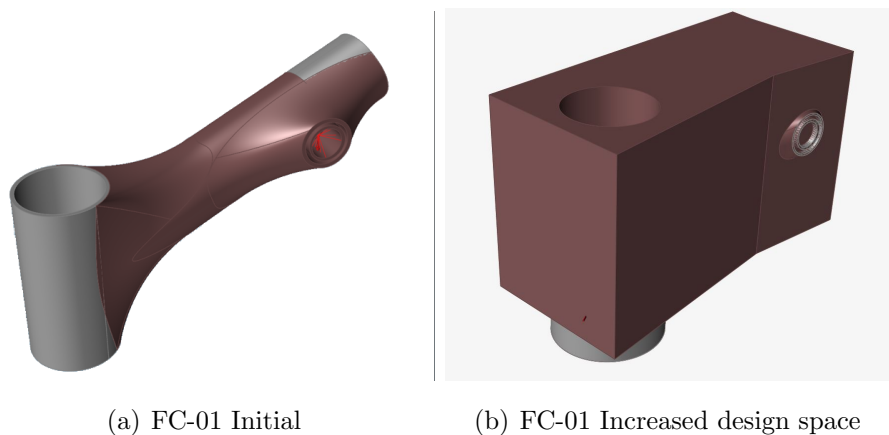
(a) FC-01 Initial

(b) FC-01 Increased design space

Figure 5.10: Front connector design space

There are two extreme load cases to consider for this component. First, the serve could cause the Player's movement transferring the weight of the Player from the rear of the wheelchair to the front castor. To account for this a load of 1500N was added to the connector where the tube is connected to the middle connector (MC-01) in the negative direction as well as a 200N load on the footrest connection point to account for the mass on the footrest. The lower face of the castor was held, which should simulate that movement sufficiently.

Another potential load case could be any potential front impact towards the front of the wheelchair. Impacts are not as common in a sport such as wheelchair tennis but there is potential for an impact with another player during a game of doubles or potentially the border of the court. To simulate such an impact the tube part of the connector was fixed in place and a force of 1500N was placed on the castor face acting in the direction towards the rear of the wheelchair.

5.4.2 Middle Connector (MC-01)

This component consists of three contact points going to the front of the wheelchair connecting to front castor connector (FC-01), to the rear of the wheelchair at the Back connector (BC-01) and its main purpose is to support the front portion of the base unit on both sides. All of the connecting points are designed to hold 25mm outer diameter tubing. Like the previous component, to increase the bonding surface area for the part and the tube, material was added so that the connector could be bonded to the inside of the tube at a diameter of 22mm as can be seen in the *Figure 5.4.2*.

(a) MC-01 initial   (b) MC-01 in assembly
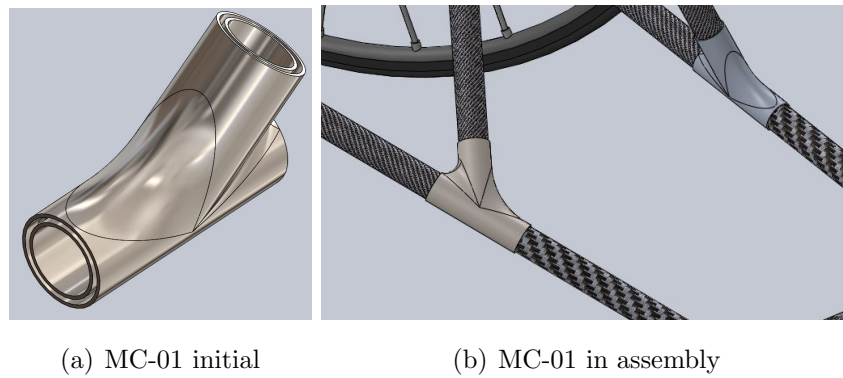
Figure 5.11: Middle connector

As with the front connector it was necessary to set a design space that high-lighted areas in which any unnecessary material can be removed, ensuring that the bonding surfaces would not be removed from the part. Each bonding surface was extruded by 20mm and set as non-design space.

As can be seen in *Figure 5.4.2* extra volume was added to the part. This reduced any geometry restrictions on the final part and ensured that the best shape possible was produced for the part.

(a) MC-01 Initial   (b) MC-01 Increased design space
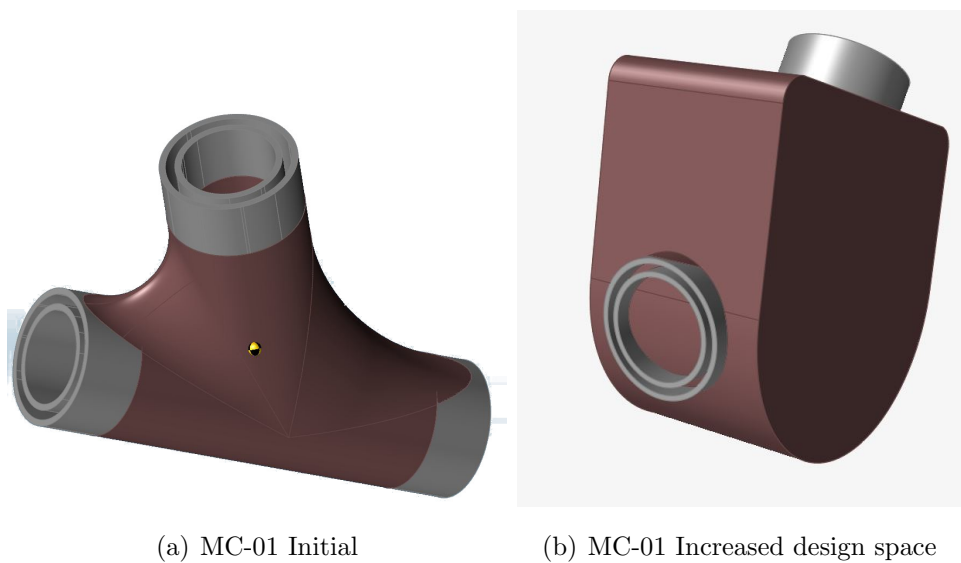
Figure 5.12: Back connector design space

MC-01 Boundary Conditions

Two of the load cases were applied to the middle connector. The serve or an aggressive turn could lead to most of the force going through this connector.

To account for this, the area where the connector joins with BC-01 and FC-01 was fixed along the axis and a load of 1500N was added to the face of the section that joins to the base unit of the wheelchair. The second load case to consider was a front impact to the wheelchair in case of collisions with doubles partners or the curb around the side of the court. To account for this impact, the parts going towards the rear connector and up to the base unit were fixed in place while a load of 1500N was added to the front face to simulate the impact.

5.4.3   Back Connector (BC-01)

This component is probably one of the most complex connectors, as it connects to four different points of the wheelchair as well as supports the driven wheels. The piece coming back then connects the middle connector (MC-01), the base unit (BU-01) and its mirrored component. All of these points are connected using 25mm carbon tubes with an inner diameter of 22mm, which are used for the rest of the space frame. All of these sections of BC-01 include the inner tube to hold the tube in place while increasing the glued surfaced area.

One design feature of the BC-01 is that it must hold the driven wheels. The connector that allows the quick release function to work is presented in *Figure 5.13* below. In RMA's current wheelchairs, the frame is threaded to allow the part to be inserted. The design space for this component, which holds the wheel, was designed so that the thread of m10 can be tapped after the part has been printed as the threads require a high tolerance. Any problems in the build could lead to some play in the driven wheels which would be unacceptable in a high-end piece of sports equipment.

(a) Back connector initial　　　　　　(b) quick relesase hub component

Figure 5.13: Back connector and quick release hub

BC-01 Boundary Conditions

As with the previous parts it was important to set the design space. As before, 20mm of material was left unedited to ensure a reasonable gluing area. BC-01 connects to the rest of the wheelchair at three points, and its mirrored component provides the stiffness in the frame. It is then connected to the middle connector and up to the main base unit of the chair. There was some difficulty as the angle between the base unit and back connector was quite small, so the part was made larger to stop the tubes colliding within the connector. As with all of the parts, the volume of the model was increased as can be seen in *Figure5.14*,to allow for the optimum part to be produced.

(a) MC-01 initial design space (b) quick relesase hub component
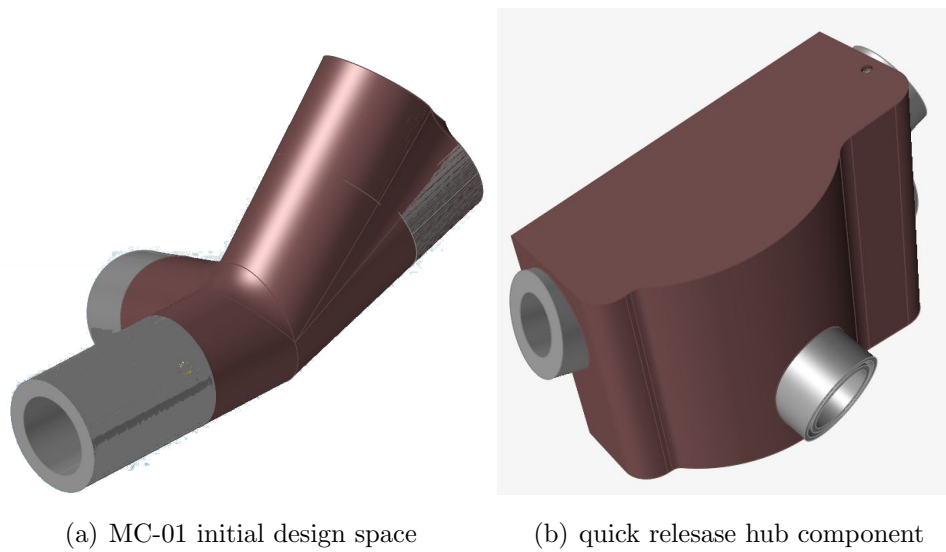
Figure 5.14: MC-01 Increased design space

There where two load cases that affect this component. First, with the wheel fixed, a force of 1500N was placed on the area that connects to the base unit in the -Z direction, while a load of 750 N was placed on the section attached to the mirrored part in that direction to simulate the players weight on the chair and the resultant tension from the other side of the part.

The second load case was an impact on the front of the wheelchair. In this case, the glued surfaces at the rear of BC-01 were fixed and a load of 1500N was placed on the tube surface towards the rear of the wheelchair.

As before the target for the optimiser was to reduce the mass of the part, with a safety factor of 1.5 and a minimum thickness of 5mm again to aid in the manufacturing of the parts while not allowing the component to become too thin and cause the build to fail.

5.4.4 Anti-Tip Connector (AT-01)

The anti-tip connector is probably the simplest of all the connectors connecting from the rear of the modular base unit down to another Frog Leg castor thus preventing the wheelchair from tipping over when the player goes to serve. Using a sprung castor could potentially aid the tennis player by adding slightly more flexible movement to the serve.

(a) AT-01 Initial

(b) AT-01 In assembly
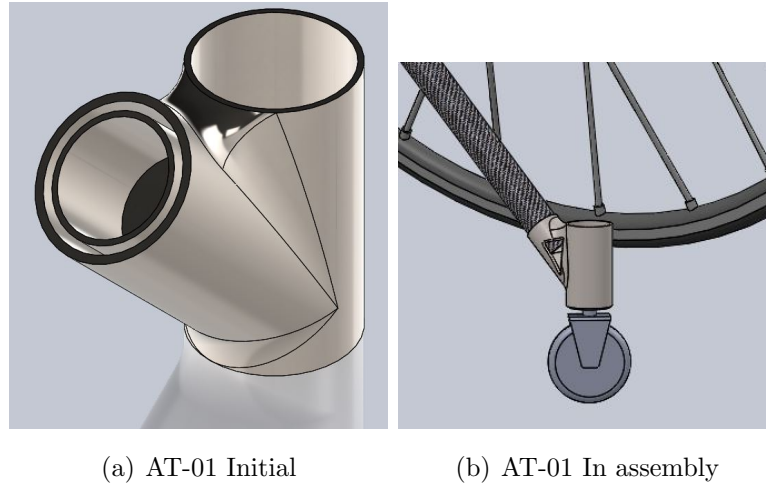
Figure 5.15: Anti tip connector

AT-01 Boundary Conditions

Setting the design space was quite simple. As with the other connectors, 20mm was kept to provide a reasonable bonding surface to hold the carbon tube in place. The other area excluded from the design space was where the castor wheel would be fitted. As with FC-01, clearance was left around this section to allow for easy assembly and to hold it in place. As with the other components the design space was increased, as seen in *Figure 7.11*. Leaving the space above the castor open allows the castor wheel to be easily fitted during the wheelchair's assembly.

The load case that is most relevant to this connector is the serve. To simulate this the face where the castor would be mounted was fixed, and a force was applied in the direction of the tube on that part of the connector.

As with the other components the optimisation was run to reduce mass with a safety factor of 1.5 and again with a minimum thickness of 2mm to reduce the chance of the build failing.

Chapter 6

Design Optimisation

This chapter focuses how the two proposed designs were optimised. First, optimising RMA's current wheelchair design, while also attempting to reduce disruption to their manufacturing processes by keeping the manufacturing methods and materials constant and adjusting the geometry of the wheelchair. Improve the design of the wheelchair in this way will helped to keep the manufacturing and design costs similar to those of the current set-up, thus preventing a negative financial impact on RMA and end users while still providing an improved wheelchair. A simple model of the current chair was developed, optimised for a reduction in mass and improved stiffness.

To optimise the modular wheelchair, a different approach was taken by breaking down the frame into separate components. The design was then improved by using a topology optimiser to remove any unnecessary material, thus reducing the overall mass of the part while maintaining the strength of each piece.

6.1 Design Optimisation

In tennis, the key movements are acceleration and quick and sharp turns. Thus, any optimisation should aim to reduce mass and increase stiffness where possible. This is because reducing the mass can increase the rate at which the wheelchair can accelerate after turning and stopping, while improving wheelchair stiffness ensures that power is not lost in the frame flex when accelerating around the court. It is important to ensure that these changes do not affect the stability of the chair, as this may affect turning and the player's ability to reach for the ball,

by keeping key parts of the tennis wheelchair geometry constant.

In the first stage of the optimisation process, the geometry was kept constant, and adjustments to the tube diameters and thicknesses were made to improve the performance of the sports wheelchair. The initial optimisation had a limited number of variables and aimed to provide an improved wheelchair design with almost no changes to RMA's manufacturing process.

The second stage involved increasing the number of variables in the optimisation by giving the coordinates of the space frame in the input file a limited amount of freedom in the X, Y, and Z directions. This identified the effect of geometry on the design goals and had a minor impact on the manufacturing process (by requiring slight alteration to some of the jigs). However, this should be easily achievable for RMA due to the company's ability to customise certain points to fit the athletes wheelchair.

The final stage of the optimisation process was to increase the number of variables further. By adding more coordinates along the length of each of the tubes in the space frame, the radius and thickness were used as variables, allowing to change along the length of the tubes. Manufacturing methods such as hydro forming, commonly used to manufacture bicycle frames, can be used to achieve the desired geometry. This stage of the optimisation process will require some changes to be made to RMA's set-up, as the tubes have custom geometry, which could lead to an expensive start-up cost, It is therefore, important for the design change to have a significant benefit.

This led to an optimisation tool that uses an algorithm to run multiple variables through a simplified three-dimensional finite element model composed of one-dimensional truss elements. This model is low-fidelity and can be run and changed quickly and easily, allowing the optimisation process to be applied to a large range of scenarios, depending on sport and customer measurements.

6.2   Exploratory Optimisation

With the model validated, the parameters could be modified to measure the effect on the wheelchair. This was performed according to the following three parameters: tube cross-section, geometry, and variable diameter tubing.

To optimise the design, it was necessary to run multiple simulations, with a wide range of design variables and multiple design goals. To achieve this, Dassault systems I sight software was used to create a design work flow process, as presented in *Figure6.1*. The optimisation module was used to alter the chosen design variables and to feed the new values back into the Abaqus model, and the mass and maximum displacement values for each load case were exported as the design goals. The optimisation module had a variety of optimisation techniques to choose from. In each optimisation step, DOE and two exploratory optimisation processes were used and the results compared to determine which one would yield the best results.

Latin hyper cube, is one of the most commonly used Monte Carlo based, sampling methods for DOE [58]. The Latin hyper cube generates a series of sample points evenly throughout the design space, splitting the design space in to subspaces based on the variables to ensure that no data points are repeated.

NSGA II, the non-dominated sorting GA is a multi-objective exploratory technique, where each objective is treated separately and optimised using a standard genetic operation. The data is then arranged based on a non-dominated sorting technique once the optimisation process has finished. A Pareto set has been constructed with points that comprise optimum designs, where improving one of the targets is impossible without affecting the other design goals.[76][77]

Multi-Objective PSO, is a population-biased search technique, where the particles location (potential solution) are continuously altered within a specified range of values. The value of the chosen parameter moves around the design space until the optimum value has been found. The random movement in the initial iteration allows for a large exploration of the design space because the starting point and directions are random for each particle. After each iteration, the particle's movement becomes more focused, depending on its movement and

the movement of the other particle's. The particles keep changing, locations until
they converge on the optimum solution. [78]
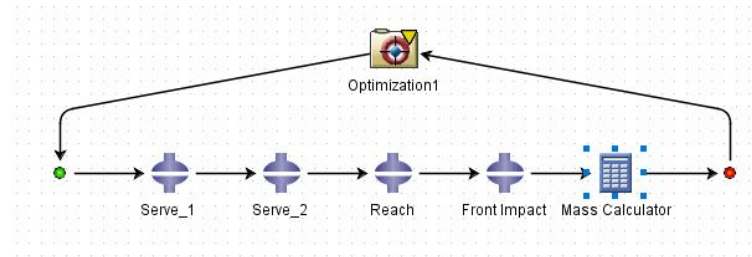
Figure 6.1: Isight optimisation loop

6.2.1 Targets

Most of the movements during a game of wheelchair tennis include short distance
sprints and quick turns. Therefore, acceleration and turning ability are key de-
sign considerations for the tennis wheelchair. The two targets chosen were mass
and stiffness.

Reducing the mass of the wheelchair should help to improve the ease with
which the it can accelerate. As the mass could not be exported from Abaqus into
Isight, a calculator was added to the optimisation loop (*Figure 6.1*), and using
the changed parameters were used to calculate the volume of each tube, then,
the density of the aluminium was used to calculate the total mass of the chair.
As with the initial Abaqus input deck, the calculator file was set so that any of
the parameters were easy to change. This made it easier for future models to
experiment with different types of materials and also when additional elements
are added to the optimiser.

To increase the stiffness of the design, at necessary target is to increase the
efficiency at which the athlete can apply force to the wheels. Another is to im-
prove the turning ability of the chair by reducing flex in the frame when their
player manoeuvres the wheelchair using the lower body. In order to set improv-
ing stiffness as a design goal, displacement values were extracted from the three
static steps at desired locations in the wheelchair, and set to target zero during
the optimisation loop. However as mass reduction was the primary goal of the
optimisation the displacement pass criteria for optimum deigns where given an

allowance of +0.1mm.

Finally, the maximum stress was extracted as a design goal from the impact load case to determine whether if it was possible, to lower the maximum stress can be lowered and the wheel chair can be re used after an impact, If the value can be brought below the yield point.

6.2.2   Tube Diameter (OP1)

The initial stage of the optimisation examined changing the tube diameter and thickness only to determine whether it would provide any mechanical benefit to the design. As previously mentioned, the benefit of starting with these two variables is that the geometry of the chair remains unchanged. Thus, if the wheelchair being optimised is part of a larger production run, there would be no need to adjust any jigs used when welding the wheelchair together. The main adjustment to the set up was to find the correct tube size.

To reduce the computational time, limits were set with a range of values that the optimiser could select. To begin with, the limits for the radius of the tubes were given a range of 3 mm above and below each of initial values.The limits for the thickness of each tube was given a range to a minimum wall thickness of 0.5 mm below and 2 mm above the current value. The smaller lower range was to prevent the tubes from becoming too thin and being difficult to manufacture.

6.3   Modular Design Optimisation

As can be seen in *figure 5.8* the modular design is made up of twelve separate printed parts. The parts that connect the frame to the base unit (SC-01) have not been optimised in this section due to assembly restrictions. For example, accessing the bolts to attach the base unit reduces the size of the design space significantly, leaving the seven lower frame connectors to optimise.

To save computational time, the parts were mirrored along the centre plane. Only one of those parts was optimised and that part was then mirrored for the build. Leaving four components (FC-01, MC-01, BC-01 and AT-01) to be optimised using INSPIRE 2019.

Altair Inspire is a generative design tool that utilises topology optimisation to create lightweight structures [79] by removing unnecessary material in the design space, due to a set boundary conditions.

The process involved importing the geometry for each component into Inspire and creating the design space as described in Section 5.4. The optimisation was conducted three times using three different materials (Steel, Aluminium, and Titanium). For each optimisation, the target goal was set to reduce the mass of each component. After the optimisation was completed, the polynurbs feature in Inspire was utilised to improve the geometry. So the parts could be exported for manufacture.

Chapter 7

Optimisation Results

The results chapter is divided into three sections. Firstly, it outlines the results of the initial simulation conducted on RMA's current tennis wheelchair, which proved the model's predictability before proceeding to the optimisation phase. Secondly, it presents the results for optimizing the current design using DOE and exploratory techniques to increase the variables in each iteration. Finally, it discusses the results of the topology optimisation for the modular wheelchair, analysing each of the lugs individually.

7.1 Initial Simulation

To save on computational time and cost in the optimisation phase, a simple 3D model represented by 1D beam elements of the frame component of RMA's current wheelchair was created in Abaqus, (*Figure5.1*). The model was then parametrised to allow the tube geometry to be changed.

The benefit of setting up the model in this way is that the geometry could easily be altered with the recommended changes after the optimisation. Separate input files for the tube dimensions and space frame coordinates were imported from the CAD model, and one file was made for each of the load cases. This also allowed the model to be easily altered so that it could potentially be used to optimise based on a player's mass and power or even altered further and applied to wheelchairs for sports like basketball or rugby.

7.1.1 The Serve (Step 1 and Step 2) Results
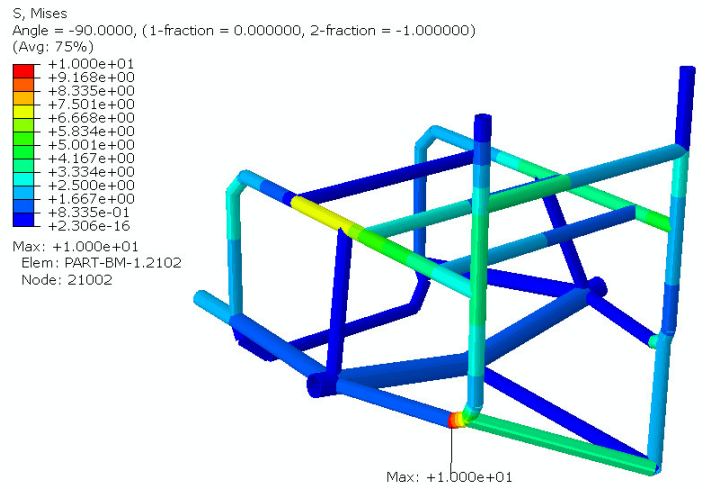
(a) Von Mises diagram for the preparation phase of the serve (Step 1)
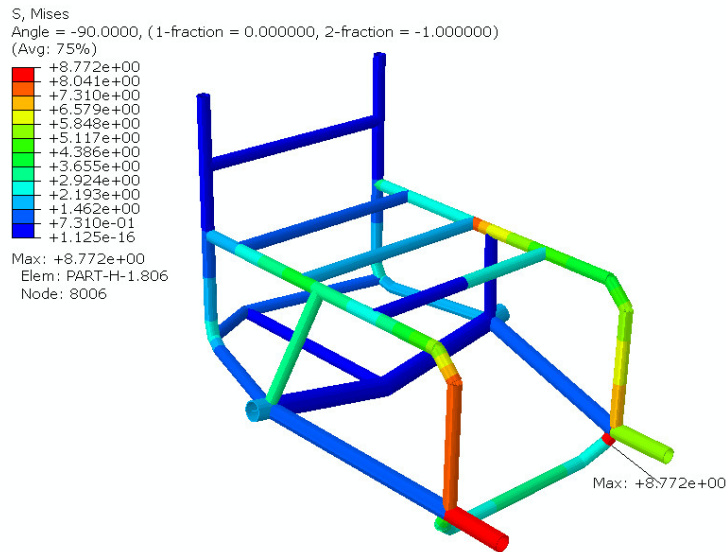
(b) Von mises diagram for the follow through stage of the serve (Step 2)

Figure 7.1: Von Misses diagram of both stages of a serve

As illustrated in *figure 7.1* for load case 1, the load was concentrated on the left side of the wheelchair as the player moved during the preparation phase of the serve. The maximum stress of 10.0 MPa occurred on the left bend, where the anti-tip wheel connected to the rest of the chair (*Figure 7.1 [a]*) and with a

maximum displacement of 0.6mm at the top left side of the backrest, (*Figure 7.2*).

The stress distribution depicted in *Figure 7.1(a)* was as expected because most of the load was focused on the left side of the wheelchair as the player's weight moved to that side at the beginning of the serve; the maximum displacement occurred at the left side of the backrest of the chair. This location is expected to experience maximum displacement due to the loads exerted on the back rest and the largest movement occurring on this unsupported element (*Figure 7.1(b)*).

The second load case was the follow-through part of the serve, where the maximum stress occurred at the front left castor and the connecting points of the foot rest, with a value of 8.77 MPa (*Figure 7.1[b]*); furthermore, a maximum displacement (*Figure 7.2*) of 0.5mm occurred slightly to the centre at the front of the seat and foot rest. For the most part, stress was distributed evenly from left to right over the front of the chair, but with a slight bias on the left castor, which matched the racket hand.
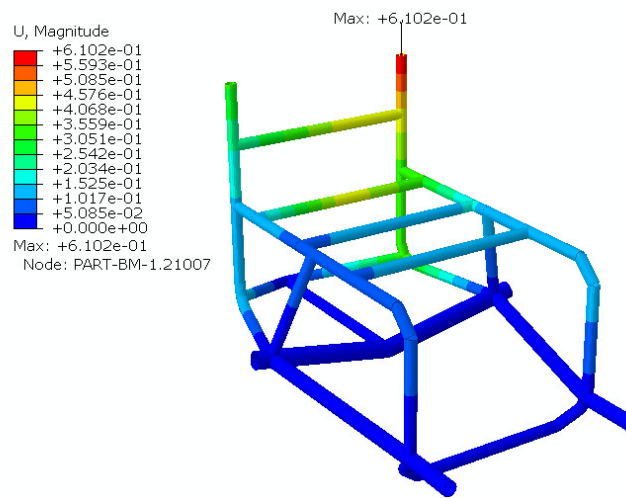
(a) Serve 1 (displacement) (Step 1)
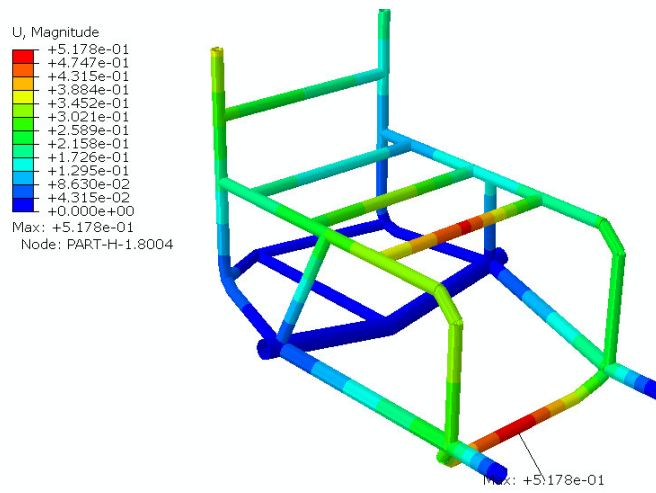
(b) Serve 2 (displacement) (Step 2)

Figure 7.2: Displacement Plots for Step 1 and Step 2

7.1.2 Reach (Step 3)
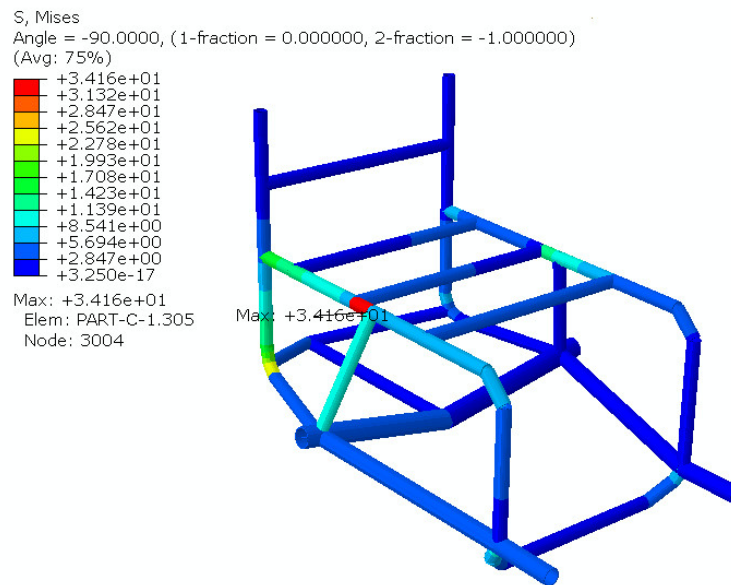
(a) Reach Von Mises stress diagram (Step 3)
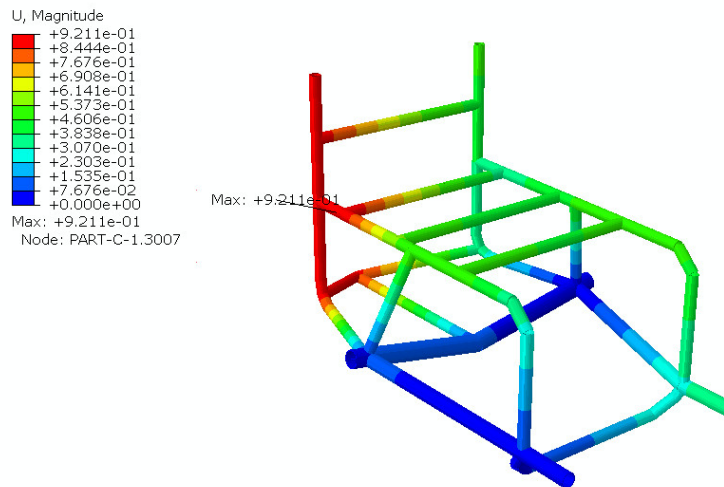
(b) Reach displacement diagram (Step 3)

Figure 7.3: Von Mises and displacement diagram of the reach load case

Compared to the other load cases, the stress distribution was quite focused on the left of the wheelchair, with a peak of 20.4 MPa, occurring where the support from the driven wheel is connected to the seat, (*Figure 7.3*). The maximum displacement of 0.7mm occurred at the top of the back rest.

7.1.3   Front Impact (Step 4)

As stated in an earlier chapter, this is an extreme load case and will not occur very often. A large stress concentration of 162 MPa occurred on the front of the seat, behind the first cross beam, and as the tubes bend to the base tubes of the wheelchair (*Figure 7.4[a]*) The maximum displacement of 0.87mm (*Figure 7.4*(b)) occurred at the top of the backrest which is quite large considering the pinned nodes. The player moving forward and exerting force on the belt anchor points had the largest effect on the wheelchair, causing both high displacement and stress concentrations in those locations.
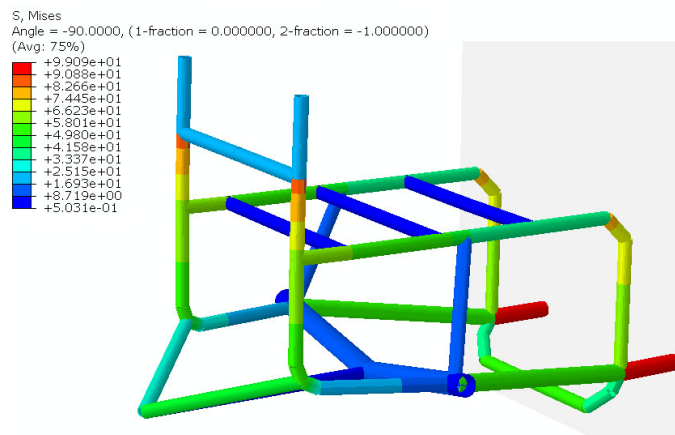
(a) Von Mises diagram of initial stage of impact
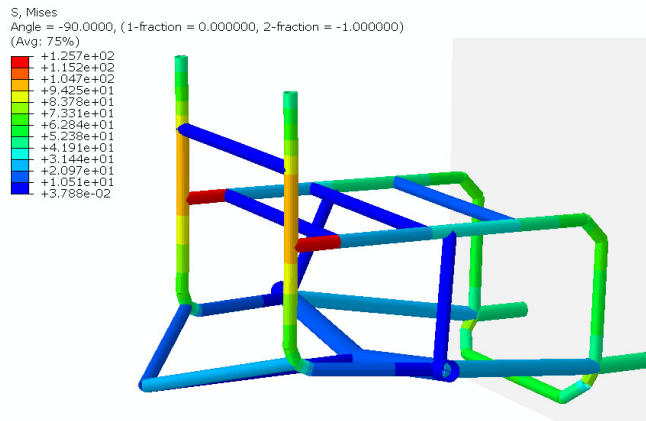
(b) Von mises diagram of largest stress during impact

Figure 7.4: Results for front impact load case

7.1.4 Model Validation

When the strain gauge results obtained in the practical tests were compared with the values in above-mentioned the simulations, some discrepancies were found in the values, with the simulated load on the wheelchair producing a much larger peak stress. This could be due to larger concentrated forces applied to the simulated tennis chair compared with those applied in the practical testing. As the simulated player's weight was 1.5 times RMA's maximum load rating of 95 kg and the test subject weighed 81kg, it is also worth noting that the test subject used was not a professional athlete and their movements might not be as aggressive.

However, when the results where compared, the wheelchair was seen to behave in the same way, with the same areas of peak load and the wheelchair acting as predicted in other regions. For example, in the preparation phase of the serve, both sets of data demonstrated that the peak loads occurred on the backrest tube on the player's racquet side when they lean back and that the load moved to the front in the follow through phase of the serve (step 2), although with discrepancies in the values.

7.2 Exploratory Optimisation Results

7.2.1 Tube Diameter Optimisation Results

Table 7.1 Presented the results from the first optimisation loop with the three different optimisation loops used, namely DOE (Latin hyper cube), GA (NSGA), and a PSO (Multi objective PSO). The table shows the design solution deemed to be the optimum by each of the techniques. As stated, each tube in the wheelchair was assigned a letter(*Figure 5.2*) and the optimum design parameters are displayed below.(*table 7.1*)

Table 7.1: Design goal output for each optimisation technique (OP1

		Original	DOE	GA	PSO
Number Of Potential Designs		1	1000	1441	751
Goals					
Mass	Mass (g)	2082.95	1889.76	1983.5	1989.5
	Difference (%)	0	9.27	4.77	4.49
Displacement	Serve 1 (mm)	0.6	0.7	0.59	0.58
	Serve 2 (mm)	0.26	0.26	0.26	0.25
	Reach (mm)	0.9	1.03	0.85	0.88
Stress	Impact (MPa)	162	141.28	131.764	142.1
Variables (mm)					
Tube A	Radius	12.7	12.53	11.9	13.9
	Thickness	1.5	1.35	1.35	1.4
Tube B	Radius	10	9.5	10.5	10
	Thickness	2	1.8	1.8	1.9
Tube C	Radius	10	9.5	10.9	9.7
	Thickness	2	1.8	1.8	2
Tube D	Radius	16	15.9	15.1	16.4
	Thickness	2	1.9	1.9	1.8
Tube E	Radius	10	9.4	9.3	9
	Thickness	2	1.44	1.5	1.44
Tube F	Radius	10	9.1	10.3	9
	Thickness	2	1.35	1.5	1.65
Tube G	Radius	10	10.3	9.1	9.3
	Thickness	2	1.5	1.4	1.4
Tube H	Radius	10	9.6	10.5	10.2
	Thickness	2	1.8	2.1	1.9
Tube I	Radius	10	9.6	10	10.5
	Thickness	2	1.9	1.8	1.9
Tube J	Radius	10	9.3	9.6	11
	Thickness	2	2.06	1.9	2
Tube K	Radius	10	10	10	9
	Thickness	2	1.8	1.9	1.9

As displayed in *Table 7.1*, all three of the optimisers were able to locate a design that met the specified targets. The DOE method was most successful at reducing the mass (primary goal) of the wheelchair, which it reduced by nearly 10 %. However, the reduction in mass came at the expense of the other targets.

Although not as impressive of a mass reduction, both the exploratory optimisation techniques managed to achieve all set goals by reducing the mass of the wheelchair and maintaining or slightly improving the stiffness of the chair, as well as achieving a reduction in the stress seen in the impact load case.

7.2.2 Frame Geometry (OP2)

Once the cross-section of each tube had been optimised, the next step was to add the geometry as a design variable; to achieve this the input deck needs to be parametrised further. With the coordinates parametrised, if the coordinates in a part were the same, they were assigned the same parameter. This has the side effect of keeping the wheelchair symmetrical, as the load cases are not symmetrical around the chair. This also helps limit the number of variables in the optimiser. As before, the amount of movement was limited to 10 mm above or below each of the X, Y and Z coordinates. This change can identify areas of the wheelchair that will require adjustment. If in the initial simulation the selected variable is close to the limits this can be adjusted accordingly in the second optimisation iteration.The optimisation results for all three loops are presented in *Table 7.2*, which also displays the changes that where made to each parameter in the optimisation loop. The changes made to the coordinates for each of the designs are indicated through the change in tube length.

Table 7.2: Design Goal Output for Each Optimisation Technique (OP2)

		Original	DOE	GA	PSO
Number Of Potential Designs Checked		1	1000	1500	1001
Goals					
Mass	Mass (g)	2082.95	1634.88	1764.29	1853.05
	Difference (%).	0	21.51	15.29849	11.03723
Displacement	Serve 1 (mm)	0.6	0.8	0.7	0.78
	Serve 2 (mm)	0.26	0.21	0.18	0.18
	Reach (mm)	-0.9	-0.93	-0.93	-0.98
Stress	Impact (MPa)	162	152.72	140	144.82
Variables (mm)					
Tube A	Radius	12.7	15	12.7	10
	Thickness	1.5	0.6	0.6	2.3
	Length	427	413	438	429.9
Tube B	Radius	10	12.1	9.9	8
	Thickness	2	1.4	1.9	1.1
	Length	610	620	600	619
Tube C	Radius	10	9.1	11	12
	Thickness	2	0.6	1.4	0.5
	Length	980	974	981	970
Tube D	Radius	16	19	15.2	16.75
	Thickness	2	0.7	1.5	3
	Length	264	268	267	262
Tube E	Radius	10	7.5	9.2	12
	Thickness	2	3	0.6	0.5
	Length	345	345	354	352
Tube F	Radius	10	7.5	10	10
	Thickness	2	1.1	0.5	0.5
	Length	345	345	343	352.3
Tube G	Radius	10	11	9.4	9.8
	Thickness	2	2.7	0.6	2
	Length	345	345	343	344.96
	Radius	10	9.6	10.9	8

Tube H	Thickness	2	2.5	0.9	1.6
	Length	423.2	425	434	442
Tube I	Radius	10	9.2	9.5	8
	Thickness	2	1.3	2.75	0.5
	Length	203.561	213	213	203
Tube J	Radius	10	12.1	8	9.3
	Thickness	2	0.65	2	0.6
	Length	240.1	238.4	252.46	245.19
Tube K	Radius	10	9	11.3	12.7
	Thickness	2	0.9	2.1	3
	Length	359	356	356	362

As *Table 7.2* indicates, adding extra variables to the optimiser affected the optimisation techniques. Again, all three techniques produced a wheelchair design that met the design targets.

The DOE Optimiser reduced the mass of the wheelchair by over 400g while keeping the other design targets within tolerance with the exception of the displacement of serve 1. The design produced through the DOE optimisation produced the most suitable results overall, as it reduced the mass of the frame by 15% and met all of the specified design targets

7.2.3   Variable Tube Diameter (OP3)

The final area of optimisation involved further adjusting the geometry of the tubes by increasing the number of variables in each of their dimensions. To this end, each of the parts assigned to each tube within the model was split into more parts. An extra coordinate was added between each coordinate in the Abaqus input file. For example, Part A previously represented the tube on the players right hand side of the wheelchair (from the castor to the driven wheel). This tube originally consisted of three coordinates that composed a single part, but now it was made up of five coordinates and four different parts (*figure 7.5*). Each part is given the same parameters stated in step one (tube diameters), which allowed the optimisation process to alter the cross-sectional area of each tube along its length. This produced a model consisted of 58 parts.

Again, limits were set on the parameters, such as the initial optimisation set-up, of 2mm above and below the radius variable and 4 mm above and 0.5 mm below the tube thickness. To fit the mirrored restriction on the wheelchair design, the mirrored parts where assigned the same parameter for the tube diameter and thickness. For example, Part AA and AAM where both assigned AA r and AA t as the tube dimensions.
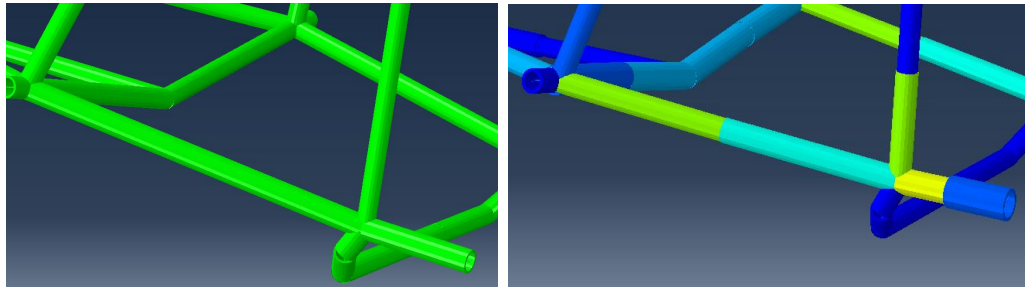
(a) Part A   (b) Part AA to Part AD

Figure 7.5: Part-A and Part-A to Part AD

Approximation

As the number of variables increased, so did the number of possible design solutions. Therefore, it was necessary to increase the ranges of the optimisers. This leads to a large increase iteration required to find the optimum design solution, thereby greatly increasing the computational time for each loop.

To reduce the computational time for OP 3, a model order reduction method was used to create an approximation model to replace the input files in the loop(*Figure 7.6*). This is an effective method for reducing design cycle times [80].
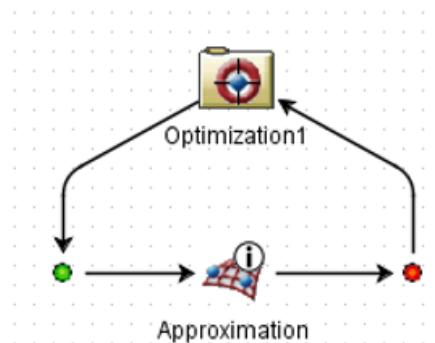
Figure 7.6: Approximation Loop in Isight

A response surface model tool in isight was used, as it is a suitable method for a problem with several variables. It requires multiple points to create the response. The initial DOE optimisation was completed using 1500 design points. Once the model had been created, 100 points were extracted from the DOE model and compared with the response calculated by the approximation the results of which are shown in *figure 7.7*
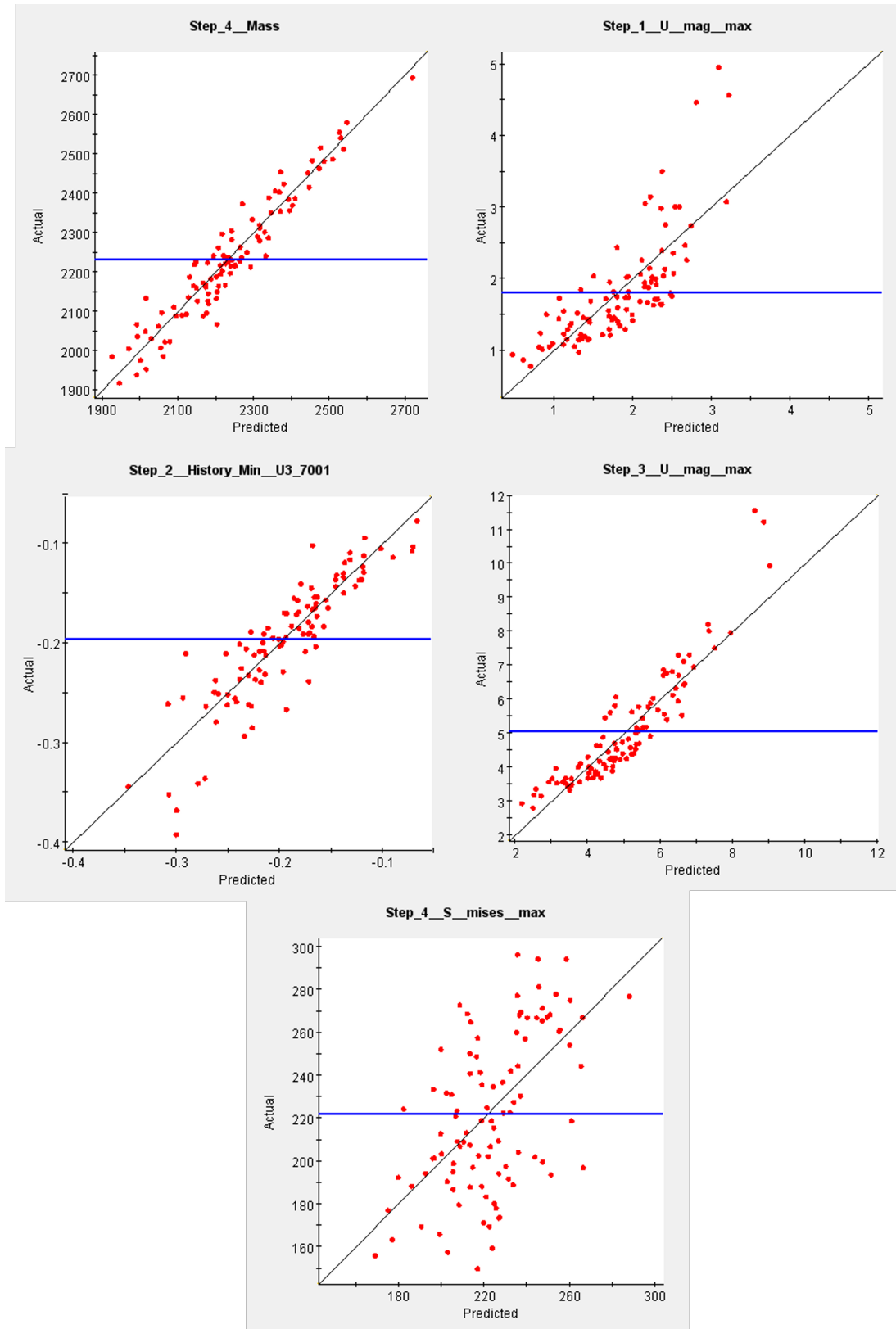
Figure 7.7: Approximation plots for outputs of OP3 DOE using 100 sample points

figure 7.7 reveals that the approximation plot for four required outputs, The displacement and mass outputs had a reasonable output with many of the plotted points close to the response curve. The outlier was the max stress output for the final as shown in *figure 7.7* this could be due to the dynamic nature of this load case being less predictable.

Due to the mass reduction being the higher priority output the approximation was used and the optimum output was re-run to confirm the results.

Variable Tube Diameter Results

Table 7.3 below shows the results from the final optimisation stage with 100 different parameters. The results reveal the different diameters along the pre existing tubes.

Table 7.3: Design Goal Output for Each Optimisation Technique (OP3)

			Original	DOE	GA	PSO
Number Of Potential Designs			1	1500	4001	1001
Goals						
Mass		Mass (g)	2082.95	1966.80	1752.00	1753
		Difference (%)	0	5.58	15.89	15.84051
Displacement		Serve 1 (mm)	0.6	0.56	0.75	0.6
		Serve 2 (mm)	0.26	0.27	-0.29	-0.2
		Reach (mm)	-0.9	-1.90	0.00	0
Stress		Impact (MPa)	162	142.00	168.00	168
Variables (mm)						
Tube A	A	Radius	12.7	14.00	10.65	9.70
		Thickness	1.5	2.90	3.85	3.17
	B	Radius	12.7	11.30	10.97	12.70
		Thickness	1.5	2.06	3.13	1.60
	C	Radius	12.7	11.27	9.84	12.70
		Thickness	1.5	0.50	2.10	1.75
	D	Radius	12.7	10.65	8.52	10.19
		Thickness	1.5	0.73	1.09	1.00
		Radius	10	10.53	11.36	12.06

	A	Thickness	2	1.89	2.32	1.61
Tube B	B	Radius	10	9.88	7.95	9.14
		Thickness	2	2.84	1.91	4.00
	C	Radius	10	9.39	7.89	10.47
		Thickness	2	2.98	2.74	4.00
	D	Radius	10	12.00	10.25	6.00
		Thickness	2	0.82	3.09	4.00
	E	Radius	10	9.90	10.13	6.38
		Thickness	2	2.20	1.64	1.17
	F	Radius	10	11.57	6.16	6.00
		Thickness	2	0.50	2.04	1.42
Tube C	A	Radius	10	10.00	10.63	11.00
		Thickness	2	4.00	1.98	1.00
	B	Radius	10	9.10	5.31	4.00
		Thickness	2	3.21	1.95	4.00
	C	Radius	10	8.47	7.59	11.00
		Thickness	2	2.17	1.33	1.00
	D	Radius	10	8.55	4.43	4.00
		Thickness	2	1.25	1.88	3.26
	E	Radius	10	6.92	10.96	8.45
		Thickness	2	3.03	2.92	1.00
	F	Radius	10	9.57	8.97	11.00
		Thickness	2	2.43	1.38	1.00
	G	Radius	10	10.00	9.10	11.00
		Thickness	2	1.19	1.07	1.00
	H	Radius	10	10.00	6.42	8.51
		Thickness	2	1.33	3.74	1.00
	I	Radius	10	8.30	10.74	4.55
		Thickness	2	3.81	1.68	1.00
'Tube D	A	Radius	16	11.36	7.13	12.00
		Thickness	2	2.92	1.12	2.31
	B	Radius	16	14.19	7.82	12.00
		Thickness	2	2.78	3.86	2.31
	C	Radius	16	2.78	6.42	12.00
		Thickness	2	2.86	1.85	2.31

Tube E	A	Radius	10	6.28	9.98	6.00
		Thickness	2	1.80	1.66	1.00
Tube F	A	Radius	10	10.00	5.22	10.00
		Thickness	2	0.50	1.86	1.00
Tube G	A	Radius	10	6.83	5.25	6.00
		Thickness	2	0.50	2.04	4.00
Tube H	A	Radius	10	9.96	10.01	7.60
		Thickness	2	2.43	2.67	1.00
Tube I	A	Radius	10	10.32	6.21	8.04
		Thickness	2	2.42	1.38	4.00
	B	Radius	10	9.65	7.03	12.70
		Thickness	2	2.80	1.91	2.94
Tube J	A	Radius	10	10.02	10.37	7.35
		Thickness	2	2.57	1.27	1.00
	B	Radius	10	10.28	7.80	6.00
		Thickness	2	2.32	1.42	1.92
Tube K	A	Radius	10	9.97	8.54	6.00
		Thickness	2	2.12	2.12	3.35
	B	Radius	10	12.00	6.55	9.73
		Thickness	2	1.58	2.82	1.39

As *Table 7.3* indicates, the three optimisation techniques were all successful in reducing the mass of the wheelchair. The GA and PSO methods both improved on the previous iteration with 12g and 100g respectively. However with more parameters the mass reduction for DOE was lower than for the two previous iterations, at 5.6% in total. This could be due to the size of the design space and the more ridged search pattern.

With regards to displacement, PSO met all of the design targets, either increasing or maintaining the displacement value of the previous wheelchair.

7.3 Modular Design Optimisation Results

As mentioned earlier, a different approach was taken to enhance the modular design. Topology optimization was used to individually improve seven out of the

twelve printed lugs. Three different materials - steel, aluminium, and titanium - were considered for each optimisation phase to determine if any effect on the geometry was observed. As before the design target where the same, to reduce the mass of the parts whilst retaining stiffness.

7.3.1 FC-01 Results

The part produced after the simulation had been run is presented in *Figure 7.8*, while the printed part in *Figure 7.13*. The mass of the initial part was 740.5g when manufactured from 316 stainless steel. After the topology optimisation and smoothing processes the mass of the part was reduced to 379.5g; thus, the weight of the part had been reduced by over 51%.

As can be seen in *Figure 7.8*, most of the material was removed as the component met the castor holder, leaving material along the load paths.
The optimiser was also run to adjust the types of materials available for printing aluminium (7075-T6) and titanium (Ti-6Al-4V) as can be seen in *Figure 7.8*, and produced some lightly different shapes. The aluminium part started at 194.48g; after optimisation using the same targets as before the weight was reduced by 32.33%. to 134.46g. The shape produced was quite different to the optimised steel part with more material lower down around the castor to compensate for aluminium's lower Young's modulus; furthermore its lower density resulted in more material being used to improve the overall stiffness of the part. The design also reduced some of the material higher up to meet the mass reduction target. Although it is worth increasing the thickness of the part on the left as can be seen in the figure, it could be a potential point of failure during the printing process.

When using titanium, the initial part weighed 334.53g which was reduced to 128.3g through topology optimisation for an approximate reduction of 61%. Although it had a similar over all shape to the 316 part, the mass was reduced further by replacing the solid material in the main body of FC-01 with a triangular structure, which explains the weight reduction in the part, as seen in (*Figure 7.8*(d)).

(a) Front lower node initial

(b) Front lower node optimised (steel)

(c) Front lower node optimised (aluminium)

(d) Front lower node optimised (titanium)
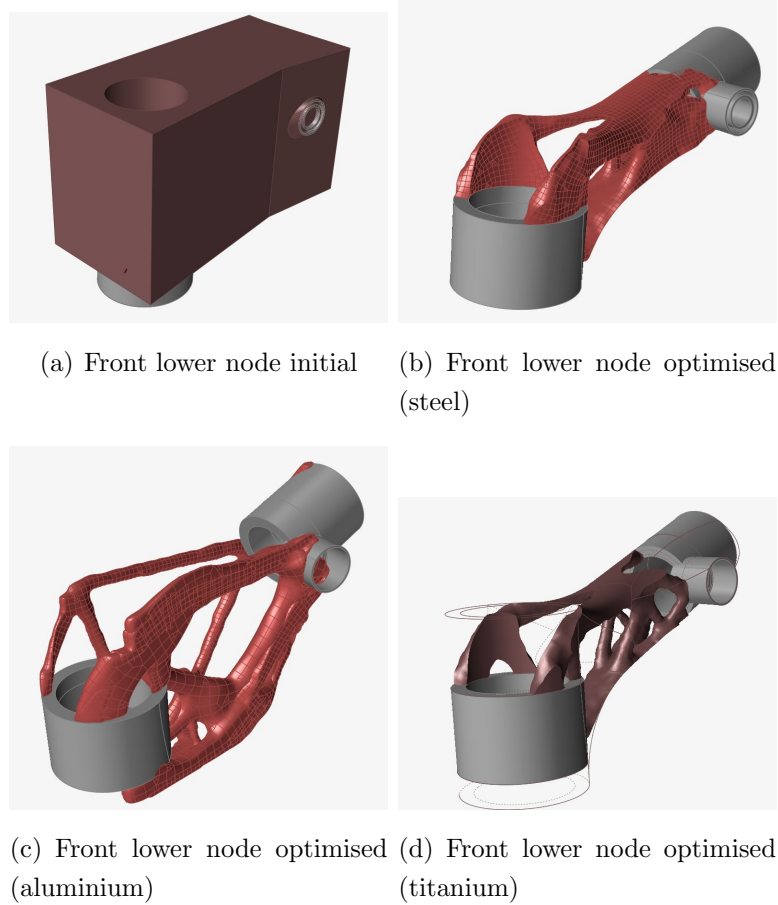
Figure 7.8: Front lower node

7.3.2 MC-01 Results

The shape produced after the simulation was presented in *figure 5.4.2*. Regarding the results for this component, it is noteworthy that despite the increased design space, the final shape that was produced was very similar to the original design. The main difference was the hollowing out of the lower section, which reduced the weight from 614g to 303g, for a weight saving of over 50%, which is considerable.

As before, the middle connector was also run using aluminium and titanium as can be seen in *Figure 5.4.2*. The aluminium part started off very light at 85.2g, and it was reduced by a further by 32%. to 58.35g removing a significant amount of material when compared with the initial design.

The titanium parts initial design was 134.89g, which was reduced to 92.48g. As

with the aluminium part much of the material was removed from the centre of the design space.
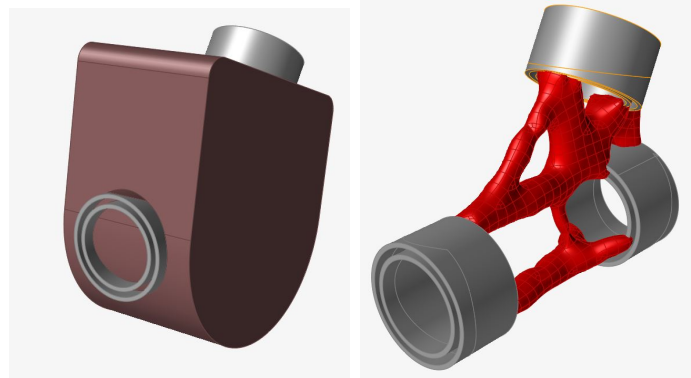
(a) Middle connector initial

(b) Middle connector optimised (steel)
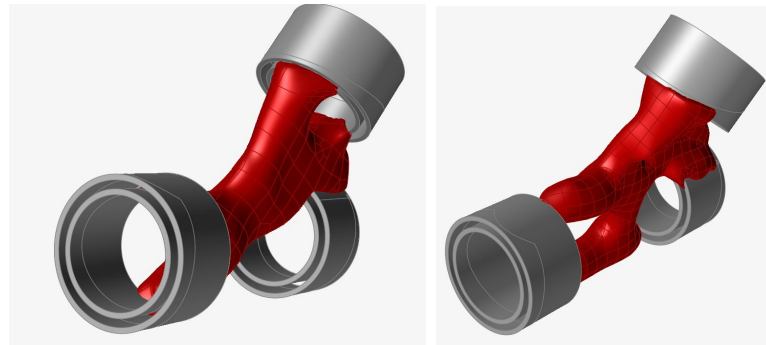
(c) Middle connector optimised (aluminium)

(d) Middle connector optimised (titanium)

Figure 7.9: Middle connector optimisation

7.3.3 BC-01 Results

As can be seen in *Figure7.10*. The design of the BC-01 took advantage of ALM to produce a shape that would be extremely difficult to manufacture in other methods. The part was originally 614.75g and was reduced to 368.81g for a 40 percent weight reduction.

As with the previous parts, the design was optimised for the other two options available, namely aluminium and titanium. The aluminium parts started at a mass of 227.49g, which was reduced to 62.6g, for a reduction while keeping most of the optimised shape similar. As can be seen in *Figure7.10(c)*, some differences

existed in the structure, increasing the amount of reinforcement in the centre of the part.

The initial mass of the titanium connector was 359.82g reduced to an optimised mass of 303.1g. The basic shape of the part was like the previous two iterations but with the volume slightly increased in the optimised section of the part.
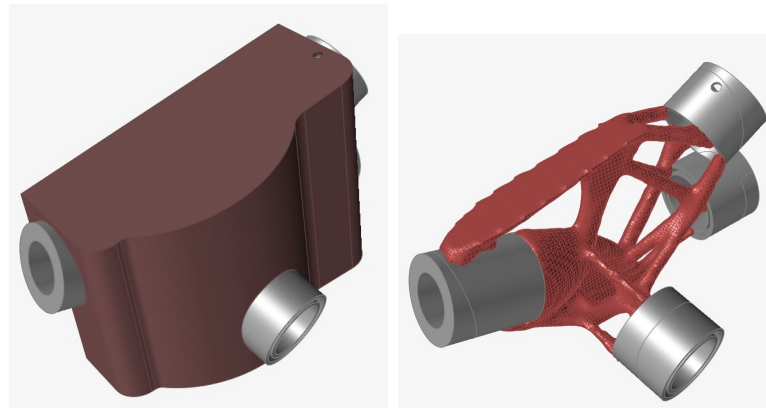
(a) Initial Back Connector (BC-01)

(b) Optamised Back Back Connector (BC-01)(Steel)
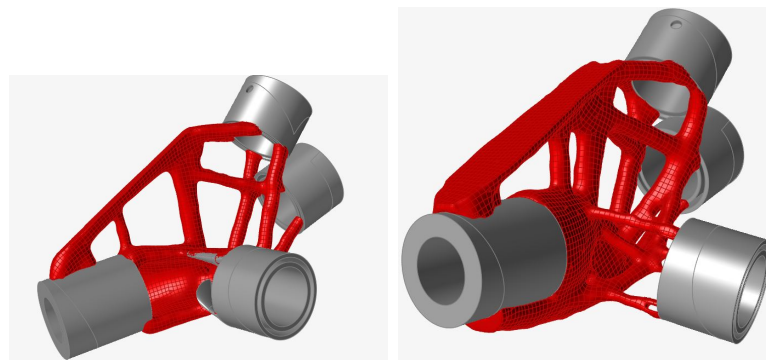
(c) Optamised Back Back Connector (BC-01) (Aluminium)

(d) Optamised Back Back Connector (BC-01)(Titanium)

Figure 7.10: Back Connector (BC-01)

7.3.4 AT-01 Results

As can be seen in *Figure7.11* most of the material was removed towards the top of the part, keeping material in the direction of the load case. The mass was reduced from an initial 165.95g to an optimised mass of 124.22g, for a reduction

of roughly 25% for the 316 steel build (*Figure7.11(b)*). The aluminium part (*Figure7.11*(c)) started at 56.01g and was reduced to 37.04g; again, the material was kept in a similar place to the optimised geometry of the 316 part, retaining material along the load path and removing more material at the base of the castor holder.

Again, the optimised titanium connector kept the material in similar places to the two previous materials with a reduced volume of material as can be seen in *Figure7.11*(d). This reduced volume brought the initial mass of the component down from 61.1g down to 54.1g for a saving of 7g.

(a) Initial anti-tip connector (AT-01)

(b) Optimised anti-tip connector (AT-01)(steel)

(c) optimised anti-tip connector (AT-01) (aluminium)

(d) Optimised anti-tip (AT-01)(titanium)

Figure 7.11: Anti-tip connector (AT-01)
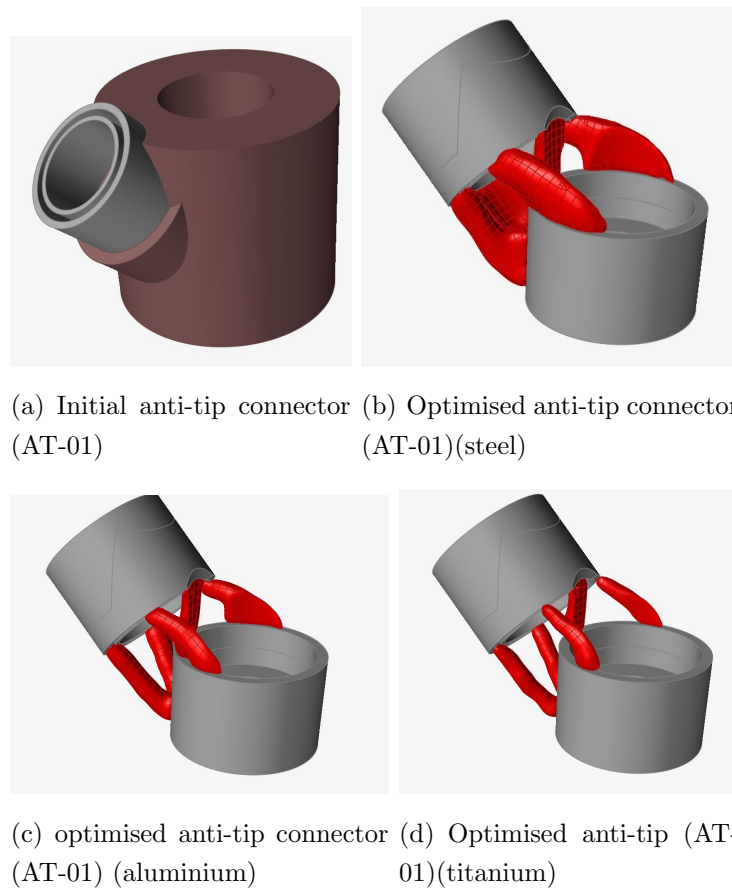
7.4 Manufacturing Optimised parts

The Renishaw AM400 system was used to manufacture the optimised wheelchair parts. When manufacturing parts on a printer it was important to consider where

to put the parts on the build plate. Twelve parts fit on a 250mm x 250mm plate, which meant one build per wheelchair. This ensured an efficient use of space as well as manufacturing time.

When placing the parts on the plate, it was important to adjust their orientation and position of the part,thereby ensuring that the number of overhangs in the build were avoided if possible as well as unnecessary support material. This helped to increase the material efficiency of the build and reduced the post processing time for removing the support material.

Another important consideration when organising the parts on the build plate was to ensure that each part have enough room to reduce the amount of heat build-up, as this could lead to residual stress in the final part and to a failed build, or problems when the parts are removed from the plate. With the set-up depicted in *Figure7.12*, the build was comprised 2564 layers at 50 microns thick, and took 58 hours to build.

(a) Finished Build Plate A   (b) Finished Build Plate B

Figure 7.12: 316 Steel completed Build plate

Once the printing process is complete, the parts can be removed using an Electronic Discharge Machine (EDM). Clearance must be ensured for the tubes to fit into each printed section. To achieve this, a final post-processing machining step is required to cut threads and make sure the tube inserts are free of build material. A machined thread has a greater tolerance than a printed thread, hence the need for this step.

Two threads must be machined into the parts. The BC-01 components require two M10 threads to hold the quick-release part of the driven wheels, and an M3 thread must be cut into all parts, as shown in the *Figure 7.13*.

When dry-fitting the wheelchair, a grub screw can be inserted to clamp the tubes in place to verify that the build is satisfactory.

7.4.1   Assembly

Once the dry fit was been deemed satisfactory, at this stage in the build, the shipping costs could be reduced if the chair can be easily assembled at the customers address, simply adding epoxy to the labelled tubes and inserting the tubes into each of the connectors. Any excess epoxy was removed from the m3 grub screw port before the grub screw was re-inserted to clamp the tube into place while the epoxy sets.

When fitting the seat connectors (SC-01) it is recommended to loosely fit them to the base unit as it can then act as a jig and reduces the chance of any issues in the final assembly.

Once the frame has set, the next step is to add the driven wheels to BC-01 and castors to the connectors FC-01 and AT-01. The final step is the seat assembly and this can be added to the top of the base unit completing the chair assembly. Once the chair had been assembled there were still some adjustments to be made to the chair, as the base unit could be adjusted in the forward and backward directions using different seat inserts to adjust the centre of gravity.

(a) Prototype dry assembly (Front)

(b) Prototype dry assembly (Rear)

(c) BC-01 printed part

(d) FC-01 printed part

Figure 7.13: Printed prototype test assembly

Chapter 8

Discussion

This chapter aims to discuss the outcomes obtained by optimizing the two suggested designs. Firstly, the improved version of RMA's current frame involves using a DOE method and two exploratory techniques to solve a multi-variable problem. This section will discuss which method achieved the most desirable result, and with which variables. Secondly, the modular design uses topology optimization to lower the mass of 3D-printed lugs that are used to assemble a space frame structure. One of the benefits of the ALM process is the ability to produce prototypes quickly, which has already been done and described further in this chapter. Finally, the chapter will compare the two proposed designs against the PDS stated at the start of this thesis to ensure that both designs meet the desired goals.

8.1   RMA Chair Optimisation Results Discussion

As *Table 8.1* indicates, the outputs differed slightly for each optimisation process as more variables were added. All of the optimisers produced viable design options, hitting the set targets and producing shapes that could be manufactured.

Of the three optimisation algorithms used the DOE achieved the best weight reduction in the second stage of the optimisation process, removing 448g (22%) from the initial design with some sacrifice to the stiffness of the wheelchair increasing the displacement in serve 1 by 0.2 mm.

The two exploratory techniques also produced optimum designs for each stage. In the final loop both the PSO and GA were able to find a better solution than DOE. This could due to the random element built into both the optimisers (i.e. mutation in GA and inertia in PSO) allowing for the larger design space to be searched more efficiently with minimum changes to the optimiser settings.

Of the three sets of parameters affected, the largest weight reduction was achieved by changing the diameter of the wall thickness. The variable tube diameters reduced the mass of the wheelchair by 100 g when the PSO method was used between optimisation loops.

Table 8.1: design goal output for each optimisation technique (Summery)

| | | Mass (g) | Displacement | | | Stress |
			Serve 1 (mm)	Serve 2 . (mm)	Reach (mm)	Impact (MPa)
Initial	1	2082.95	0.6	0.26	-0.9	162
DOE	OP1	1889.76	0.7	0.26	1.03	141.28
	OP2	1634.88	0.8	0.21	-0.93	152.72
	OP3	1966.8	0.56	0.27	-1.9	142
GA	OP1	1983.5	0.59	0.26	0.85	131.764
	OP2	1764.29	0.7	0.18	-0.93	140
	OP3	1752	0.75	-0.29	0	168
PSO	OP1	1989.5	0.58	0.25	0.88	142.1
	OP2	1853.05	0.78	0.18	-0.98	144.82
	OP3	1753	0.6	-0.2	0	168

Due to the mass saving in the DOE OP2 loop that was deemed the most suitable design to proceed with and compare against the PDS set at the start of this thesis.

8.2 Topology Optimisation results discussion

Using topology optimisation for these parts has been very beneficial in reducing the mass of the modular chair design. As can be seen in *Table8.2* reducing the mass of the components by up to 50%. in the case of the steel parts. As can be seen in the table below the lightest of the three materials used was the aluminium components with a mass of 528.37g for all twelve of the connectors. This is almost four times lighter than that of the steel parts. This identifies aluminium as the ideal material for the finished chair.

Using the aluminium lugs instead of the steel lugs used to make the prototype the total mass of a frame can be calculated. Aluminium lugs:732.44g, base module:637g and 554g for the tubes gave a total mass of 1.92kg a mass saving of only 160g when compared to RMA's current frame. but this design does allow for more adjustability and customisation.

Table 8.2: Total Mass of Printed Components

	Steel	Aluminium	Titanium
Total initial mass (g)	4647.71	1260.81	2030.36
Total Optimised mass (g)	2407.10	732.44	1412.64
Total mass saved (g)	2240.61	528.37	617.72
Percentage saved (%)	48.21	41.91	30.42

8.3 PDS Review

It is crucial to evaluate the two designs presented in this thesis with the PDS discussed earlier in the thesis *Chapter3.1. Table* **??** which demonstrates how each of the designs has met or missed the desired objectives.

Table 8.3: Product Design Specification Checklist

No.	Requirement	Class	Standard Space frame	Printed Modular Frame
1	Design Target			
1.1	Reduce Mass	1	Pass: 448g saved in space frame. Using similar components reduces the mass of the wheelchair to 9.152 kg	Pass: The total mass of optimised aluminium Lugs were 732g carbon tubes 554g and 637g for the base module The total mass of 1.92kg 160g less than RMA's current wheelchair.
1.2	Increase or maintain Stiffness	2	Pass: The benchmark set by the current wheelchair was used as a design goal in the optimisation phase	Pass: Was set as one of the design goals for as part of the optimisation process
2	User requirement			
2.1	Fit a range of body shapes	2	Pass: Optimisation Phase restricted movement of points that affected fit. So design will fit the same range of players of current	Pass: Adjustability in design allows the wheelchair to fit a wide range of body shapes
3	Componants			

Table 8.3 continued from previous page

No.	Requirement	Class	Standard Space frame	Printed Modular Frame
3.1	Quick release driven wheels	2	Pass: Like the current RMA wheelchair design brackets can be welded to the space frame	Pass: Base unit design allows for attachment points for the seat belt
3.2	Castors	2	Pass: Follows same design as the RMA wheelchair using inserts in tube to attach castors	Pass: As discussed on the boundary conditions, FC-01 was designed to fit the castors
3.3	Seat	1	Pass: As with the current Wheelchair design. the fit of the seat can be adjusted with the soft material added to the seat.	Pass: The adjustability of the base unit allows for the sides to be adjusted to hold the player in place
4	Environmental Considerations			
4.1	Cannot cause damage to court	1	Pass	Pass
4.2	Distractions to other players	1	Pass	Pass

Table 8.3 continued from previous page

No.	Requirement	Class	Standard Space frame	Printed Modular Frame
4.3	Tight Turning circle	1	Pass Minimal Changes to geomatry means that the wheelchairs ability to turn has not been hindered	Pass: Key points of the wheelchair geomatry not changed to affect the handeling of the wheelchair
4.4	Removable wheels	2	Pass: As part of the boundary conditions in the optamisation process allowed room for a boss to be welded into place	Pass: Space was kept in connector BC-01for the current boss used to be fixed in place with a threaded hub
5	Load Cases			
5.1	Serve	1	Pass: Set as part of the boundary conditions	Pass: Set as part of the boundary conditions
5.2	Acceleration and turning	1	Pass: Set as part of the boundary conditions in the optimisation phase	Pass: Set as part of the boundary conditions
5.3	Forehand and backhand	1	Pass: Set as part of the boundary conditions	Pass: Set as part of the boundary conditions
5.4	Impact	3	Pass: Set as part of the boundary conditions	Pass: Set as part of Boundary conditions Specific to FC-01

Table 8.3 continued from previous page

No.	Requirement	Class	Standard Space frame	Printed Modular Frame
6	Manufacturing			
6.1	Cost	2	Pass: Manufacturing process and materials have not changed so does not have an impact on cost	Pass; Printed Lugs:£1470 Carbon Tubes: £190 Base;£50 (From prototype build) Total:£1710 when compared to cost to produce an elite level wheelchair
6.2	Avalability	2	Pass; Key feature of this design was to use manufacturing methods already avalible to RMA	Fail: ALM machines not readily available at RMA's factory. However this manufacturing method can be sub-contracted

Table 8.3 continued from previous page

No.	Requirement	Class	Standard Space frame	Printed Modular Frame
6.3	Design and manufacturing time scale	2	Pass: The current design can be manufactured just as quickly as the new design, using a similar assembly process with jigs and fixtures to hold the tubes in place.	Pass; Lugs take 58 hrs to print assembly can be done quickly. The ALM process allows for adjustments to be made to the design without an effect on manufacturing time
6.4	Large-scale production	2	Pass: Design can be manufactured on a similar scale to the current sports chair	Fail: Currently, ALM is not suited to large-scale manufacture.
6.5	Small batch, bespoke	2	Pass: Wheelchair can be made bespoke. however may need some changes to jigs	Pass: Due to the nature of the ALM process all of the wheelchairs can be tweaked and have the potential to be bespoke.

Table?? shows that both proposed wheelchair designs have mostly met the targets set in the PDS. The optimum designs have successfully reduced the weight of the wheelchair. The new RMA chair reduced the weight by nearly 450g by adjusting the tube diameter and lengths of the current wheelchair. The modular wheelchair had a weight reduction of 160g which is less than the other first design but is more versatile with adjustable seat position and the potential to swap tube lengths.

However, the AM modular design failed to meet two of the required targets, namely the ability to produce the wheelchairs in large quantities and the availability of AM. There is potential for the parts to be made either by investing in the necessary equipment or subcontracting the parts. With that said both of the wheelchair designs have proven to be an improvement on RMA's Current design with the mass reduction in the new optimised RMA's chair and the increased adjustability for the modular wheelchair.

Chapter 9

Future Work and Improvements

Upon reflecting on the areas that were covered in this project, it has become apparent that certain aspects require improvement or further work. Particularly, the practical testing and the two optimization phases need attention. Suggestions have been made to enhance the testing procedure during the practical testing stage, to obtain more reliable results. Second, the exploratory techniques optimization model will be employed to develop a tool that can be utilised by RMA and potentially be applied to other sports. Lastly, some design enhancements can be made to the modular wheelchair.

9.1   Practical testing future work

It is possible to improve the testing of wheelchairs in the future. Firstly, using a group of professional athletes as test subjects could lead to more consistent results, especially in cases where the load is more predictable, such as during a serve.

Secondly, updating the equipment by using an online motion detection system to replace the existing GoPro and data logging system could improve the number of data points recorded. The new system would feed directly into the online motion detection system, eliminating any potential errors in syncing the data sets.

9.1.1 Online Motion Detection

An online motion detection system would be the next stage in using the video to analyse the player's movements in the required space. Key points should be identified on the player and their chair to monitor their movement in relation to the speed and velocity of the chair [81].
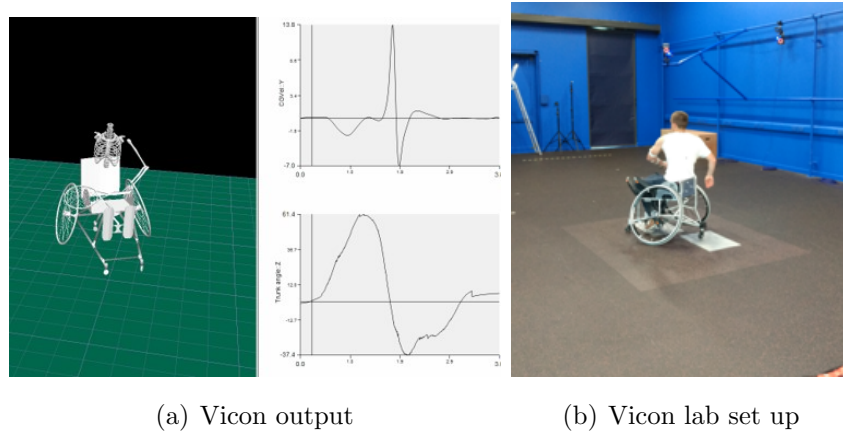

(a) Vicon output   (b) Vicon lab set up

Figure 9.1: Vicon

9.1.2 Purpose-Built Data logger

Furthermore, a purpose-built data logger could be built using two Arduinos mounted on the back seat of the wheelchair and linked to the strain gauge points on the left and right of the wheelchair, thus reducing the length of the wires and potential for noise. A third Arduino would be used to send a signal to both the data-logging Arduinos and via Bluetooth to the Vicon data collection box connected to a PC to enable the data to be paired after the tests had been completed. The data collected by the Arduinos could be transmitted to the PC, providing live data during the test. As this set up would be lighter than the P3 data logger, it would be less intrusive on the player's movement and could be used for a full game.
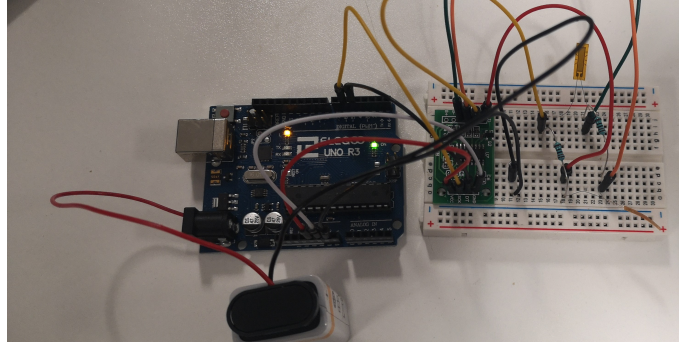
Figure 9.2: Strain gauge Arduino setup

9.2 Further Work in RMA Chair Optimisation

To determine whether the current design could be further improved, further changes could be made to the algorithms, experimenting with the parameters for each algorithm and noting the effects, for example, the number of particles could be increased in the PSO, the number of iterations in the GA could be increased and potentially more specific design targets could be set.

Once the process has been improved, more variables could be added such as the tube shape or material, or the current variables could be given a wider range of values to consider.
The end goal would be to create a tool that can be used to generate a wheelchair design quickly for RMA based on the players weight and the sport they want to play. Providing a design for the technician to manufacture.

9.3 Modular Design

To further improve the customisation aspect of the modular design a clamping mechanism was added to allow for the quick adjustment of tube lengths. To achieve this, and retain the stiffness of the frame, inspiration was taken from the bicycle industry using a similar design, to the seat clamp of the Giant Propel Advanced Aero road bike design as seen in *Figure9.3*. The clamp is made from three sections of 1075 aluminium machined to shape, as seen in *figure9.3*. The lower third section of the clamp has a m5 thread cut. As the clamp is tightened, the middle section is pushed into the carbon tube and upper and lower sections

are pushed out into the connector as can be seen on the *figure9.3*. This method should allow the design to be completely modular and adjustable with only a hex key required to assemble and adjust the wheelchair.

The initial design can be used as a moveable jig for the tennis players to find the perfect geometry. Furthermore, this fully adjustable design will be useful when testing geometry to see how different lengths affect different play styles for creating a wheelchair that is bespoke to the player. This could lead to a second stage in RMA's fitting service after the initial contour body mapping, providing a dynamic test before settling on a more permanent geometry.

A potential possibility for this design is for younger players to have the chair geometry altered as they mature, thus negating the need to replace the entire wheelchair when it has been outgrown, thereby, saving costs and material waste. This could result in wheelchair sports becoming more accessible to younger Athletes.
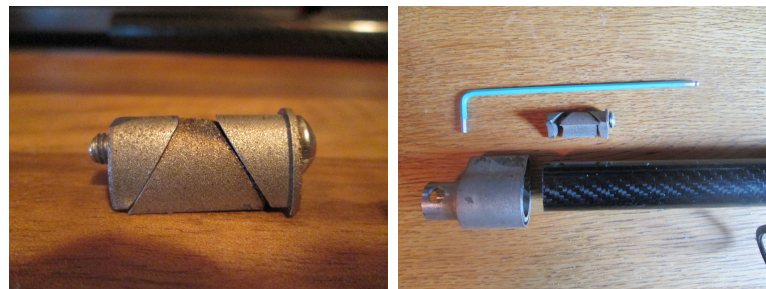
(a) Three part inline clamp

(b) Clamp Compnents
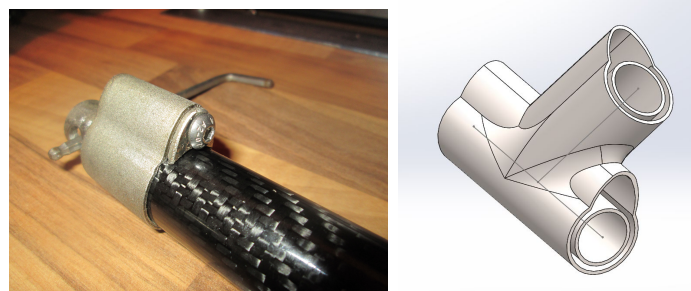
(c) Inline Clamp Full Assembly

(d) MC-02 with clamp locator

Figure 9.3: Temporary joint modular clamp

Chapter 10

Conclusion

The aim of this project was to investigate new techniques for designing and optimising tennis wheelchairs. In the first step current wheelchairs on the market were researched, looking initially at the sports wheelchairs designed by the sponsoring company RMA, before moving on to those produced by their competitors. With the exception of Stéphane Houdet's bespoke wheelchair, the tennis wheelchairs shared key characteristics: all weighed between 8 and 10 kg, had a steel or aluminium space frame chassis, using two driven wheels and three or four stabilising castor wheels. Moreover, the majority of the entry level wheelchairs had some adjustability on the seat, rear castors, and footplate. The adjustability was removed from the tennis wheelchairs aimed at intermediate to professional players, favouring a more bespoke fit to improve mechanical properties. Areas that could impact the design, such as user size, wheelchair components, and environmental factors, were highlighted in this chapter to aid in creating the PDS.

With the aid of the previous section and the gathered data, a PDS was created, the aim of which was to highlight the following: the design goals (reducing mass and improving stiffness), restrictions (rules and manufacturing) and player requirements (size and components).This information was then presented as PDS in table form to guide future designs.

The next stage was to develop a method to test RMA's current wheelchair to identify how it reacts during a game and to investigate any movements the player makes that would affect future designs. To achieve this, strain gauges were applied to a tennis wheelchair in locations predicted to have the largest loads.

The user then simulated the main movements that occur during a tennis match namely service, ball returns, acceleration, and steering. The strain gauge data were synchronised with camera footage, allowing the strain values to be paired with the relevant movement. For the most part the peaks in strains did align with peaks in the stress data, confirming the load cases; however, the standard deviation for each load case was quite large. There were a few ways that which the experiment could be improved to eliminate this problem in future tests. First, a professional athlete might exhibit more consistent loads compared with the user in the experiment. A larger test group would also be beneficial. Additionally, further improvements could be made to the experiment, such as the use of a data logger that can record data more frequently so the load cases can be understood better. In future work the camera equipment could also be improved by introducing a motion capture system such as Vicon to gather more data during the testing stage and to determine the constancy of the movement.

Once load cases have been identified, a 3-dimensional FEA model was constructed with 1D beam elements. This was a low fidelity model to allow for quick runs and easy changes to be made during the optimisation phase. When the load cases where calculated, the input Abaqus file was parametrised to allow for the variables to be adjusted. Dassults systems Isight was then used to create an optimisation loop with the design targets of reducing the mass and increasing the stiffness of the chair.

Three optimisation techniques were used in the optimiser; DOE (Hypercube), multi-objective PSO and NSGA. The number of variables in the optimiser where increased with each run. starting with the tube diameter and wall thickness being altered by 2mm above and below. The second stage allowed for the adjustment of the wheelchair geometry by giving design freedom to the coordinates that comprised the frame. The coordinates where allowed to move by 10 mm in any direction. The final step required some adjustment to the input file by splitting existing tubes into separate parts. Each part was assigned its own tube radius and thickness which were set as the new variables to determine whether any savings could be made with variable diameter tubing. The best design was highlighted in the second optimisation loop using the DOE method.Producing a design with a total weight saving of almost 450g.

In the future, the optimiser could be improved by initially editing the settings

with in the optimisers to determine whether the results can be improved. For example increasing the number of particles in the multi objective PSO, would allow for a broader search of the design area. Once the optimisation process has been completed, it would be possible to increase the number of variables in the optimiser or increase the range of variables (e.g. tube shape).

The final stage of the project involved designing and optimising a printed modular wheelchair using ALM to allow custom geometry for each wheelchair. This was achieved by taking inspiration from companies within the bicycle industry, designing a space frame that can be assembled from 12 printed lugs and carbon fibre tubes and using an adhesive to permanently bond the tubes in place.

As the lugs would be printed, it was decided to take advantage of the near net manufacturing technique and improve the mechanical properties of the lugs using the topology optimisation software Altair Inspire. All the parts were given a large design space, so as not to hinder any shape that was generated. Steel, aluminium, and titanium versions of the parts were optimised to measure which material would be optimal for the wheelchair design. The optimisation was successful and reduced the total mass of the parts by 48% for steel, 42% for aluminium and 30% for titanium parts. Aluminium lugs emerged as the best option, and the total mass of the 12 connectors came to 528g. However due to availability, the parts were printed from 316 stainless steel to prove the concept.

A future development of this design would be to remove the need for adhesive, making all the joints temporary. Using an in-line clamp to hold the tubes in place would allow the whole space frame to be assembled with only a hex key, making geometry adjustments to the wheelchair throughout the product's life cycle. This could be useful to customers if they participated in multiple wheelchair sports and as they could adjust the frame components and geometry easily. Furthermore this style of wheelchair would be beneficial to younger athletes who adjust the geometry as they grow.

In the last phase, the two designs that were proposed were compared with the PDS set earlier in the project. Both designs met majority of the targets. However, the modular design did not meet some of the targets due to the availability of the manufacturing process.

In conclusion, the aim of the project was to investigate alternative designs for high-performance tennis wheelchairs for RMA Sport. This has been achieved by proposing two design approaches: firstly, a design based on current manufacturing methods, and secondly, a design utilizing alternative materials and manufacturing methods. Both approaches can be customised to suit player-specific requirements.

Bibliography

[1] "Wheelchair Tennis - About." [Online]. Available: https://www.paralympic.org/wheelchair-tennis/about

[2] Roma Medical, "About - Roma Medical," 2017. [Online]. Available: http://romamedical.co.uk/about/

[3] "RMA Sport About Us About Us About Us." [Online]. Available: https://rmasport.com/about/

[4] "RMA Sport - Shop - Spinergy Wheels, Tyres, Castors and more." [Online]. Available: https://rmasport.com/shop/

[5] "Top End Eliminator Racing wheelchair - Invacare United Kingdom." [Online]. Available: https://www.invacare.co.uk/manual-wheelchairs/top-end-sports-wheelchairs/top-end-eliminator-racing-wheelchair

[6] "RMA Sport Rugby Wheelchair Made to Measure Rugby Landing Page %." [Online]. Available: https://rmasport.com/rugby-landing/

[7] ITF Tennis, "Paralympic tennis event, Rio 2016," 2016. [Online]. Available: http://www.rio.itftennis.com/paralympics/organisation/{%}2Fparalympics{%}2Forganisation{%}2Frio-2016

[8] "ITF Rules oF TennIs." [Online]. Available: http://www.itftennis.com/media/248215/248215.pdf

[9] "The Mountain Trike Self Propelled, All Terrain Off... — Mountain Trike." [Online]. Available: https://www.mountaintrike.com/products/mountain-trike

[10] "RMA Sport Tennis Wheelchairs Tennis Club Wheelchair - Adult." [Online]. Available: https://rmasport.com/product/tennis-club-wheelchair-adult/

[11] "Tennis Club Wheelchair – Child -." [Online]. Available: https://rmasport.com/product/tennis-wheelchair-youth/

[12] "RMA Tennis Wheelchairs Made to Measure & Club Wheelchairs." [Online]. Available: https://rmasport.com/tennis/

[13] A. Welch, "Core values," pp. 35–38, 2012. [Online]. Available: http://www.rgklife.com/rgk-core-values-sport-and-daily-made-to-measure-wheelchairs.html

[14] "Tennis Wheelchair - Made to Measure — RGK Wheelchairs." [Online]. Available: https://rgkwheelchairs.com/wheelchairs/sport-wheelchairs/grandslam.html

[15] "Grandslam X Best Tennis Wheelchair — RGK Wheelchairs." [Online]. Available: https://rgkwheelchairs.com/wheelchairs/sport-wheelchairs/grandslamx.html

[16] "GrandSlam CX Carbon Fibre Basketball Wheelchair — RGK Wheelchairs." [Online]. Available: https://rgkwheelchairs.com/wheelchairs/sport-wheelchairs/grandslam-cx-tennis-wheelchair-carbon-fibre-seat-rgk-wheelchairs.html

[17] "Brand Advocates and RGK Wheelchair Athletes." [Online]. Available: https://rgkwheelchairs.com/athletes.html

[18] BroMakin, "Bromakin Tennis Evo." [Online]. Available: https://www.bromakin.co.uk/index.php/products/sports/wheelchair-tennis/bromakin-tennis-evo

[19] "Bromakin Tennis XL." [Online]. Available: https://www.bromakin.co.uk/index.php/products/sports/wheelchair-tennis/bromakin-tennis-xl

[20] "Bromakin Tennis Evo." [Online]. Available: https://www.bromakin.co.uk/index.php/products/sports/wheelchair-tennis/bromakin-tennis-evo

[21] "Invacare ® Top end ® T-5 7000 Series Tennis," 2012. [Online]. Available: www.invacare.co.uk

[22] "Invacare ® Top end ® pro Basket-Ball / Tennis," 2012. [Online]. Available: www.invacare.co.uk

[23] ITF Tennis, "ITF Tennis - WHEELCHAIR - Player Profile - HOUDET, Stephane (FRA)." [Online]. Available: http://www.itftennis. com/wheelchair/players/player/profile.aspx?playerid=100089994

[24] "Wheelchair Tennis HOUDET Stephane - Tokyo 2020 Paralympics." [Online]. Available: https://olympics.com/tokyo-2020/paralympic-games/en/ results/wheelchair-tennis/athlete-profile-n1358156-houdet-stephane.htm

[25] "Jeux Paralympiques - De l'or pour Stéphane Houdet et Nicolas Peifer en double aux Jeux Paralympiques de Rio." [Online]. Available: https://www.lequipe.fr/Tennis/Actualites/ De-l-or-pour-stephane-houdet-et-nicolas-peifer-en-double-aux-jeux-paralympiques-de-rio/ 727743

[26] "Rio 2016 : Stéphane Houdet et Nicolas Peifer en finale du double - Coeur Handisport." [Online]. Available: https://www.coeurhandisport.fr/tennis/ f42da0bae837613e11b4a9be7f22d615.php

[27] J. P. Parkerson and L. W. Schaper, "Design considerations," *Advanced Electronic Packaging*, no. February, pp. 437–485, 2006.

[28] H. Factors and U. States, "Topic 1: Human Factors & Ergonomics."

[29] A. Data, P. Page, B. Height, B.-k. Length, B.-p. Length, E. R. Height, E. R. Height, G. Length, E.-w. Length, E. H. Approximation, E. Height, E. Height, F.-f. Breadth, F.-h. Length, F. G. Reach, F. G. Reach, F. L. Length, H. Breadth, H. Circumference, H. Length, H. Breadth, K. Height, L. Arm, L. Leg, O. F. Reach, P. Height, S. Height, S. Height, S.-e. Length, S.-w. Length, S. Height, S. Inseam, T. Breadth, T. Reach, U. A. Length, V. G. Reach, V. Grip, R. Down, V. G. Reach, V. Index, F. Reach, V. Index, F. Reach, and V. T. Reach, "A n t h r o p o m e t r i c d a t a."

[30] "Factors of Safety." [Online]. Available: https://www.engineeringtoolbox. com/factors-safety-fos-d{_}1624.html

[31] K. Koehler, T. Abel, D. M. Bellar, and J. L. Flueck, "Article 1 Flueck JL (2020) Body Composition in Swiss Elite Wheelchair Athletes," *Front. Nutr*, vol. 7, p. 1, 2020. [Online]. Available: www.frontiersin.org

[32] "About Us — Spinergy." [Online]. Available: https://www.spinergy.com/ about-us

[33] "Spinergy Rugby Wheels Spinergy - Sport Lite Extreme." [Online]. Available: https://rmasport.com/product/spinergy-slx-sport-light-extreme/

[34] "Titanium Axle - 1/2" — Spinergy." [Online]. Available: https://www.spinergy.com/products/titanium-axle-12

[35] "PHASE-ONE – Frog Legs Inc." [Online]. Available: https://froglegsinc.com/collections/forks/products/phase-one

[36] "WCMX - RMA Sport - Made to Measure, Club & Youth Skate Wheelchairs." [Online]. Available: https://rmasport.com/wcmx/

[37] "RGK Club Sport Tennis Wheelchair - RGKCLUBSPORT-TENNIS." [Online]. Available: https://www.epc-wheelchairs.co.uk/wheelchairs-powerchairs/sports-wheelchairs-wheelchair-tennis/rgk-club-sport-tennis-wheelchair

[38] "RGK-Grandslam." [Online]. Available: https://www.epc-wheelchairs.co.uk/wheelchairs-powerchairs/sports-wheelchairs-wheelchair-tennis/rgk-grandslam-tennis-wheelchair

[39] "How to Start a Sporting Goods Store in 2022." [Online]. Available: https://www.magestore.com/blog/how-to-start-a-sporting-goods-store/{#}s12

[40] T. Rietveld and R. J. K Vegter, "The interaction between wheelchair configuration and wheeling performance in wheelchair tennis: a narrative review," 2021. [Online]. Available: https://doi.org/10.1080/14763141.2020.1840617

[41] "Sports graphic packages on Behance." [Online]. Available: https://www.behance.net/gallery/9259117/Sports-graphic-packages

[42] K. Masubuchi, *Analysis of Welded Structures: Residual Stresses, Distortion, and Their ... - Koichi Masubuchi - Google Books*, 1st ed., 1980. [Online]. Available: https://books.google.co.uk/books?hl=en{&}lr={&}id=TUgvBQAAQBAJ{&}oi=fnd{&}pg=PP1{&}dq=welded+structures{&}ots=4w9UVuff-X{&}sig={_}fUOwhAZ-8JAghY3ZquOenpP94E{&}redir{_}esc=y{#}v=onepage{&}q=weldedstructures{&}f=false

133

[43] B. Wu, J. Li, and C. Myant, "Beyond the hype: 3D printing grows up," 2016. [Online]. Available: http://www.imperial-business-partners.com/wp-content/uploads/2016/06/Additive-Manufacturing-Briefing-Note-20062016.pdf

[44] "About - Bastion Cycles." [Online]. Available: https://www.bastioncycles.com/about/

[45] "TECHNOLOGY — Athertons." [Online]. Available: https://www.athertonbikes.com/technology

[46] Renishaw, "First metal 3D printed bicycle frame manufactured by Renishaw for Empire Cycles," 2014. [Online]. Available: http://www.renishaw.com/en/first-metal-3d-printed-bicycle-frame-manufactured-by-renishaw-for-empire-cycles--24154

[47] K. S. Prakash, T. Nancharaih, and V. V. Rao, "Additive Manufacturing Techniques in Manufacturing -An Overview," *Materials Today: Proceedings*, vol. 5, no. 2, pp. 3873–3882, 2018. [Online]. Available: https://doi.org/10.1016/j.matpr.2017.11.642

[48] "Green Mechanic: Comparison between Selective Laser Melting (SLM) and Selective Laser Sintering (SLS)." [Online]. Available: https://www.green-mechanic.com/2016/12/comparison-between-selective-laser.html

[49] M. Grujicic, G. Arakere, P. Pisu, B. Ayalew, N. Seyr, M. Erdmann, and J. Holzleitner, "APPLICATION OF TOPOLOGY, SIZE AND SHAPE OPTIMIZATION METHODS IN POLYMER METAL HYBRID STRUCTURAL LIGHTWEIGHT ENGINEERING," *Multidiscipline Modeling in Mat. and Str*, vol. 4, pp. 305–330, 2008. [Online]. Available: www.brill.nl/mmms

[50] E. C. Wai-fah, "Space Frame Structures," *Handbook of Structural Engineering*, pp. 1239–1288, 2020.

[51] M. Kociecki and H. Adeli, "Engineering Applications of Arti fi cial Intelligence Shape optimization of free-form steel space-frame roof structures with complex geometries using evolutionary computing," *Engineering Applications of Artificial Intelligence*, vol. 38, pp. 168–182, 2015. [Online]. Available: http://dx.doi.org/10.1016/j.engappai.2014.10.012

[52] J. A. Nelder and R. Mead, "A Simplex Method for Function Minimization," *The Computer Journal*, vol. 7, no. 4, pp. 308–313, jan 1965. [Online]. Available: https://academic.oup.com/comjnl/article/7/4/308/354237

[53] "Cauchy and the Gradient Method." [Online]. Available: http://mathdoc.emath.fr/cgi-bin/oetoc?id=OE{_}CAUCHY{_}1{_}

[54] S. Katoch, S. S. Chauhan, and V. Kumar, *A review on genetic algorithm : past , present , and future.* Multimedia Tools and Applications, 2021.

[55] M. Kociecki and H. Adeli, "Two-phase genetic algorithm for size optimization of free-form steel space-frame roof structures," *JCSR*, vol. 90, no. 2013, pp. 283–296, 2018. [Online]. Available: http://dx.doi.org/10.1016/j.jcsr.2013.07.027

[56] M. O. Okwu and L. K. Tartibu, "Particle Swarm Optimisation," *Studies in Computational Intelligence*, vol. 927, pp. 5–13, 2021.

[57] M. Jafari, E. Salajegheh, and J. Salajegheh, "Optimal design of truss structures using a hybrid method based on particle swarm optimizer and cultural algorithm," *Structures*, vol. 32, no. January, pp. 391–405, 2021. [Online]. Available: https://doi.org/10.1016/j.istruc.2021.03.017

[58] S. J. Bates, J. Sienz, and V. V. Toropov, "Formulation of the optimal latin hypercube design of experiments using a permutation genetic algorithm," *Collection of Technical Papers - AIAA/ASME/ASCE/AHS/ASC Structures, Structural Dynamics and Materials Conference*, vol. 7, pp. 5217–5223, 2004. [Online]. Available: https://arc.aiaa.org/doi/10.2514/6.2004-2011

[59] M. Tomlin and J. Meyer, "Topology Optimization of an Additive Layer Manufactured (ALM) Aerospace Part," Tech. Rep., 2011.

[60] "SRAM — Generative Design — Autodesk." [Online]. Available: https://fom.autodesk.com/sram/p/1

[61] D. Brackett, I. Ashcroft, and R. Hague, "TOPOLOGY OPTIMIZATION FOR ADDITIVE MANUFACTURING."

[62] S. Odenwald, "Test Methods in the Development of Sports Equipment," in *The Engineering of Sport 6.* Springer New York, 2006, pp.

301–306. [Online]. Available: https://link.springer.com/chapter/10.1007/978-0-387-46051-2{_}54

[63] D. J. Stefanyshyn and J. W. Wannop, "Biomechanics research and sport equipment development," *Sports Engineering*, vol. 18, no. 4, pp. 191–202, dec 2015. [Online]. Available: https://link.springer.com/article/10.1007/s12283-015-0183-5

[64] "RMA Sport UK Wheelchairs Rugby WCMX Tennis - Basketball." [Online]. Available: https://rmasport.com/

[65] "Wheelchair Testing & Mobility Aids Testing — WO — TÜV Rheinland." [Online]. Available: https://www.tuv.com/world/en/wheelchair-scooter-tests.html

[66] "EN 12183:2022 - Manual wheelchairs - Requirements and test methods." [Online]. Available: https://standards.iteh.ai/e-library/reader/8c690140-b2f8-11ee-8497-734bb1f9fff7

[67] R. Tricker, "The Medical Devices Directive (93/42/EEC)," Tech. Rep. June 1993, 2020.

[68] "Made to Measure wheelchairs custom Made Wheelchairs." [Online]. Available: https://rmasport.com/wheelchairs-made-measure/

[69] W. Montero, R. Farag, V. Díaz, M. Ramirez, and B. L. Boada, "Uncertainties Associated with Strain-Measuring Systems Using Resistance Strain Gauges," *The Journal of Strain Analysis for Engineering Design*, vol. 46, no. 1, pp. 1–13, jan 2011. [Online]. Available: http://journals.sagepub.com/doi/10.1243/03093247JSA661

[70] K. Hoffmann, "Applying The Wheatstone Bridge Circuit," in *Hottinger*, 3rd ed., 1986. [Online]. Available: http://paginas.fisica.uson.mx/horacio.munguia/aula{_}virtual/Cursos/InstrumentacionII/Documentos/TeoriaCtosPuentes.PDF

[71] "865-6235 — ET16744636 — RS Pro — RS Pro Wire Lead Strain Gauge 4mm, 120Ω -30°C +180°C — Enrgtech." [Online]. Available: https://www.enrgtech.co.uk/product/strain-gauges/ET16744636/865-6235

[72] "Strain gauges and Wheatstone bridges — Basic instrumentation and new applications for electrical measurement of non-electrical quantities — IEEE Conference Publication — IEEE Xplore." [Online]. Available: https://ieeexplore.ieee.org/abstract/document/5767428

[73] "Strain Gauges — Electrical Instrumentation Signals — Electronics Textbook." [Online]. Available: https://www.allaboutcircuits.com/textbook/direct-current/chpt-9/strain-gauges/

[74] A. Sánchez-Pay, R. Martínez-Gallego, M. Crespo, and D. Sanz-Rivas, "Key physical factors in the serve velocity of male professional wheelchair tennis players," *International Journal of Environmental Research and Public Health*, vol. 18, no. 4, pp. 1–11, feb 2021.

[75] T. Janssen, J. Lenton, V. De Baare, Y. Bakker, F. Bos, V. Goosey-Tolfrey, and S. De Groot, "Acceleration Profile during 20-m Sprints in Elite Wheelchair Tennis Players."

[76] Alex, "Isight Design Optimization Methodologies," 2010. [Online]. Available: www.asminternational.org

[77] "IEEE Xplore Full-Text PDF:." [Online]. Available: https://ieeexplore.ieee.org/stamp/stamp.jsp?tp={&}arnumber=996017

[78] "Multi-Objective Particle Swarm Technique."

[79] N. Ferede, "Topology Optimization of Automotive sheet metal part using Altair Inspire," *International Journal of Engineering and Management Sciences*, vol. 5, no. 3, pp. 143–150, 2020.

[80] Jim Soltisz, "Approximation Models in Isight for Reduced Order Modeling," jan 2023. [Online]. Available: https://www.inceptra.com/approximation-models-in-isight-for-reduced-order-modeling/

[81] C. J. Payton and R. M. Bartlett, *Biomechanical evaluation of movement in sport and exercise: The British association of sport and exercise sciences guidelines.* Routledge, 2007. [Online]. Available: http://whel-primo.hosted.exlibrisgroup.com/primo{_}library/libweb/action/display.do?ct=display{&}fn=search{&}doc=44WHELF{_}SWA{_}ALMA{_}DS2164148400002417{&}indx=1{&}recIds=44WHELF{_}

SWA{_}ALMA{_}DS2164148400002417{&}recIdxs=0{&}elementId=0{&}
renderMode=poppedOut{&}displayMode=full{&}fr